Application of Radiotracers and Energetic Beams in Sciences

Volume 6

Extended abstract of the invited lectures and contributed papers of

The Fifth International Conference on Application of RadiotraCers and Energetic Beams in Sciences (ARCEBS 2023)

January 31 – February 05, 2023

EDITORS

Nabanita Naskar
Susanta Lahiri

Organized by
Sidho-Kanho-Birsha University
Purulia, India

In Cooperation with

International Atomic Energy Agency (IAEA)

Published
January 31, 2023

Printed at

DHAR BROTHERS
4 Rammohan Roy Road, Kolkata 700009
Ph 033-23508103

ARCEBS 2023

Conference Chair: Susanta Lahiri

International Advisory Committee

Hannah Affum IAEA
Navin Alahari, FRANCE
A. Chatt, CANADA
Swapan Charropadhyay, USA
J. G. Correia, PORTUGAL
Christoph Düllmann, GERMANY
Flavia Groppi, ITALY
Hiromitsu Haba, JAPAN
Férid Haddad, FRANCE
Xiaolin Hou, DENMARK
Karl Johnston, CERN
Dinakar Kanjilal, INDIA
S. Kannan, INDIA
Dipak Kumar Kar, INDIA
Gunther Korschinek, GERMANY
P. K. Mohapatra, INDIA
Yuichiro Nagame, JAPAN
Vandana Nanal, INDIA
Bernd Neumaier, GERMANY
S. M. Qaim, GERMANY
Zsolt Revay, GERMANY
Tetsuya K Sato, Japan
Thierry Stora, CERN
Zoltan Szücs, HUNGARY
B. S. Tomar, INDIA
Md. Mohi Uddin, BANGLADESH
Meera Venkatesh, INDIA
Bert Wolterbeek, THE NETHERLANDS

National Organizing Committee

Dipak Kumar Kar, Vice-Chancellor, SKBU, Purulia --- Chairperson
Chiranjib Barman, SKBU, Convener
Tapas Das, BARC, Mumbai
Sandeep Ghugre, UGC DAE CSR, Kolkata
Sunali Khanna, Mumbai
Pankaj Kumar, IUAC, New Delhi
Moumita Maiti, IIT ROORKEE
Gopal Mukherjee, VECC, Kolkata
Sandip Kumar Mukhopadhyay, MoES, GoI
Vaishali Nayek, VECC, Kolkata
R. C. Ramola, Tehri Garhwal
R. Ravishankar, VECC-BARC, Kolkata
Bhupinder Singh, ICAR-IARI, New Delhi
Suparna Sodaye, BARC, Mumbai
Alok Srivastava, PU, Chandigarh
Diwakar Tiwari, MZU, Aizwal

Local Organizing Committee

Chairperson	Dipak Kumar Kar, Vice-Chancellor, SKBU	
Convener	Chiranjib Barman, SKBU	
Joint Conveners	Sonjoy Mondal, SKBU	Biswanath Mukherjee, SKBU
LOC Members	Nachiketa Bandyopadhyay, SKBU	Punarbasu Chaudhuri, CU
	Subal Chandra De, SKBU	Kaushik Gangopadhyay, CU
	Supriya Gangopadhyay, SINP	Tilak Kr. Ghosh, VECC
	Probodh Kumar Kuiri, SKBU	Susanta Lahiri, DHWU & SKBU
	Debdas Mandal, SKBU	Sushanta Kr. Mondal, SKBU
	Rajib Nath, SKBU	Ardhendu Sekhar Patra, SKBU
	Subrata Raha, SKBU	Rajarshi Raut, UGC DAE CSR
	Kamalika Sen, CU	
Secretary	Nabanita Naskar, Diamond Harbour Women's University	
Secretarial Team	Saheli Chowdhury, JU	Sayantan Mitra, SKBU
	Joydeep Mukherjee, SKBU	

ARCEBS 2023 – Scientists' Commitment Towards Good Science

The First International Conference on Application of Radiotracers in Chemical, Environmental and Biological Sciences (ARCEBS-06) was held at the Saha Institute of Nuclear Physics (SINP), Kolkata during January 23-27, 2006. Thereafter ARCEBS conferences were held every four years, ARCEBS-2010, ARCEBS-2014 and ARCEBS-2018. After ARCEBS-2010, the name of the conference was changed to Application of RadiotraCers and Energetic Beams in Sciences keeping the acronym, ARCEBS, and the logo unchanged. The last ARCEBS, i.e., the fourth conference in this series was held at Ffort Raichak, a tranquil place beside river Hooghly during November 11-17, 2018. ARCEBS-2018 was more than a grand success.

The scientific and all other creative activities suddenly stopped about a year after ARCEBS-2018. Due to the pandemic COVID-19, we lost about 7 million fellow human beings including dedicated doctors and scientists. Worldwide, people were anxious. Everyone received or sent emails with the same subject line "How are you?". We all were expecting the end of covid-19 after two months, three months, or even six months! No one in this world could expect and accept that it would last for more than two years, new vocabularies came, second wave, third wave, fourth wave, etc.

Naturally in this situation, it was not possible to organize ARCEBS in 2022. When at the beginning of 2022, the Covid situation was under control, slowly activities started under the so-called "new normal style", we and our colleagues from the Department of Physics, Sidho-Kanho-Birsha University, humbly placed the proposal of organizing ARCEBS in 2023 in offline mode (another vocabulary that became popular in last 2-3 years) to Professor Dipak Kumar Kar, Hon'ble Vice Chancellor of Sidho-Kanho-Birsha University. He instantly accepted the proposal and encouraged us to organize the conference in SKBU in offline mode. Just expressing gratitude to him for his courageous decision would not be enough.

In the meantime, another shock was waiting for the human being, the shock of war, the shock of killing human beings, the shock of destroying the environment of our beloved blue planet. Covid and the war hand-in-hand ruined the world economy. Both of these have made a difference not only in global crisis but also in widespread human rights violations. Scientists and especially the fundamental sciences have been affected much due to the economic crisis. In many countries, financial embargos have been

imposed against travel and attending conferences. In this situation, it was a real challenge to organize the conference in offline mode. Thankfully we received an enormous response from scientists from abroad and from India. It is true, that ARCEBS-2023 cannot touch the success of ARCEBS-2018 in numbers, but considering all the constraints, the numbers of ARCEBS 2023 should be multiplied by at least a factor of 10, and in that way, ARCEBS 2023 is highly successful.

Since 2006, world leaders from renowned organizations are attending ARCEBS. The most important feature of ARCEBS 2023 is the presence of young leaders who have taken the torch of nuclear science for the betterment of human beings. Thanks to the world leaders and the young delegates for agreeing to deliver invited talks in ARCEBS 2023.

The success of the conference primarily depends on the contributions of the participants. Thanks to the contributors for making again ARCEBS a benchmark conference. The reviewers from all corners of the world by their stringent reviews helped to maintain the standard of ARCEBS, our heartiest thanks to them. We extend our heartfelt thanks to The International Atomic Energy Agency (IAEA) for extending their cooperation and The Ministry of Earth Science (MoES), Govt of India, for supporting the conference. The Journal of Radioanalytical and Nuclear Chemistry (JRNC) has always been a strong supporter of the ARCEBS conference series. Since 2006. JRNC is publishing the selected papers of ARCEBS and ARCEBS 2023 is no exception. Thanks to Professor Zsolt Revay, Editor-in-Chief, JRNC and the members of the editorial board for their continued support.

Last, but not least, the organization of ARCEBS-2023 is made possible due to the culmination of yearlong hard efforts by the SKBU team headed by Dr Chiranjib Barman, convenor of ARCEBS 2023. Thanks to Dr Barman and his team.

Looking forward to meeting you, dear friends, in ARCEBS-2023. We believe that ARCEBS will continue, therefore, looking forward to meeting you again in ARCEBS 2026. We are optimistic and hopeful to have a safe, peaceful and better world ahead.

Nothing in life is to be feared,
it is only to be understood.
Now is the time to understand more,
so that we may fear less.

----------Marie Curie

Nabanita Naskar
Susanta Lahiri

CONTENTS

Keynote and Invited Lectures (Mini Symposium on Earth and Environmental Sciences)

Contributed Papers (Main Symposium)

Contributed Papers
(Mini Symposium on Earth and Environmental Sciences)

Keynote and Invited Lectures

(Main Symposium)

Are Alpha Beams of Interest to Produce Medical Radionuclides?

Férid Haddad[1,2], Cyrille Alliot[1,3], Anne-Cecile Bonraisin[1], Etienne Nigron[1], Thomas Sounalet[2], Arnaud Guertin[2]*

[1] Groupement Intranet Public ARRONAX, 44800 – Saint Herblain, France.
[2] Laboratoire Subatech, Nantes Université, IMT Atlantique, CNRS/IN2P3, France.
[2] CRCI^{2}NA, INSERM, CNRS, Nantes Université, France.
*Email: haddad@arronax-nantes.fr

With the rise of radio ligand therapy and of the theranostic approach, there has been a renewed interest in alternative radionuclides in nuclear medicine. Most common production routes use low-energy protons or neutrons. In some cases, these methods are not well suited. The aim of this study is to illustrate the interest in using α particles as projectiles to produce radionuclides for medical applications through the presentation of three relevant examples, ^{211}At, ^{43}Sc and ^{97}Ru.

The best-known example of the use of α beam is the production of ^{211}At, an α emitter that can be used for internal targeted therapy. It is produced through the (α,2n) nuclear reaction on ^{209}Bi. Cross-section data allows for optimizing both the production and purity of the final product considering the co-production of ^{210}At, the main contaminant that needs to be avoided. In the case of ^{43}Sc, a β+ emitter with $T_{1/2}$= 3.9h, irradiation with an α beam allows the use of ^{nat}Ca as the target material instead of ^{43}Ca which has a very low natural abundance and therefore is very expensive. The last example corresponds to the production of ^{97}Ru ($T_{1/2}$=2.83d), which is emitting 215 keV γ-rays (85.62%) and can be used for single photon emission tomography. In this case, the use of α beam allows starting from ^{nat}Mo whereas the proton beam requires the use of a radioactive ^{99}Tc target. Recent new cross-section values [1] have been measured up to 70 MeV allowing optimizing irradiation parameters.

For each of these 3 radionuclides, cross-section data will be discussed, production yields will be calculated from experimental data we have measured, those present in the literature or calculated from the TALYS code [2] and discussed. These three examples show that it is of interest to consider α beam to produce medical radionuclides that can be hardly obtained by other means. At the ARRONAX facility, ^{211}At production is routinely produced every week whereas the 2 other radionuclides have been studied for research.

References:

/1/ M. Sitarz, et al., Instruments 3 (2019) 7.

/2/ A.J. Koning, D. Rochman, Modern. Nucl. Data Sheets, 113 (2012).

Chemical Studies of The Heaviest Known Elements: Nihonium (Element 113), Flerovium (Element 114), and Moscovium (Element 115)

Christoph E. Düllmann[1,2,3] on behalf of the TASCA chemistry collaboration (a GSI – HIM – JGU – HS Mannheim – U. Liverpool – Lund U. – U. Jyväskylä – U. Oslo – LLNL – TAMU – RIKEN – JAEA – IITR – SINP – ANU – ITE collaboration)*

[1]Johannes Gutenberg-Universität Mainz, 55099 Mainz, Germany.
[2]GSI Helmholtzzentrum für Schwerionenforschung GmbH, 64291 Darmstadt, Germany.
[3]Helmholtz-Institut Mainz, 55099 Mainz, Germany.
*Email: c.e.duellmann@gsi.de

All elements up to oganesson (Og, element 118) have been discovered and officially accepted, filling the 7th period of the periodic table of chemical elements. Experimental chemical investigations of the heaviest elements have made tremendous progress in the last decades. The current focus is on copernicium (Cn, E112), nihonium (Nh, E113), flerovium (Fl, E114), and mocovium (Mc, E115). Relativistic effects render Cn, Nh, and Fl more chemically inert than their lighter homologs due to energetic stabilization and spatial contraction of the outermost $7s_{1/2}$ and $7p_{1/2}$ orbitals, as was realized already in the 1970s [1] and is confirmed in current state-of-the-art molecular, cluster, and solid-state relativistic calculations (e.g., [2]). Experimentally, such effects are explored using in gas phase chromatography studies of single atoms of these elements, probing volatility and reactivity towards hetero-surfaces like silicon oxide or Au, also in relation to properties of the lighter homologs and the noble gas radon [3,4].

Chemical properties of Cn have been reproducibly studied [4] and shown that the trend in adsorption strength on an Au surface established by the lighter homologs is followed by Cn [5]. Only fragmentary and unconfirmed information, mostly gained in studies that suffered from considerable background, is available on Nh [4,6]. For the past ten years, Fl has been the focus of chemical studies, with its chemical character having been disputed for many years. Results obtained at FLNR Dubna [7] and at GSI [8] were interpreted to point at a noble-gas-like and a metallic character, respectively, based on the distribution of Fl decays in Au-covered gas phase chromatography columns. New data from GSI allowed settling the question, once the inhomogeneous morphology of the Au surface, leading to sites differing in chemical reactivity, was considered [9]. Fl generally exhibits very low reactivity in the

interaction with the Au surface; at reactive sites, though, Fl forms weak metallic bonds [9], showing that Fl is not a noble gas. This allows explaining the full data set of measured Fl data, including data from [7]. On the way to settling the question of the chemical character of Fl, the safe identification of its nuclear decay chains has proven difficult [4,10]. The coupling of chemistry setups to an electromagnetic separator [8,9,11,12] provides the necessary suppression of the primary beam and of the products of multi-nucleon transfer reactions, and thus a gain in sensitivity for the unambiguous identification of single atoms of the heaviest elements. This facilitates sensitive chemical studies and even allows exploring nuclear properties in chemistry experiments [8,11].

At GSI Darmstadt, SHE studies have been a pillar of the program over the past many decades [13]. The gas-filled TransActinide Separator and Chemistry Apparatus (TASCA) serves as a physical pre-separator, along with its ancillary systems including the Cryo-Online Multidetector for Physics and Chemistry of Transactinides (COMPACT) [8,9,11,14] and its upgraded version miniCOMPACT [6,15] has been continuously improved during the last decade. The current focus of the SHE chemistry experiments behind TASCA is on Nh, Fl, and Mc, using isotopes with half-lives down to ≈0.2 s. The interesting chemical behavior of Fl [9] as well as the first data on Mc and its daughter Nh gained more recently at GSI Darmstadt will be discussed. To progress to the next heavier element, livermorium (Lv, element 116), developments towards a faster technique based on electrical field guidance rather than gas-flow extraction to transport the species of interest to the gas chromatography and detection system have started [11]. Preparatory experiments were performed at Texas A&M University and at GSI Darmstadt and show the path forward to chemical studies of yet heavier elements.

References

/1/ O.L. Keller et al., J. Phys. Chem. 74 (1970) 1127; K.S. Pitzer, J. Chem. Phys. 63 (1975) 1032.
/2/ V. Pershina, Radiochim. Acta 107 (2019) 833; L. Trombach et al., PCCP 21 (2019) 18048.
/3/ V. Pershina, A. Türler, Chem. Rev. 113 (2013) 1237.
/4/ A. Türler et al., Nucl. Phys. A 944 (2015) 640.
/5/ R. Eichler et al., Angew. Chem. Int. Ed. 47 (2008) 3262.
/6/ A. Yakushev et al., Front. Chem. 9 (2021) 753738.
/7/ R. Eichler et al., Radiochim. Acta 98 (2010) 133.
/8/ A. Yakushev et al., Inorg. Chem. 53 (2014) 1624; Ch.E. Düllmann et al., Radiochim. Acta 110 (2022) 417.
/9/ A. Yakushev et al., Front. Chem. 10 (2022) 976635.
/10/ Ch.E. Düllmann, Radiochim. Acta 100 (2012) 67.
/11/ J. Even et al., Science 345 (2014) 1491; J. Even et al., J. Radioanal. Nucl. Chem. 303 (2015) 2457.
/12/ D. Wittwer et al., Nucl. Instrum. Meth. B 268 (2010) 28.
/13/ Ch.E. Düllmann et al., Radiochim. Acta 110 (2022) 417.
/14/ L. Lens et al., Radiochim. Acta 106 (2018) 949.
/15/ S. Götz et al., Nucl. Instrum. Meth. B 507 (2021) 27; V. Varentsov et al., *ibid*. A 940 (2019) 206.

Retention Behaviour of Actinides and Long-Lived Fission Products in Na-Montmorillonite and Fe-Montmorillonite

*B.S. Tomar**

Homi Bhabha National Institute, Training School Complex, Anushakjtinagar, Mumbai 400094, India.
*Email: bstomar1957@gmail.com

1. Introduction

Closed nuclear fuel cycle is considered a preferred mode for harnessing fission energy for electricity production, particularly by countries which do not have an abundant inventory of uranium. However, this option comes with challenges, with regard to the disposal of the high-level waste (HLW), generated during the reprocessing of the spent nuclear fuel to recover, Plutonium and leftover Uranium. Though, the HLW is considered a rich source of useful radioisotopes, such as ^{137}Cs, ^{90}Sr, etc., even after their recovery, the waste has enough radioactivity and hence needs to be managed properly so that it does not get into the biosphere. Vitrification of the HLW into suitable glass matrices is being used as one of the methodologies for immobilizing the waste, which, after an interim storage period of a few decades, will be buried in a deep geological repository. The waste form, the overpack, the engineered barrier (e.g., bentonite clay) and the host rock are expected to retain the actinides and long-lived fission products for a period of hundreds of thousands of years. Typical waste forms include the borosilicate glass matrix containing the HLW encased in carbon steel overpacks, which will come in contact with the engineered barrier, namely, backfill materials, such as bentonite clay. Over a long period of time corrosion of carbon steel will result in the release of Fe(II)which may alter the Na-montmorillonite, the main component of the clay. Further, the actinides and long-lived fission products once released by leaching from the waste form may come in contact with groundwater. The complexing anions, both inorganic and organic, present in groundwater may influence the migration of the long-lived radionuclides in the geosphere.

In the present talk, the studies carried out towards understanding the retention behavior of actinides (Am(III)) and long-lived fission products(^{137}Cs and ^{90}Sr) by the montmorillonite-based clays

will be discussed. To begin with, sorption of Eu(III), an analogue of Am(III) by simple model mineral oxide, such as, Alumina in presence of inorganic and organic complexing anions, namely, sulphate, malonic acid and picolinic acid was studied with the view to model the sorption process [1-3]. Subsequently the alteration of Na-montmorillonite to Fe(II)-montmorillonite was studied and the sorption behavior of the above-mentioned radionuclides by these clays was studied [4-6]. Lastly, the diffusion of long-lived radionuclides through these clays was studied using the diffusion out method [7]. These studies will help in the long-term performance of the deep geological repository in retaining actinides and long-lived fission products.

References

/1/ M.A. Patel, A.S. Kar, S. Kumar, et al., Radiochim. Acta 107 (2019) 115-128.

/2/ M.A. Patel, A.S. Kar, V.V. Raut, et al., Environ. Sci. Processes and Impacts 22 (2020) 329-339.

/3/ M.A Patel, A.S. Kar, V.V. Raut, et al., J. Environ. Sci. 100 (2021) 181-192.

/4/ S. Chikkamath, M.A. Patel, A.S. Kar, et al., Radiochim. Acta 109 (2021) 73-83.

/5/ S. Chikkamath, M.A. Patel, A.S. Kar, et al., Aq. Geochem. 27 (2021) 31-47.

/6/ S. Chikkamath, M.A. Patel, A.S. Kar, et al., Radiochim. Acta 107 (2019) 387-396.

/7/ S. Kasar, S. Kumar, R.K. Bajpai, et al., J. Environ. Radioact. 151 (2016) 218-223.

Radiotracers in Agriculture: Deciphering The Regulators of Plant Mineral Nutrition and Source-Sink Dynamics in Crops

*Bhupinder Singh**

Division of Environment Science, Nuclear Research Laboratory building, ICAR-Indian Agricultural Research Institute, New Delhi-110 012, India.
*Email: bhupindersinghiari@yahoo.com

1. Introduction

An outstanding feature of life is the capability of living cells to take up substances from the environment and use them for the synthesis of their own cellular components or as an energy source, radioisotopes can be effectively used for improving the nutrient and water use efficiency of crop plants. Root surface can be considered as a boundary process where the inorganic domain impinges upon the living world. Both stable isotopes and radio-isotopes have been exceptionally useful in the effort to understand the various aspects of ion and water uptake, translocation and utilisation. The advantages of radio-isotopes are that they can be easily traced and measured in minute quantities and the situations *in vivo* are uncomplicated by the presence of large cellular pools of the ions in question [1]. Radioisotopes also have applications in tracing metabolic biosynthetic pathways.

1.1 *Radiotracer application for determining source-to-sink transfer of photoassimilates and nutrient uptake and transport dynamics*

1.1.1 Contribution of stem assimilates towards grain filling: Use of radiotracer ^{14}C, strongly indicated that stem assimilates (^{14}C) are transported to basal grains in preference to middle and apical spikelet grains during the onset of flag leaf senescence in wheat [2]. Besides immense applications of radiotracers in delineating the abiotic stress tolerance mechanism in plants are documented [3].

1.1.2 Assessing the role of old leaves in floral bud emergence in Kinnow: An experiment was conducted to know the role of old fully opened leaves in the emergence of new inflorescence leaves and floral buds by using ^{14}C labelling [4]. The study clearly shows that the pruning of the upper leaves

is not likely to affect fruit productivity since it is the middle leaves and not the basal or the upper leaves that contribute carbon resources majorly to regulate bud development.

1.1.3 $^{14}CO_2$ labelling technique for measuring total root exudation and vascular sap flow: The ^{14}C release by the roots was compared against the ^{14}C transport in the vascular sap [3]. An experimental hypothesis that a higher ^{14}C level in the vascular sap would indicate a higher root release of carbon by the roots into the rhizosphere was verified. The biosynthesis of phytosiderophore as affected by S-nutrition is also delineated [5].

1.1.4 Role of phytosiderophore biosynthesis and release in zinc efficiency: Short-term uptake studies with bread and durum wheat in mono- and mixed-culture, employing ^{65}Zn-DMA, revealed that Zn-acquisition of Zn-inefficient durum wheat is increased when co-cultivated with the Zn-efficient bread wheat. While Zn-efficient and inefficient wheat types did not differ in the uptake of ^{65}Zn-PS (DMA). Differences in PS release among the two wheat types were related to PS synthesis, evidenced by a differential expression of nicotianamine synthase (NAS) and nicotinamide amino transferase (NAAT), the chief enzymes involved in PS biosynthesis [6].

2. Conclusion

Innovative radiological tools like Positron Emission Tomography (PET) where short-lived positron-emitting radiation provides time-dependent data that are critical for developing models of metabolite transport and resource distribution in plants and their microenvironments or the real-time radioisotope imaging for studying nutrient uptake and translocation are now indispensable analysis tools in understanding the biological activity of plants.

References

/1/ B. Singh, ICAR PG textbook “Radioisotopes in soil and plant studies ICAR, New Delhi (2021) ISBN: 9788171642298; pp 319

/2/ B Singh, S Ahuja, P Yadav, J. Radioanal. Nucl. Chem. 321 (2019) 255-262.

/3/ W.B. Naguib, P.R. Divte, A. Chandra, et al., Physiologia Plantarum 173 (2021) 1421-1433.

/4/ A. Attri, M. Thakre, P. Yadav, et al., J. Radioanal. Nucl. Chem. 317 (2018) 1447-1454.

/5/ V. Sharma, A. Anand, B Singh, J. Radioanal. Nucl. Chem. 323 (2020) 291-301.

/6/ R. Khobra, B Singh, J. Plant Nutrition 41 (2018) 679-688.

Medical Radioisotope Production Research at The Reactor Institute Delft, The Netherlands

Robin de Kruijff, Svenja Trapp, Sabarish Ravi, Antonia Denkova*

Reactor Institute Delft, Delft University of Technology, Mekelweg 15, 2629 JB Delft, The Netherlands.
*Email: r.m.dekruijff@tudelft.nl

1. Introduction

In recent years, the world has seen a turnaround in the use of medical radioisotopes for diagnostic, but even more so for therapeutic purposes. While ^{99m}Tc is still the workhorse of nuclear medicine, with about 75% of all procedures relying on this isotope, many other radioisotopes are finding their place in the medical landscape. For instance, ^{68}Ga-based radiopharmaceuticals are increasingly employed as indicators for the efficacy of, amongst others, ^{177}Lu-based radiotherapeutic agents. In the Netherlands alone, two ^{177}Lu-based tumor therapies have already found their way to the clinic; ^{177}Lu-octreatate for the treatment of neuroendocrine tumors, and ^{177}Lu-PSMA for metastasized prostate cancer [1]. As researchers and clinicians are continuing their quest for the development of new radiopharmaceuticals, moving from β^--emitters to the use of α-emitters such as ^{225}Ac and ^{213}Bi, it is up to the radiochemists and radionuclide producers to ensure these essential radioisotopes will be abundantly available. In this talk, I will highlight recent development at the Reactor Institute Delft, the Netherlands, where we work on 1) innovative irradiation facilities, 2) targets materials, and 3) separation methods.

2. Irradiation facility development

At our in-pool irradiation facilities, there are thermal, epithermal and fast neutrons, as well as gamma-rays incident on target materials. We have designed an innovative flexible irradiation facility, the FlexBeFa, to specifically block neutron/gamma energies whilst letting others pass. For instance, the use of lead shielding material at the FlexBeFa has been shown to significantly decrease the gamma flux, while having little impact on the neutron flux. As a direct consequence, we have been able to irradiate holmium microspheres, used for the radioembolization of hepatic malignancies [2], up to three times longer than without the flexible shielding material. This significantly increased the

produced activity and specific activity, allowing for the shipment of the ^{166}Ho-microspheres to hospitals throughout Europe.

3. Novel target materials

^{99}Mo, the mother radioisotope of ^{99m}Tc, is currently produced through the fission of ^{235}U, resulting in long-lived nuclear waste associated with fission-based production. While ^{99}Mo can also be produced through direct activation of stable molybdenum isotopes, this direct production route results in very low specific activity ^{99}Mo. Existing ^{99}Mo/^{99m}Tc generators have too low an adsorption capacity to adsorb the same ^{99}Mo activity produced through any of the direct routes. We have therefore synthesized molybdenum-based nanomaterials, where we focused on high stability and large surface areas. These materials have been designed to function as both target and generator materials to replace current low-capacity aluminium oxide adsorbers, allowing for selective ^{99m}Tc extraction.

4. Radioisotope separation

Given the generally short half-lives and high activities associated with radionuclide production, fast, automatable separation strategies are warranted. To this end, we are working on an alternative to the current lengthy separation strategies. Our primary focus was the separation of ^{68}Ga from liquid zinc nitrate targets, where we developed a two-step solvent extraction process to recover ^{68}Ga in under 15 minutes. Solution compositions ranged from 1 - 5 M $^{nat}Zn(NO_3)_2$ in 0.01 - 1 M HNO_3 and the organic extracting phase consisted of 200 mM BPHA dissolved in chloroform. Using microfluidic solvent extraction using a membrane separator, a ^{68}Ga extraction efficiency of 99.2% ± 0.3% from the target solution was realized. Because all zinc nitrate solutions were used without any modification, this method should allow for direct recycling of the target solutions after the extraction process.

5. Conclusion

Our research at the research reactor in Delft focuses on novel irradiation and extraction strategies for medical radioisotope production. Through this research, we aim to help bring radionuclide production to a level where patients worldwide can benefit from the medical opportunities they offer.

References

/1/ R.P. Baum, H.R. Kulkarni, C. Schuchardt, et al., J. Nucl. Med. 57 (2016) 1006-1013.

/2/ M.A.D Vente, T.C. De Wit, M.A.A.J. Van Den Bosch, et al., Eur. Radiol. 20 (2018) 862-869.

Production of Radioisotopes for Application Studies at RIKEN RI Beam Factory – Search for New Elements through Diagnosis and Therapy of Cancer

*Hiromitsu Haba**

Nishina Center for Accelerator-Based Science, RIKEN, Wako, Saitama 351-0198, Japan.
*Email: haba@riken.jp

At RIKEN RI Beam Factory (RIBF), Wako, Japan, we have been developing production technologies of radioisotopes (RIs) for application studies in the fields of physics, chemistry, biology, engineering, medicine, pharmaceutical and environmental sciences [1,2]. With light- to heavy-ion beams from the AVF cyclotron, we produce more than 100 RIs from ^{7}Be (atomic number Z= 4) to ^{262}Db (Z= 105). In the chemistry of superheavy elements (SHEs), the distribution coefficients of Rf (Z= 104) were determined in hydrochloric acids by observing extraction equilibrium with the automated batch-type solid-liquid extraction apparatus for repetitive experiments of transactinides (AMBER) [3]. Reversed-phase extraction behavior of Rf with 2-thenoyltrifluoroacetone in HF/HNO_3 was investigated using the JAEA automated rapid chemistry apparatus (ARCA) [4]. Recently, co-precipitation of Rf was investigated in basic solutions containing NH_3 or NaOH using a semi-automatic suction filtration apparatus (CHIN) [5]. In nuclear medicine, we often produce ^{211}At in the ^{209}Bi(α,2n)^{211}At reaction for targeted α-particle therapy (TAT) [6-8].

RIs of a large number of elements (multitracer) are simultaneously produced from metallic targets such as ^{nat}Ag and ^{197}Au irradiated with a 135-MeV/nucleon ^{14}N beam from RIKEN Ring Cyclotron [9]. The multitracer is useful to trace the behavior of many elements simultaneously under an identical experimental condition. Recently, ^{225}Ac was produced in the ^{232}Th(^{14}N,$xnyp$)^{225}Ac reaction for TAT [10].

A gas-jet transport system was installed on the RIKEN gas-filled recoil ion separator (GARIS) at the RIKEN linear accelerator (RILAC) as a novel technique for SHE chemistry [11]. ^{261}Rf^{a,b}, ^{262}Db, ^{265}Sg^{a,b} (Z= 106), and ^{266}Bh (Z= 107) were produced in the heavy-ion induced reactions on a ^{248}Cm target and their decay properties were investigated in detail using a rotating wheel apparatus for α and SF spectrometry [12-15]. After the successful chemical synthesis of $Sg(CO)_6$ by the Univ. Mainz and

GSI groups [16], a detailed experiment to investigate the stability of the metal carbon bond in $Sg(CO)_6$ is in progress with a thermal decomposition setup developed by the PSI group [17]. Also, syntheses and properties of Tc, Ru, Rh, and Re carbonyls were studied with the ^{252}Cf fission source at IMP and GARIS for future studies on Bh, Hs (Z = 108), and Mt (Z = 109) carbonyls [18-20]. In 2020, RILAC was upgraded as the superconducting RILAC (SRILAC) with a 28 GHz superconducting ECR ion source and a superconducting quarter-wavelength resonator [21]. A synthesis experiment of element 119 is ongoing in the $^{248}Cm(^{51}V,xn)^{299-x}119$ reaction using a new gas-filled recoil ion separator GARIS III at SRILAC.

References

/1/ H. Haba et al., in Handbook of Nuclear Chemistry (2nd ed.), edited by A. Vértes, S. Nagy, Z. Klencsár, R. G. Lovas, and F. Roesch, Vol. 3, Springer, (2010) 1761-1792.

/2/ RIKEN Accel. Prog. Rep., Sect. Radiochemistry and Nuclear Chemistry in each volume, (https://www.nishina.riken.jp/researcher/APR/index_e.html).

/3/ T. Yokokita et al., Dalton Trans. 45 (2016) 18827.

/4/ A. Yokoyama et al., Radiochim. Acta 107 (2019) 27.

/5/ Y. Kasamatsu et al., Nature Chem. 13 (2021) 226.

/6/ K. Fujiki et al., Chem. Sci. 10 (2019) 1936.

/7/ H. Takashima et al., Cancer Sci. 112 (2021) 1975.

/8/ S. Manabe et al., ACS Omega 6 (2021) 14887.

/9/ H. Haba et al., Radiochim. Acta 93 (2005) 539.

/10/ X. Yin et al., RIKEN Accel. Prog. Rep. 54 (2021) 162.

/11/ H. Haba et al., Chem. Lett. 38 (2009) 426.

/12/ H. Haba et al., Phys. Rev. C 83 (2011) 034602.

/13/ H. Haba et al., Phys. Rev. C 85 (2012) 024611.

/14/ H. Haba et al., Phys. Rev. C 89 024618 (2014).

/15/ H. Haba et al., Phys. Rev. C 102 (2020) 024625.

/16/ J. Even et al., Science 345 (2014) 1491.

/17/ R. Eichler et al., EPJ Web Conf. 131 (2016) 07005.

/18/ Y. Wang et al., Phys. Chem. Chem. Phys. 17 (2015) 13228.

/19/ S. Cao et al., Phys. Chem. Chem. Phys. 18 (2016) 119.

/20/ Y. Wang et al., Phys. Chem. Chem. Phys. 21 (2019) 7147.

/21/ H. Haba, Nature Chem. 11 (2019) 10.

The ISOLPHARM Project at LNL: A New Production Method of High Specific Activity Medical Radionuclides

Stefano Corradetti[1], Alberto Andrighetto[1], Elisa Vettorato[1], Luca Morselli[1], Michele Ballan[1], Alberto Arzenton[1,2], Daniele Scarpa[1], Marianna Tosato[3], Valerio Di Marco[3], Francesca Mastrotto[4], Paolo Caliceti[4], Aldo Zenoni[5,6], Antonietta Donzella[5,6], Silva Bortolussi[6], Marcello Lunardon[7,8], Lisa Zangrando[8], Mattia Asti[9]*

[1]INFN, Laboratori Nazionali di Legnaro, Viale dell'Università, 2, 35020 Legnaro (PD), Italy.
[2]Department of Physical sciences, Earth and environment, University of Siena, Strada Laterina, 8 53100 – Siena, Italy.
[3]Department of Chemical Sciences, University of Padua, Via Marzolo, 1 35131 – Padova, Italy.
[4]Department of Pharmaceutical Sciences, University of Padua, Via Marzolo, 5 35131 – Padova, Italy.
[5]Department of Mechanical and Industrial Engineering, University of Brescia, Via Branze 38, 25123 Brescia, Italy
[6]INFN, Pavia Department, Via Bassi 6, 27100 Pavia, Italy.
[7]Department of Physics and Astronomy, University of Padova, 35131 Padova, Italy.
[8]INFN, Padua Department, Via Marzolo 8, 35131, Padua, Italy.
[9]AUSL – IRCCS Reggio Emilia viale Risorgimento 80, 42122 RE, Italy.
*Email: stefano.corradetti@lnl.infn.it

1. Introduction

Radionuclides of interest in nuclear medicine are generally produced in cyclotrons or nuclear reactors, with associated issues such as highly enriched target costs and undesired contaminants (carrier-added). In this context, the ISOLPHARM project (ISOL technique for RadioPHARMaceuticals) at the SPES (Selective Production of Exotic Species) facility at INFN-LNL (Istituto Nazionale di Fisica Nucleare-Laboratori Nazionali di Legnaro) aims at producing high purity (no-carrier added) radionuclides for nuclear medicine applications (Figure 1). Besides being operated for nuclear physics studies, the facility may play a pivotal role in producing medically relevant radionuclides employing the ISOL (Isotope Separation On-Line) technique. This technique will enable the production of radiopharmaceuticals hardly obtained in standard production facilities. Both traditional and innovative radionuclides from many different regions of the nuclide chart will be produced with high specific activities, going beyond the state of art of radiopharmaceuticals research.

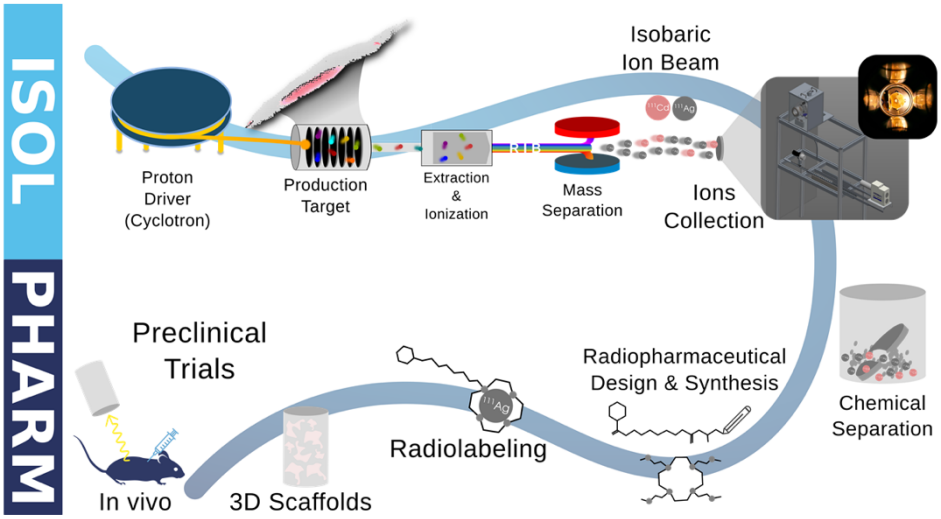

Figure 1: The ISOLPHARM method

2. The ISOLPHARM project

ISOLPHARM is a comprehensive project started at INFN–LNL and developed in collaboration with many University departments, with the aim of applying this technology to produce high-specific activity beta-emitting radionuclides as radiopharmaceutical precursors. As an example, ^{111}Ag, a β-emitter (360 keV with mean tissue penetration of 1 mm) with a medium half-life (7.45 d) and a low percentage of γ-emission, can be produced in carrier-free form only when a costly ^{110}Pd enriched target is used with classical irradiation methods. Alternatively, the ISOL method could be suitable to produce ^{111}Ag with high purity and high production rate. The ISOLPHARM project has three main goals, based on the application of the ISOLPHARM method to the production of ^{111}Ag radionuclides as radiopharmaceuticals precursors: a) Physics: production of ^{111}Ag, spectroscopy studies, laser ionization of Ag [1], b) Radiochemistry: synthesis and characterization of chelators, linkers, targeting agents and purification of isotopes [2], c) Biology: biological characterization on cells, scaffold production and 3D cell cultures, in vitro and in vivo studies [3].

References

/1/ M. Ballan et al., Appl. Radiat. Isot. 164 (2020) 109258.

/2/ M. Tosato et al., Inorg. Chem. 59 (2020) 10907.

/3/ M. Verona et al., Molecules 26 (2021) 918.

Radioactive Molecular Beams – From ISOL Targets to Fundamental Symmetries

*J. Ballof**

FRIB, 640 S Shaw Ln, East Lansing, MI 48824, USA
*Email: ballof@frib.msu.edu

The *in-situ* synthesis of radioactive molecules has proven to be a powerful tool within and beyond the scope of the isotope separation online (ISOL) technique for the production of radioisotope beams [1, 2]. The thick targets exploited by ISOL are both a blessing and a curse. While their areal densities of typically above several g/cm^2 enable high production rates, chemical and physical interactions within the target hamper the extraction of some species. The governing diffusion and effusion processes are temperature-dependent and often require operation at the highest possible temperatures to achieve maximum yield for short-lived isotopes. However, the target material and structural materials of the target and ion source unit limit the approach to use increasingly higher temperatures. Typically, temperatures around 2000 °C mark the limit. In Fig. 1, radioactive ion beam yields measured at ISOLDE are compared to the melting and boiling points of the elements. The latter are correlated via the vapour pressure to the adsorption enthalpy, which limits the effusion time and renders the extraction of some elements impossible. Molecular beams serve to overcome this limitation of the ISOL technique. By providing favourable conditions for the formation of volatile carrier molecules, refractory elements like carbon or boron have been successfully extracted as ISOL beam. The formation of a carrier molecule is often promoted by the injection of reactive gases (like CF_4).

The second application of molecular sidebands is the purification of beams. A wide range of radioisotopes is produced in reactions with energetic light particles with heavy targets in spallation, fission and fragmentation reactions. The isotope of interest is typically selected by mass-over-charge ratio with a dipole magnet. However, in some cases, isobaric impurities are present which can be of overwhelming intensity. The formation of a molecule changes the mass of an isotope as seen by the separation magnet and can shift away from contamination. The strategy is particularly successful if the mass of the molecule exceeds the mass of the target material. Nuclides significantly exceeding the

mass of the target material are not typically produced. The method was, *e.g.*, successfully used for the production of pure and intense alkaline earth fluoride [3] beams.

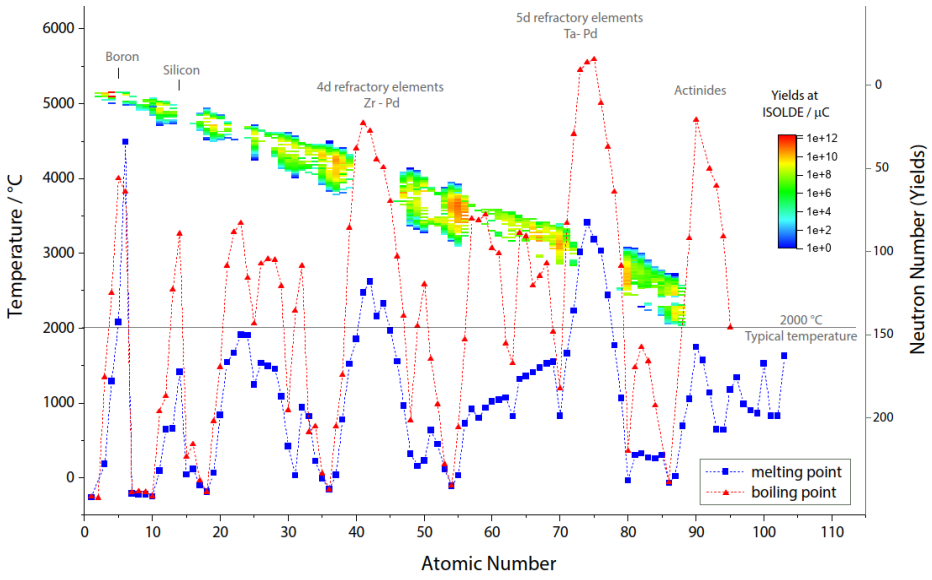

Figure 1: Radioactive ion beam yields at ISOLDE in comparison with the melting and boiling point of the elements

Recently, a strong interest in studying radioactive molecules was emerging. It was proposed that molecules like RaF could be sensitive probes to study Beyond Standard Model physics [2].

In this contribution, available radioactive ion beams along with recent developments will be summarized. As an example of a radioactive ion beam application to study Beyond Standard Model physics, the in-design FRIB-EDM^3 instrument will be presented.

References

/1/ U. Köster et al., Eur. Phys. J. Special Topics 150 (2007) 285

/2/ N.R. Hutzler et al. (2020), 10.48550/ARXIV.2010.08709

/3/ H.L. Ravn, S. Sundell, L. Westgaard, J. Inorg. Nucl. Chem. 37 (1975) 383.

Development of Radiolabeled Antibodies for Radioimmunotherapy: From bench to bed

Tapas Das[1,2]*

[1]Radiopharmaceuticals Division, Bhabha Atomic Research Centre, Mumbai 400085, India.
[2]Homi Bhabha National Institute, Anushaktinagar, Mumbai 400085, India.
*E-mail: tdas@barc.gov.in

'Radioimmunotherapy' (RIT) is a treatment modality in which the affinity of immune proteins towards the tumor-associated specific antigens or antigen receptors is exploited for delivering a therapeutic radionuclide to the target of interest for providing a lethal dose of cytotoxic radiation to the cancerous lesions [1]. As a large number of cancerous cells can be destroyed by targeting a limited number of cancer cells in the tumor mass owing to the cross-fire effect exerted by the particulates generated due to the decay of the associated radionuclide, RIT is expected to be more efficacious compared to 'immunotherapy', which uses unlabeled antibodies for destroying the cancer cells. Additionally, the amount of antibody required for RIT is significantly lower compared to that needed for immunotherapeutic modality, as the role of antibody in the former is just limited to shedding off the radiation load at the target of interest and this reduces the chemotoxic dose burden of the immunotherapy to a significant extent. Therefore, developing suitable RIT agents for targeted radionuclide therapy (RNT) is a subject of much interest and intense research for the last few decades.

Although considerable efforts have been directed to develop radiolabeled antibodies for the treatment of various types of cancers, no RIT agent has reached the clinical domain to date for regular utilization. This is primarily attributable to the use of antibodies of murine origin, short *in-vivo* residence time, generation of human anti-mouse antibody response etc. [2]. Significant progress made in recent time in genetic engineering have helped to overcome the majority of these short-comings and this has regenerated the interest in using various unlabeled as well as radiolabeled antibodies for the treatment of human maladies.

The use of two radiolabeled anti-CD20 antibodies, namely Zevalin® (^{90}Y-labeled) and Bexxar® (^{131}I-labeled) has been approved by US-FDA (Food and Drug Administration of United States of America) for targeted RNT of B-cell lymphomas. At present, a host of other radiolabeled antibodies

are being evaluated for RIT applications and these agents are in different stages of clinical evaluation. Trastuzumab (Herceptin®), a humanized monoclonal antibody, is one such antibody whose use has been approved by US-FDA for the treatment of patients suffering from metastatic breast cancers over-expressing Human Epidermal Growth Factor Receptor 2 (HER2) antigen receptors. Although its use in radiolabeled form is yet to receive approval for human administration, clinical trial involving radiolabeled trastuzumab has been initiated in the recent past [3]. The presentation will comprise the efforts undertaken in the author's laboratory for the formulation of ^{177}Lu-labeled trastuzumab patient dose and its preliminary clinical evaluation in patients suffering from HER2-positive metastatic breast cancer [4].

Acknowledgement: The author gratefully acknowledges all the members of Radiopharmaceuticals Division of Bhabha Atomic Research Centre who are involved in this exciting development and clinical collaborators.

References

/1/ S. M. Larson, J. A. Carrasquillo, N. K. V. Cheung, et al., Nat. Rev. Cancer. 15 (2015) 347-360.

/2/ M. R. Chamarthy, S. C. Williams, R. M. Moadel, et al., Biol. Med. 84 (2011) 391-407.

/3/ P. Bhusari, R. Vatsa, G. Singh, et al., Int. J. Cancer. 15 (2017) 938-947.

/4/ M. Guleria, R. Sharma, J. Amirdhanayagam, et al., RSC Med. Chem. 12 (2021) 263-277.

MXenes: 5th Generation Emerging Graphene-like 2D materials; Recent Progress, Challenges and Outlook

M. M. Uddin[1], M. H. Kabir[1], S. Mandal[2], A. Arifutzzaman[3], M. A. Ali[1], M. M. Hossain[1], M. U. Khandaker[4], D. Jana[5]*

[1]Department of Physics, Chittagong University of Engineering and Technology, Chattogram-4349, Bangladesh.
[2]Vidyasagar College, 39, Sankar Ghosh Lane, Kolkata-700006, India.
[3]Research Centre for Carbon Dioxide Capture and Utilisation (CCDCU), School of Engineering and Technology, Sunway University, Bandar Sunway, 47500 Selangor, Malaysia.
[4]Centre for Applied Physics and Radiation Technologies, School of Engineering and Technology, Sunway University, 47500 Bandar Sunway, Selangor, Malaysia.
[5]Department of Physics, University of Calcutta, 92 A P C Road, Kolkata-700009, India.
*E-mail: mohi@cuet.ac.bd

1. Introduction

MXenes are a new family of 2D early transition metal carbides, carbonitrides and nitrides that were discovered in 2010 and emerged in the world of 2D materials beyond graphene [1,2]. MXenes can be used in many applications such as lithium-ion and sodium-ion energy storage systems, electromagnetic interference (EMI), water purification, printable 5G and many more. The archetypical MXenes with high metallic conductivity, hydrophilicity and high negative surface charge that allows dispersion in water, forming stable colloidal solutions of single-layer flakes that combine the best properties of GO and reduced graphene oxide (rGO) and take those to an extreme (5-10 times higher conductivity compared to rGO films). Therefore, researchers are interested to explore useful properties that enable applications of MXenes and hype (yesterday- nanotubes, today - graphene, or tomorrow – MXene). In this talk, the prospects, challenges and outlook of the MXenes research have been discussed.

2. Experiment

More than 70 structures of MXenes have already been reported, besides numerous solid solutions and ordered double transition metal structures. MXenes were taken birth with an unintentional event, researchers are intended to create more space for electrochemical Li intercalation/de-intercalation for the Li-ion battery anodes, by selectively etching A layer from MAX phase precursor using HF at room

temperature, besides observing the fascinating properties of energy storage capacity they discovered first MXene material Ti_3C_2 with a large family of 2D materials.

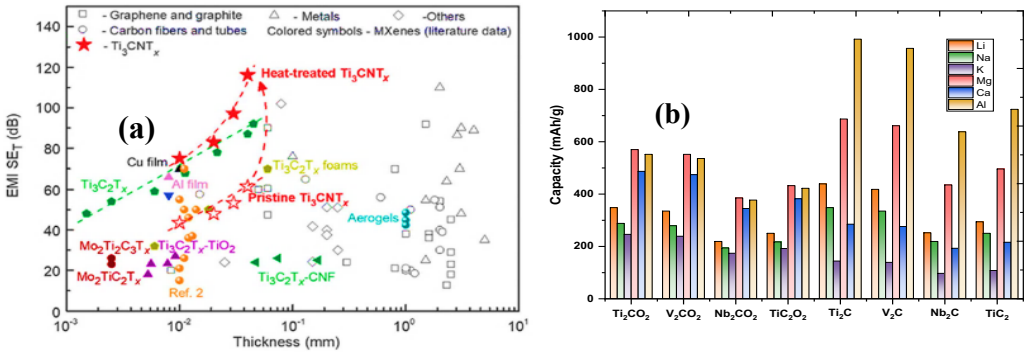

Fig 1: (a) Radiation efficiency comparison of $Ti_3C_2T_x$ with other materials (b) Storage capacity comparison of different MXene materials

3. Results and Discussion

***3.1 Radiation shielding and antenna applications*:** High metallic conductivity and radiation efficiency make the MXenes more useful in electromagnetic interference (EMI) shielding. The EMI shielding has been performed in various MXenes that are strongly dependent on their structure and compositions. The thickness dependence of EMI shielding of different MXenes and conventional materials is illustrated in Figure 1(a). It is seen that 1 -2 μm thick $Ti_3C_2T_x$ exhibits EMI shielding efficacy ~ 50 dB (99.999% protection) and 92 dB at 45 μm thickness.

***3.2 Energy Storage applications of MXenes*:** Storage capacities of different ion batteries of oxygen-terminated and bare MXenes are presented in Figure 1(b). Bare MXenes provide better performance because of their reduced weight, and oxygen-terminated MXenes can decompose into bare MXene. Moreover, an additional metal layer results in almost double its capacity for different ions.

4. Conclusion

The evolving applications of MXenes in the area of electronics, optoelectronics, spintronics devices, sensors, high-performance and transparent electrodes, and nanocomposites have been discussed.

Acknowledgement: CUET/DRE/2020-2021/PHY/009 and S. K. Mandal thanks CSIR, GOI for the fellowship.

References

/1/ B. Anasori, M.R. Lukatskaya, Y. Gogotsi, Nat. Rev. Mat. 2 (2017).

/2/ M. Naguib, M. Kurtoglu, V. Presser, et al, Adv. Mat. 23 (2011).

Radiation Dosimetry with Carbon Based Media for Medical and Industrial Applications

Mayeen Uddin Khandaker[1, 2], Siti Nurasiah Mat Nawi[3], S.F. Abdul Sani[4], S.E. Lam[1], D.A. Bradley[1, 5]*

[1]Centre for Applied Physics and Radiation Technologies, School of Engineering and Technology, 47500, Bandar Sunway, Selangor, Malaysia.
[2]Department of General Educational Development, Faculty of Science and Information Technology, Daffodil International University, DIURd, Dhaka 1341, Bangladesh.
[3]Department of Medical Sciences, School of Medical and Life Science, 47500, Bandar Sunway, Selangor, Malaysia.
[4]Department of Physics, Faculty of Science, University of Malaya, 50603, Kuala Lumpur, Malaysia.
[5]Department of Physics, University of Surrey, Guildford, GU2 7XH, UK
*Email: mu_khandaker@yahoo.com

Effective clinical uses of ionising radiation (IR) have involved dosimetric procedures. Thermoluminescence (TL) dosimetry show useful in a variety of fields, such as clinical research, individual dosimetry, and environmental dosimetry, amongst others. However, it is well documented that ionizing radiation has various effects on human health, typically regarding deterministic and stochastic biological risks associated with DNA alterations, genetic mutation, etc. It means that the risk of ionizing radiation can overweigh the benefits if it has not been used in a controlled manner. Thus said, to protect society from the potentially harmful effect of radiation, it is critical to measure the radiation dose received by patients as well as radiation workers. Therefore, a dosimeter is a device that plays an important role in the undertaking of radiation protection monitoring and quality control of radiation therapy treatment. Over the past few decades, in the quantification of absorbed dose and also in QA programs, several dosimeters such as semiconductor diodes, radiographic and radiochromic films, thermoluminescence dosimeters (TLDs) and metal–oxide field effect transistors have been utilized. Note that each type of dosimeter has its inherent limitations including poor spatial resolution, non-tissue equivalence, and the requirement of high bias voltage to achieve an acceptable collection of charges, especially for ionization chambers. Therefore, there is a need to develop new technologies that offer low-cost and high spatial resolution dose monitoring systems throughout the treatment process to improve the accuracy of the treatment delivery.

Worldwide, there is ongoing intensive research into the adaptation of graphite for a wide variety of applications. The present study has explored the potential of highly uniform 2B and HB grade polymer pencil lead graphite (PPLG) for safe clinical radiation applications. Herein, the TL dosimetric properties of PPLG samples irradiated by X-ray, gamma-ray, electron and neutron have been investigated. The investigation has been made of key dosimetric properties such as glow curve, dose-response, sensitivity, reproducibility, energy dependence, sensitivity and fading. Following optical characterisation, the structural alterations of PPLG dosimeters are observed via state-of-the-art techniques, including Raman, Photoluminescence and X-ray diffraction spectroscopy in order to understand the nature and distribution of defects in its crystal lattice structures that produce the luminescence signal. All of the samples were found to have a good linear response over the whole dosage range that was investigated, with 2B grade PPLGs demonstrating a higher level of sensitivity than both HB grade and graphite sheet samples. Additionally, the level of sensitivity shown by each of them is highest at the lowest dosage that was given, and it decreases as the dose that was delivered rises. The excellent TL properties of a 2B grade pencil demonstrate its usefulness as a passive radiation dosimeter. As a consequence, the findings suggest that graphite-rich materials have the potential to be useful as a low-cost passive radiation dosimeters, with applications in radiotherapy and manufacturing.

The LARAMED Project at INFN-LNL: Direct Production of Medical Radionuclides with The SPES Cyclotron

Gaia Pupillo[1], Alessandra Boschi[2], Sara Cisternino[1,3], Lucia De Dominicis[1,3], Petra Martini[2], Liliana Mou[1], Gabriele Sciacca[1], Juan Esposito[1]*

[1]Istituto Nazionale di Fisica Nucleare, Laboratori Nazionali di Legnaro (INFN-LNL), Legnaro (Padova), Italy.
[2]University of Ferrara and INFN-FE, Ferrara, Italy.
[3]University of Padova, Padova, Italy.
* Email: gaia.pupillo@lnl.infn.it

1. Introduction: The LARAMED facility at the INFN-LNL

The LARAMED project, an acronym for LAboratory of RAdioisotopes for MEDicine [1, 2] is funded by the Italian Ministry of University and Research (year 2014 and 2016) at the INFN-LNL, in the framework of SPES (Selective Production of Exotic Species). The heart of SPES is the 70 MeV proton-cyclotron, capable of providing intense beams (up to 700 μA) also in the dual-extraction configuration. LARAMED has been conceived, since the beginning, to meet a double scope. The first one was to develop a more efficient production for well-established radionuclides already playing a key role in nuclear medicine (e.g. ^{99m}Tc), while the other was to investigate unexplored production routes for novel radionuclides having potential interest in medicine, but still unavailable. As emerging infrastructure, the LARAMED and ISOLPHARM projects at the INFN-LNL are included in the PRISMAP consortium as emerging infrastructures for the production of medical radionuclides, exploiting the direct activation method and the ISOL technique, respectively.

The LARAMED facility is currently under completion and it includes the RI#3 and A9c bunkers, used in the next years to perform research activities on medical radionuclides and nuclear cross-section measurements; no.2 additional bunkers, RI#1 and RI#2, devoted in further years to produce massive amounts of radioisotopes, in collaboration with a private partner, to supply hospitals and clinical departments, for both routine and clinical research purposes; the RILAB Radiochemistry laboratory, covering all the radiochemical processing aspects and designed to carry out R&D activities on radioisotope production, separation/purification, up to perform all the requested quality control procedures; and the RILAB Target-preparation laboratory, where all the new/alternative cold-

chemistry technologies devoted to target manufacturing are implemented by the LARAMED research group. This work will outline the status of the LARAMED facility.

2. The LARAMED research activities

Thanks to a wide national and international network of collaborations, the LARAMED research activities started 10 years ago with the following projects:

- APOTEMA and TECHN-OSP (2012-2017), dedicated to the direct ^{99m}Tc production using isotopically enriched ^{100}Mo targets at medical cyclotrons;
- COME (2016), dedicated to the first measurements of the ^{70}Zn(p,x)^{67,64}Cu nuclear reactions above 35 MeV and the ground of the INFN patent on ^{67}Cu multi-layers target;
- PASTA (2017-2018), dedicated to the nuclear cross-section measurements for ^{47}Sc production;
- E_PLATE (2018-2019), dedicated to thin target manufacturing exploiting the High-Intensity Vibrational Powder Plating (HIVIPP) technique;
- METRICS (2018-2021), dedicated to $^{51/52}$Mn accelerator-based production and to the development of innovative radiopharmaceuticals for PET/MRI dual-imaging purposes;
- INTEFF_TOTEM (2021-2022), dedicated to the further development of the INFN patents on targetry for the production of medical radionuclides;
- REMIX (2021-2023), dedicated to the measurements of the ^{49,50}Ti(p,x)^{47}Sc nuclear reactions (exploiting the thin targets developed with the HIVIPP technique) and Tb-radionuclides production (^{149}Tb, ^{152}Tb, ^{155}Tb and ^{161}Tb);
- STarDiS (2023), dedicated to the development of a solid target dissolution system integrable on automatic commercial modules for radiopharmaceutical synthesis;
- CUPRUM-TTD (2023-2025), dedicated to the Target Technology Development for the massive production of $^{67/64/61}$Cu radionuclides.

This work will present some results obtained by the LARAMED team in these years with a focus on the most recent outcomes and future perspectives.

References

/1/ J Esposito et al., Molecules 24 (2019) 20.

/2/ G Pupillo et al., AIP Conference Proceedings 2295 (2020) 020001 DOI 10.1063/5.0032898.

Measurement of Beta Decay Feeding Intensity: The Case Of ^{126}Sb

*Gopal Mukherjee**

Variable Energy Cyclotron Centre, 1/AF Bidhannagar, Kolkata 700064, INDIA
*Email: gopal@vecc.gov.in

The odd-odd, neutron-rich isotope of ^{126}Sb (Z = 51) is an important nucleus from the reactor decay-heat point of view as well as an interesting one in the field of nuclear structure research. The calculations show that it has a reasonably large yield in U^{233}, U^{235} and Pu^{239} fissions [1]. Therefore, it is one of the key nuclei for which detailed information on the decay is important for decay heat calculations for both PHWR (or BWR) and FBR. In order to assess the decay heat, accurate data on the beta feeding intensities are necessary. However, the spin and parities (J^{π}) of many of the states populated in ^{126}Te from the β^- decay of ^{126}Sb are not firmly assigned [2]. One of the methods to determine the β-feeding intensity is via high-resolution γ-ray spectroscopy. In this method, the β-feeding intensity of a level is determined from the difference in feeding and decay intensities of the γ-ray transitions. Hence, if the J^{π} of a level is uncertain, the β-feeding intensities will also be tentative as multipolarities and type (Eλ/Mλ) of the γ rays from and to the corresponding levels (necessary to calculate the internal conversion coefficient) could not be estimated properly. It is also worth noting that the long-lived ($T_{1/2}$ = 2.3 x 10^5 a) ^{126}Sn decays to ^{126}Sb and the decay scheme of that is also not well known. Recently, the decay scheme of the tin/antimony-126 ensemble has been studied [3]. In this work, the absolute photon emission intensities in the decay of ^{126}Sn were measured with improved accuracy. The isomeric branching ratio of ^{126}Sb^m was deduced to be 18.6 (6)%. However, the primary information on the decay of the ground and isomeric states of 126Sb is still from the earlier work done in the 1970s [4].

Therefore, it is important to study the decay of ^{126}Sb, particularly from its ground state ($T_{1/2}$ = 12.35 (6) d). In the last few decades, tremendous improvement has happened in gamma detection systems. Many efficient and precise measurements are now possible with the arrays having modern day state of the art detectors like clover HPGe detectors.

At VECC, we have planned to study the decay of 126Sb from the measurement of the gamma rays using clover detectors. To make a cleaner measurement, ^{124}Sn(^{4}He, pn)^{126}Sb fusion evaporation reaction will be used to populate ^{126}Sb. In addition, the CeBr3 scintillator detectors will be used to measure the lifetimes of the states. The use of coincidence measurement will enable us to use the angular correlation method to determine the spin parity of the states.

The beta-feeding intensities are also measured by the Total Absorption Gamma Spectroscopy (TAGS) technique as well, which is free from the pandemonium effect. A modular TAGS setup with BaF2 scintillator detectors has been successfully tested and used in beta decay studies.

The use of different techniques in the beta-decay studies will be presented in the context of the beta-decay measurement of ^{126}Sb.

References

/1/ S. Mukerji, Private communication.

/2/ H. Iimura, J. Katakura, S. Ohya, Nucl. Data Sheets 180 (2022) 1
and https://www.nndc.bnl.gov/ensdf/EnsdfDispatcherServlet.

/3/ L. Ferreux, M.-C. Lepy, M.-M. Be, et al., Appl. Radiat. Isot. 68 (2010) 1571.

/4/ Chr. Bargholtz et al., Z. Phys. A 272 (1975) 3.

Industrial Applications of Radiotracer Technology at the International Atomic Energy Agency: Status and Prospects

*Hannah Asamoah Affum**

Radioisotopes Production and Radiation Technology Section, Division of Physical and Chemical Sciences, Department of Nuclear Sciences and Application, International Atomic Energy Agency, Vienna, Austria
*Email: H.Affum@iaea.org

Consistent with its statutory mandate "to accelerate and enlarge the contribution of atomic energy to peace, health and prosperity throughout the world", the International Atomic Energy Agency (IAEA) continues to pursue and lead advances in nuclear science and technology for the development of member states. To this end, the Agency continues to assist Member States with capacity-building, research and development in the nuclear sciences and supports them in using nuclear methods for a variety of practical industrial applications.

One such method is the Radiotracer technology which plays an important role in the industry as it is used for the investigation of industrial unit processes and troubleshooting with optimisation in mind. Though the technology is applicable across a broad industrial spectrum, the petroleum and petrochemical industries, mineral processing and wastewater treatment sectors are identified as the most appropriate target beneficiaries of radiotracer applications.

Due to the technically complex and continuous nature of processes in chemical and petrochemical plants, radiotracer techniques are very competitive and largely applied for troubleshooting inspection and process analysis as they provide more comprehensive information than conventional techniques. The Agency supports needs-based development efforts through coordinated research projects and provides assistance for scientific and technical aspects of IAEA technical cooperation projects. This presentation will discuss some key principles undergirding the radioactive tracer technology, share some member states' success stories, outline the Agency's programmes and activities related to radiotracer technology in the industry among member states and highlight ongoing and future coordinated research projects as well as training and certification

courses for practitioners of the technology. Ongoing and planned activities for the International Standardisation of the technology which is crucial to improve the confidence of practitioners will be outlined. The role of partnerships, through the IAEA Collaborating Centres, in the accomplishment of this area of nuclear application will be underscored.

Radionuclides For Theranostic Applications

Flavia Groppi, Simone Manenti, Michele Colucci*

L.A.S.A., Radiochemistry Laboratory, Università degli Studi di Milano, UNIMI and Istituto Nazionale di Fisica Nucleare, INFN, Via F.lli Cervi 201, I-20090 Segrate, MI, Italy.
*Email: flavia.groppi@mi.infn.it

1. Introduction

The use of High Specific Activity Radionuclides HSARNs, obtained by either proton, deuteron or alpha cyclotron irradiation, followed by selective radiochemical separation from the irradiated target in *No Carrier Added* (*NCA*) form, is a powerful analytical tool for plenty of applications in pure and applied sciences and technologies. The main applications of these RNs are in medical radio-diagnostics and metabolic radiotherapy in addition to toxicological, environmental and industrial studies. Nowadays the new challenge in Nuclear Medicine is the so-called theranostic medicine, a relatively novel paradigm that involves specific individual 'dual-purpose' radionuclides or radionuclide pairs with emissions that are suitable for both imaging, therapy and monitoring the response to therapy. The theranostic radionuclides would potentially bring us closer to the age-long dream of personalized medicine [1]. Different radionuclides with the suitable characteristics to be used as theranostics can be produced by bombardment of targets by charged particle beams in No Carrier Added form with very high A_S, with irradiations made with deuteron beams that present some more advantages. Recently there is an increasing interest in the terbium family, due to the four medically relevant radioisotopes ^{149}Tb, ^{152}Tb, ^{155}Tb and ^{161}Tb, which could be employed either in diagnostic or therapy. We present our results of the cross-section determination of nuclear reactions induced by deuterons on ^{nat}Dy targets.

2. Experiment

At the Radiochemistry Laboratory of LASA, a wide range of high specific activity accelerator-produced radionuclides have been produced since the 70-ties in *NCA* form. Presently, nuclear activations are carried out at the cyclotron IBA K=70 of ARRONAX Center in Nantes France, which can deliver proton and alpha beams, with variable energy up to 70 MeV and deuteron beams of energy up to 35 MeV. The gamma and X-ray spectra are measured at Physics Measurements Laboratory in

LASA with several 15 % efficient, 2.3 keV (FWHM) resolution, coaxial 50 cm^3 active volume HPGe detectors relative to 3"x3" NaI(Tl) and a Compton to peak ratio of 30:1 at the 1332 keV photo-peak of ^{60}Co connected to Ortec mod. 918 and 919A MCAs. All detectors are calibrated with reference sources and standard geometries with overall uncertainties of no more than 3 % at 1 σ. To avoid corrections for the different geometry configurations, all samples are measured in the same geometrical assembly as the calibration sources. The quality control tests are carried out for both chemical and radiochemical purities, using electrothermal atomic absorption spectrometry, instrumental neutron activation analysis in conjunction with a liquid scintillation counter and HPGe spectrometry.

3. Results and Discussion

The production of ^{149}Tb, ^{152}Tb, ^{155}Tb and ^{161}Tb by deuteron beams irradiation with particular attention to the ^{155}Tb and ^{161}Tb production with the long-lived interferences has been investigated [2] in the energy range of 12.5 – 32 MeV and the coproduction of terbium and dysprosium contaminants ($^{156,160}Tb$ and $^{155,157,159}Dy$). The experimental cross-sections for the different reactions were determined with the well-known staked foil technique and compared with only one set of data present in the literature [3], showing a generally good agreement. The curves of theoretical calculations with EMPIRE-II, EMPIRE-3.2.2 and TALYS 1.96 run with default options and fail to predict the experimental data in most cases. Also, the Thick Target Yields, obtained as the integration of the thin target yields, and the radionuclidic Purity are calculated for ^{155}Tb and ^{161}Tb radionuclides and compared with protons irradiation production as well. For ^{161}Tb the results obtained with deuterons are better, reaching a RNP at the highest energy and energy loss of about 70 %. For ^{155}Tb better results are obtained for proton irradiation, suggesting to try to can have a larger energy interval for deuterons irradiations or to study the indirect production via the decay of ^{155}Dy in a ^{155}Dy-^{155}Tb generator but taking into account the unavoidable presence of ^{157}Dy with a TTY higher than ^{155}Dy.

Acknowledgement: Thanks to INFN financial support (Gr V—Interdisciplinary Commission—REMIX experiment) and to all the staff of the ARRONAX Cyclotron.

References

/1/ S.C. Srivastava. Semin. Nucl. Med. 42 (2012) 151.

/2/ M. Colucci, S. Carminati, F. Haddad, et al., Eur. Phys. J. Plus 137 (2022) 1.

/3/ F. Tarkanyi, F. Ditroi, S. Takacs, et al., Appl. Radiat. Isot. 83 (2014) 18.

Chemistry of The Elements at The End of The Actinide Series Using Their Low-energy Ion-beams

*Tetsuya K. Sato[1,2]**

[1]Advanced Science Research Center, Japan Atomic Energy Agency, Tokai, Ibaraki 319-1195, Japan.
[2]Graduate School of Sci. and Eng., Ibaraki Univ., Mito, Ibaraki 310-8512, Japan.
*Email: sato.tetsuya@jaea.go.jp; tetsuya.sato.she@vc.ibaraki.ac.jp

Studies of the chemical properties of the elements at the uppermost end of the Periodic Table are extremely challenging experimentally and theoretically. One of the most important and exciting subjects is to clarify the basic chemical properties of these elements as well as to elucidate the influence of relativistic effects on their electronic configuration. Isotopes of these elements produced at accelerators, however, are short-lived, and the number of produced atoms is so small; any chemistry to be performed must be done on one atom-at-a-time basis that imposes stringent limits on experimental procedures.

At Japan Atomic Energy Agency (JAEA), we investigated the atomic properties of heavy actinide whose atomic number is greater than 100 using the ISOL (Isotope Separator On-Line) technique. We have successfully produced low-energy ion-beams of the elements at the end of the actinide series, fermium (Fm, atomic number Z = 100), mendelevium (Md, Z = 101), nobelium (No, Z = 102), and lawrencium (Lr, Z = 103), using a surface ion-source installed in the ISOL at the Tandem accelerator facility of JAEA and applied to measurements of the first ionization potentials (IP_1) of these elements [1,2]. The experimental setup is

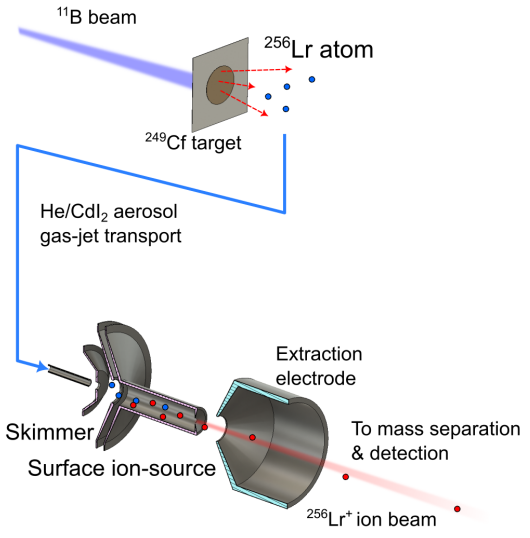

Fig. 1 experimetal setup for ion-beam production of heavy

shown in Figure 1. The nuclear reaction products transported to the ion source can be surface ionized and mass-separated to produce low-energy ion beams. The IP_1 values were evaluated based on the relationship between IP_1 and the ionization efficiency of the surface ionization process.

The successful measurement of the IP_1 values of the actinides motivated us to apply this technique to investigate the chemical properties of the heaviest actinide, the volatility of elemental Lr, and to improve the production of various ion-beam by employing a new ion source.

The surface ion-source application range is limited to elements whose IP_1 value is lower than about 7 eV, so its main ionization target elements of groups 1, 2, and 3. To produce more various elements, we have been developing a new ion-source, EBGP (Electron Beam Generated Plasma) ion-source [3], coupled to the He/CdI_2 gas-jet transport system (Figure 2). The ion source has a cylindrical shape perforated anode electrode. The anode is covered with a cathode electrode surrounded by two filaments. Thermal electrons produced on the inside surface of the cathode are accelerated by a potential difference between the anode and the cathode, 100 ~ 200 V, and introduced into the anode via its holes to ionize nuclear reaction products transported by the aerosol gas-jet transport system by electron bombardment. By using the EBGP technique, the production of ion-beam of elements with higher IP_1 can be expected.

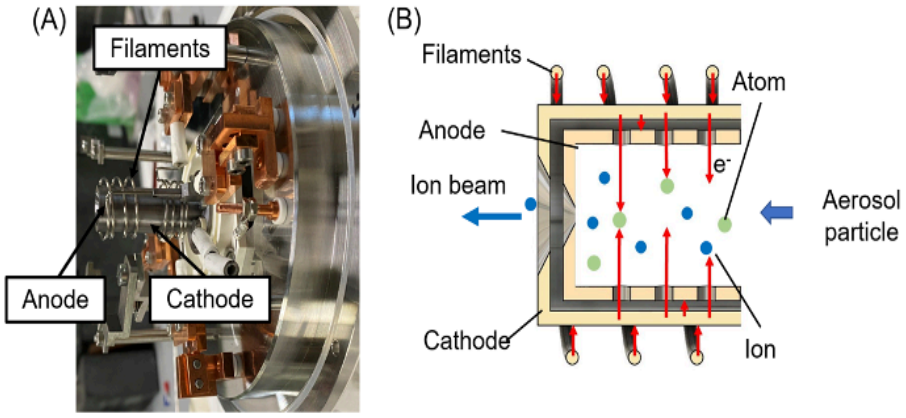

Fig. 2 EBGP (Electron Beam Generated Plasma) ion-source coupled to the gas-jet transport system. (A) Photo of the EBGP ion-source, (B) Schematic cross section of the ion-source.

At the presentation, the current status of superheavy element chemistry at JAEA based on the ISOL will be presented.

References

/1/ T. K. Sato et al. Nature 520 (2015) 209-211.

/2/ T. K. Sato et al., J. Ame. Chem. Soc. 140 (2018) 14609-14613.

In-source Laser Resonance Ionization For Efficient And Selective Radioactive Ion Beam Production And Nuclear Structure Investigations At CERN-ISOLDE

Reinhard Heinke for the ISOLDE-RILIS collaboration*

CERN SY-STI-LP, Esplanade des Particules 1, 1211 Meyrin, Switzerland.
*Email: reinhard.heinke@cern.ch

1. Introduction: Radioactive ion beam production using laser ionization

The Resonance Ionization Laser Ion Source RILIS [1], employing laser radiation in a hot cavity ion source directly coupled to the isotope production target, has become a principal method for the production of radioactive ion beams worldwide, such as at CERN-ISOLDE [2] or -MEDICIS [3]. The inherent chemical selectivity of the technique, using stepwise resonant excitation and subsequent detachment of an electron by laser radiation tuned to element-unique atomic shell transitions, allows for highly efficient enhancement of abundance of the desired isotope in the mass-separated ion beam.

Purity may be influenced by isobaric contamination stemming from different mechanisms - mainly surface ionization in the hot cavity heated to around 2000 °C needed for atomization and volatilization of the required species. Specifically tailored ion source designs tackle this by spatially separating the hot cavity from a cold and clean laser interaction volume in an RFQ structure directly downstream. These types of sources, namely ISOLDE's LIST [4] or TRIUMF's IG-LIS [5], achieve contamination suppression by several orders of magnitude, yet at a cost of 20 to 50-fold reduced efficiency.

2. Nuclear structure studies and isomer-pure beams – New prospects with PI-LIST

Besides its application as part of the production infrastructure, RILIS is proven to be a highly sensitive tool itself for laser spectroscopy nuclear structure investigations on isotopes with low production and extraction yields [6]. While the efficiency of this technique is unrivalled, the spectral resolution is ultimately limited to the range of 1 – 10 GHz by thermal Doppler broadening. Precise measurements of

nuclear parameters often require resolving hyperfine structure splitting well below the GHz regime. Additionally, such resolution capabilities can be employed to selectively ionize single isomeric states of nuclei for pure ion beam delivery.

We present an adaption of ISOLDE's LIST ion source to achieve experimental linewidths of 100 – 200 MHz, an order of magnitude below usual limitations. Fig. 1 shows the layout, targeting only transversal velocity components of the atom beam effusing from the hot cavity via perpendicular laser irradiation in the LIST corpus [7], thus greatly reducing the remaining Doppler broadening. Following development work at Mainz University, where this method is now a standard tool for nuclear structure studies [8], the Perpendicularly Irradiated LIST (PI-LIST) was employed at ISOLDE in 2022 for the first time. Results of an experimental campaign on neutron-rich actinium isotopes to pin down the borders of assumed octupole deformation in this part of the nuclear chart as predicted by recent Energy Density Functional theories [9] are presented, and future developments and prospects are discussed.

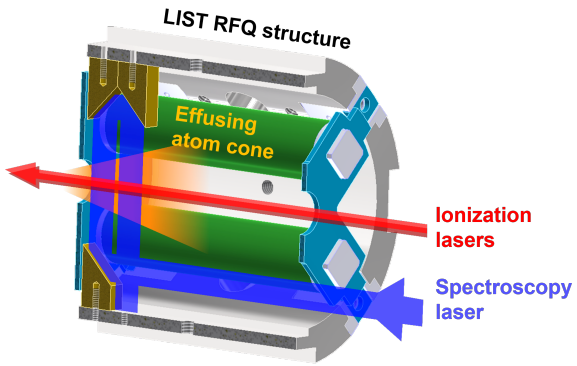

Figure 1: The Perpendicularly Illuminated Laser Ion Source and Trap PI-LIST. A narrow-bandwidth spectroscopy laser is introduced in cross geometry to only address lateral velocity components, thus greatly reducing the Doppler broadening as the limit for experimental resolution

References

/1/ V. Fedosseev, et al., J. Phys. G: Nucl. Part. Phys. 44 (2017) 084006.

/2/ R. Catherall, et al., J. Phys. G: Nucl. Part. Phys. 44 (2017) 094002.

/3/ C. Duchemin, et al., Front. Med. 8 (2021) 693682.

/4/ D.A. Fink, et al., Nucl. Instrum. Methods Phys. Res. A, 344 (2015) 83-95.

/5/ S. Raeder, et al., Rev. Sci. Instrum. 85 (2014) 033309.

/6/ B.A. Marsh, et al., Nature Phys. 14 (2018) 1163-1167.

/7/ R. Heinke, et al., Hyperfine Interact. 238 (2016).

/8/ D. Studer, et al., Eur. Phys. J. A. 56 (2020).

/9/ E. Verstraelen, et al., Phys. Rev. C 100 (2019) 044321.

Laser Spectroscopy of Fm and No Isotopes at GSI

Michael Block[1,2,3]*

[1]GSI Helmholtzzentrum für Schwerionenforschung, Planckstrasse 1, 64291 Darmsta. dt Germany.
[2]Helmholtz Institute Mainz, Staudingerweg 18, 55128 Mainz, Germany.
[3]Johannes Gutenberg-Universität, Department Chemie – Standort TRIGA, Fritz-Strassmann-Weg 1, 55128 Mainz, Germany.
*E mail: m.block@gsi.de

The atomic structure of actinide and transactinide elements is influenced by relativistic effects leading to changes their atomic and chemical properties compared to lighter homologs. Laser spectroscopy with its high spectral resolution provides experimental access to determine several properties such as level energies, lifetimes of excited states, and the ionization potential [1]. Precise measurements allow us to validate and improve theoretical calculations that are challenging due to electron correlations and quantum electrodynamics in a non-perturbative regime.

In addition, there is a strong interest in determining nuclear properties of the heaviest elements that owe their existence to their nuclear shell structure [2]. In the heavy actinides around Z= 100, N= 152 that are well deformed sizeable shell gaps appear providing extra stability to nuclei in this region. The shell gap is reflected in binding energies and can be experimentally obtained from mass measurements [3] and nuclear spectroscopy. Data on the shape and size of these heavy nuclei are more difficult to obtain, and often nuclear-model dependent. Hyperfine laser spectroscopy reveals gives access to the nuclear quadrupole moment, and by measuring the isotope shift of atomic transitions one can obtain information on the changes in the mean-square charge radii [1].

While such information has become available for many radionuclides in recent years, the elements above proton number Z= 100 were inaccessible due to low production rates and often short half-lives. For the actinide elements up to fermium (Z= 100), long-lived isotopes can be bred in Femto- to picogram quantities that are sufficient for offline studies. This had been demonstrated in the group of Backe et al. in 2003 when seven atomic levels in Fm were observed in challenging experiments [4]. They utilized resonance ionization mass spectrometry in a gas cell to study the long-lived isotope ^{255}Fm that was available in femtogram quantities for offline studies at the University of Mainz.

Based on the work by Backe et al. pioneering online experiments were performed at the GSI in Darmstadt, Germany utilizing the RADRIS method. These resulted in the first-ever laser spectroscopy of nobelium isotopes [5-7] demonstrating that laser experiments are feasible under these difficult conditions. Recently, laser spectroscopy measurements have been extended to a chain of eight Fm isotopes on either side of the N= 152 shell gap. To this end, online experiments at the GSI with RADRIS were combined with offline measurements at the RISKO mass separator at Mainz University. Using resonance ionization laser spectroscopy, the Fm isotopes ^{245,246,248,249,250,254,255,257}Fm have been investigated. The measurement scheme had to be optimized for each case based on the half-life and the production scheme using different customized detector setups.

In my contribution, I will briefly introduce the employed methods and present the latest experimental results obtained within the FAIR phase-0 campaign at the GSI in Darmstadt, Germany.

References

/1/ M. Block, et al., Prog. Nucl. Phys. 116 (2021) 103834.

/2/ S.A. Giuliani, et al., Rev. Mod. Phys. 91 (2019) 011001.

/3/ S.A. Sewtz, et al., Phys. Rev Lett. 90 (2003) 163002.

/4/ M. Block, Nucl. Phys. A 944 (2015) 471.

/5/ M. Laatiaoui, et al., Nature. 583 (2016) 495.

/6/ S. Raeder, et al., Phys. Rev. Lett. 120 (2018) 232503.

/7/ P. Chhetri, et al., Phys. Rev. Lett. 120 (2018) 263003.

Radiations And Their Applications: Making Our Lives Better, Safer and Healthier – A Glimpse

*Meera Venkatesh**

Former Director, Division of Physical and Chemical Sciences, International Atomic Energy Agency, Vienna; Former Head, Radiopharmaceuticals Division, Bhabha Atomic Research Centre and Former Senior General Manager, Board of Radiation and Isotope Technology, Department of Atomic Energy, India.
*E mail: prof.mvenkatesh@gmail.com

1. Introduction

Although the word 'Radiation" is often seen with a negative connotation, "Radiations" are wonderful tool yielding enormous benefits to humans in diverse sectors. It is gratifying to understand and use the huge potential of radiation. Radiations are bundles of energy – be it from the Sun or from a radioactive nucleus or produced in machines. This talk will primarily focus on nuclear radiation. The pioneering works during the past century by several Nobel Laureate scientists opened the floodgate for the production of artificial radionuclides and paved the way for the use of radioisotopes/radiation. Easy detectability of radiation enables the use of radioisotopes as tracers in many fields. Deposition of the energy when radiation passes can be used to produce novel materials; or its deleterious effect on living cells can be used in the treatment of cancers, radiation sterilization, food irradiation, and sanitization of effluents. Attenuation of radiation on passage through matter can provide useful information about the material it travels through and could aid in the examination of material in a non-destructive manner.

2. Applications of Radiations

Radiations have made a great impact in several areas that touch our daily life, such as healthcare, food and agriculture, industries, hydrology, environment and numerous research fields. Nuclear medicine (NM) is a speciality wherein radiopharmaceuticals (RP) are used for diagnosis or therapy. Diagnostic NM enables the visualisation of organs/ their functions and abnormal growths. Nearly all vital organs and their functions and most of cancers can be imaged now. Since the use of radioiodine (I-131) in the 1940s for treating thyroid cancers, therapeutic NM has grown enormously. 'Theranostics', the synchronised use of diagnosis and therapy for personalised treatment, is growing. RPs are also used in

drug development, for quick screening and assessing the efficacy of drugs. In 'Teletherapy', radiation from an external source is used for cancer therapy, while 'Brachytherapy' employs radioactive sources in close contact with the cancerous tissue/organ. Radioimmunoassay (RIA), a Nobel prize-winning technology, is a boon for measuring minute levels of bio-molecules. Radiation is used to sterilize medical products, such as implants, disposable syringes, needles etc. Blood irradiation for safe transfusion, especially in immune-compromised persons is mandatory in several countries. Radiation polymerized hydrogels and novel polymers have applications in medicine.

Radiation is used in many ways for food safety and security. Radiation processing of food is used to disinfest, sanitize/sterilize, delay sprouting/ripening and make it safe for consumption. Food irradiation is routinely followed in several countries and is mandatory for the export of a few products such as spices. Crop mutation induced through radiation has been successful in developing robust crop varieties and has helped in achieving food security in many countries.

Radiotracers/radiation-based technologies are used in several industries. Radiotracers aid in the optimization of chemical processes, and the quick detection of leaks in underground pipelines, dams etc. Radiography, akin to X-radiography in humans, is extensively used in many industries for QC/QA and troubleshooting. Nucleonic gauges, based on the attenuation principle of radiation are used routinely in several manufacturing industries. Radiation cross-linking of wires and cables enhances their performance significantly and is currently followed worldwide.

Radiation treatment of industrial effluents and used waste oil from transformers makes them amenable for disposal. Radiation treatment of sewage effluent effectively hygienizes the waste and makes it a bio-fertilizer. Radiation treatment of gaseous effluents from thermal power plants can drastically reduce acid rain-causing emissions and yield valuable fertilisers as by-product.

Radiotracers have been used for a long in research. Radioactive sources find applications in space industries. A niche use of radiation is in art and cultural heritage, in the treatment of valuable artefacts to save from damages due to fungi etc. and many countries use it to restore damaged artefacts and books. The field of 'art and museums' also uses radiography for assessing the internal integrity and vulnerability of art pieces, especially while moving them. And, many unique applications of radiation are continuously emerging!

3. Conclusion

In conclusion, radionuclides and radiation play important roles in many fields that contribute to human welfare and well-being. Particularly, the impact of healthcare applications is very gratifying.

Radiation and Kolkata: A Twosome Tale

*S. S. Ghugre**

UGC-DAE CSR Kolkata Centre, Sector II, LB-8, Bidhan Nagar, Kolkata 700106, India.
*Email: ssg.iuc@gmail.com

Radiation, since its discovery more than a century ago, has evolved into an indispensable tool of use in myriad domains that impact us at all scales. Apart from the many research pursuits of the global academia, and the path-breaking accomplishments therefrom, radiation is now a panacea to numerous theranostic challenges as well as an elixir for evolving impediments in the areas of national security, quality control (of industrial products) and processing/sterilization needs.

This presentation aspires to take its audience on a tour of some of the endeavours in radiation centric pure and allied sciences that have happened in the speaker's part of the world in general and at the Kolkata Centre of the UGC-DAE Consortium for Scientific Research in particular, and that is often left untold in the narrations on the city of joy.

Starting from the installation of the first Cyclotron in the country to the development of accelerators for research in different energy domains to the facilities of nuclear medicine the city of Kolkata has a long and cherished history of practising radiation science.

UGC-DAE Consortium for Scientific Research (UGC-DAE CSR), was established in the year 1990 for providing state-of-the-art equipment & facilities for the benefit of researchers especially from teaching institutes. The broad objective of the Consortium is to promote research in front-line areas of science and technology by providing an institutional framework for optimum utilization of the research facilities of the Department of Atomic Energy (DAE), along with the in-house facilities. The Kolkata Centre of UGC-DAE CSR has been pursuing multi-disciplinary research, with emphasis on ionizing radiation in its diverse role as a characterization tool, a causative agent, and a probe. The Centre has nurtured an organic collaborative linkage between the university system and DAE over the period of more than thirty years, in these domains.

The Nuclear Physics Group at the Kolkata Centre has been associated with the activities of the Indian National Gamma Array (INGA) a multi-clover detector setup for pursuits in experimental nuclear structure physics. In the recent INGA campaign at the Variable Energy Cyclotron Centre

(VECC), Kolkata, the Digital Data Acquisition System based on digital signal processing, conceptualized by the group has been extensively used by the user community in several routines as well as challenging experiments.

The developments in the domain of efficient pulse processing as well as the data analysis using state-of-the-art algorithms, used primarily for results from INGA have been extended to results obtained using X-ray Fluorescence in arriving at elemental concentration even at the ppm level.

The Centre has hosted a gamma-ray irradiation facility to probe the response of biological systems to radiation-induced stress. The research activities of the Radiation and Stress Biology Group at the Kolkata Centre are centred around the application of radiation for probing biological activity in cancer cells and related bioanalytical developments.

The Macromolecular and Radiation Chemistry Group studies the interaction between radiation and chemical species, which have been exploited to create novel nanomaterials of relevance.

The research activities which would be presented would highlight the efforts of the Kolkata Centre in their humble attempts to pursue activities which are expected to have societal relevance.

Bioanalytical and Biochemical Neutron Activation Analysis to Study Total, Bioaccessible and Speciation of Elements

*Amares Chatt**

Trace Analysis Research Centre, Department of Chemistry, Dalhousie University
6274 Coburg Road, Room 212, PO BOX 15000
Halifax, Nova Scotia, B3H 4R2, Canada.
*Email: a.chatt@dal.ca

1. Introduction

Neutron activation analysis (NAA) is a powerful analytical technique for the simultaneous measurement of multielement concentrations in a variety of complex sample matrices. When applied directly to analyze solid, liquid and gaseous samples, without any pre-treatment such as chemical separation, the technique is referred to as instrumental NAA (INAA) which is the most common form of NAA. It has many unique characteristics from the viewpoint of precision and accuracy. Preconcentration NAA (PNAA), where a chemical separation is carried out before irradiation, and radiochemical NAA (RNAA), where the separation is done following irradiation, still have these unique features while increasing the number of elements that can be determined at ultra-trace levels in somewhat more difficult sample materials. We have further extended the scope of NAA by using it in combination with several common chemicals, bioanalytical and biochemical separation methods to study biologically important trace elements and their species. A few examples are given below.

2. Biochemical neutron activation analysis (BNAA)

We are interested in developing biochemical neutron activation analysis (BNAA) methods by combining biochemical methods with NAA for the separation, purification, and characterization of metalloproteins and protein-bound trace elements. In these studies, we need an analytical technique capable of analyzing a few milligrams of samples non-destructively, and of determining ultra-low levels of several elements simultaneously within a short time in a matrix largely composed of carbon, hydrogen, nitrogen, oxygen and sulfur. The technique should provide excellent precision, accuracy,

sensitivity, and detection limits. NAA meets all of these requirements. The biochemical techniques of interest are dialysis, ammonium sulphate precipitation, gel filtration, ion exchange and hydroxyapatite chromatography, high-performance liquid chromatography, chromatofocusing, isoelectrofocusing, isotachophoresis, sedimentation equilibrium and enzymatic assay. We called the combination of these two techniques BNAA and it is ideally suited for studying metalloproteins and protein-bound trace elements. We observed that most of the trace elements in bovine kidneys were largely concentrated in the cytosol fraction. More than 70% of As, Br, Cl, Co, K, Na and Rb, about 65% of Cd, and 30-35% of other elements except for Se (14.4%), Cr (15.6%) and Mo (24.6%) were detected in this fraction. Elements such as Ca, Cr, and Se were more abundant in the nuclei fraction with concentrations of 34%, 75% and 73%, respectively. The dialysis experiments showed that more than 90% of Ca, Cd, Cu, Fe, Mg, Mn, Mo, Se, V and Zn, and possibly As, and I, and about 20% of Br were bound to macromolecules, mainly proteins. Most of these proteins were stable in the pH range of 3.5 to 10.5. Examples of these species with particular emphasis on Se will be presented.

3. Speciation neutron activation analysis (SNAA)

We wanted to extend the scope of NAA by determining the species of an element. We called it speciation NAA (SNAA). We have further extended SNAA to simultaneously determine several species and termed it simultaneous SNAA (SSNAA). Since the toxicity of an element largely depends on its physicochemical forms, there is an increasing interest in studying its speciation. We have used SSNAA for: (i) simultaneous multielement speciation with high specificity, (ii) speciation of elements which are not chemically similar such as Cd, Mn and Se, (iii) speciation of elements such as Cl, Br and I which are rather difficult to determine by most other techniques, etc. We have developed various methods for the detection, identification and measurement of proteic, lipidic and ionic species of a number of trace elements in biological materials, for example, iodine in milk. The total iodine concentrations ($\mu g\ mL^{-1}$) for milk with various fat content (MF) were: 0.40±0.01 (in 3.25% MF), 0.40±0.01 (2% MF), 0.42±0.01 (1% MF), 0.42±0.01 (<0.05%), and 0.96±0.01 (1% MF+Ca). Iodine bound to various fractions of the milk samples analyzed, in percent of total iodine content, ranged: (0.05-1.8), (1.9-4.8), (90-95) for the lipidic, proteic and anionic inorganic fractions respectively. Iodine recovery in all cases was higher than 96%. We have also estimated bioaccessible fractions of elements such as Se in individual food items and duplicate diets. In addition to NAA, we have used solvent extraction, gas and liquid chromatography, mass spectrometry, and nuclear magnetic resonance spectrometry. Recently we have used various X-ray techniques employing synchrotron radiation for speciation analysis at macromolecular to cellular levels.

Application of Nuclear Techniques in Material Science Research: Perspective of a Nuclear Chemist

*Alok Srivastava**

Department of Chemistry, Panjab University, Chandigarh-160 014, India.
*Email: alok@pu.ac.in

The successful application of nuclear techniques has been demonstrated by researchers from around the world in subject areas as varied as geology, archaeology, chemistry, physics, agriculture, space science, biology, agriculture science, medical science etc., for several decades. The ARCEBS conference series is one such platform which has been trying to offer researchers a platform to showcase novel applications of radiochemical tracers and energetic beams in different areas of natural sciences.

The study of novel polymers synthesized by employing energetic ion beams has become one such interesting area of material science research due to the increasing application of polymers in different fields including hard radiation environments similar to those encountered in space-crafts, satellites, power plants, particle accelerators, sterilisation irradiators etc. A review of the literature shows that exposure of matter to ionizing radiation leads to irreversible changes in chemical, structural, physical, optical, magnetic, and electrical properties etc. some of which can be exploited for technological applications.

Conducting and non-conducting polymer films of varying thickness obtained commercially as well as synthesized in our laboratory were exposed to gamma rays as well as swift heavy ion beams of carbon, silicon and nickel employing the 15 UD Pelletron Accelerator Facility of Inter-University Accelerator Centre (IUAC) located in New Delhi, India. The physicochemical characterization was carried out first and if promising properties were displayed by the irradiated material it was further investigated for technological applications.

The invited talk which is related to research work carried out in collaboration with researchers from India and Germany will try to illustrate that new polymeric materials with the desired color, thermal stability, optical band gap energy, electrical conductivity and dielectric constant have the potential for application as lightweight plastic capacitors and gas sensors can be prepared by using

gamma rays of different dose besides energetic ion beam approach through control of ion fluence and the energy of the swift heavy ions besides the thickness of the polymeric material. The future prospects of technological applications of polymeric materials prepared using the energetic ion beam approach will also be presented to explore the possibility of multilateral research collaboration.

A Comprehensive Study of Break Up Fusion Reactions at Near Barrier Energies

*B. P. Singh**

Department of Physics, Aligarh Muslim University, Aligarh - 202002, India.
*Email: bpsinghamu@gmail.com

1. Introduction

The study of fusion reactions in heavy ion (HI) collisions has been a topic of importance for many years [1]. As the projectile fuses with the target nucleus, referred to as the complete fusion (CF), a fully equilibrated compound nucleus (CN) is formed, provided the driving input angular momentum $\ell \leq \ell_{crit}$. If the angular momentum (ℓ) of the composite system is not sustainable, the projectile may break up into parts and one of the constituents fuses with the target nucleus, while the other goes on moving in the forward direction as a spectator leading to the break-up fusion (BUF) reaction [2]. Results have indicated that being a strongly bound structure, the α-particle is favoured as an emitted particle in BUF. Several models have been proposed to explain the BUF reaction dynamics but none of these is found to reproduce the data at energies as low as ≈4-7 MeV/nucleon. Moreover, some of the most debated issues related to BUF reactions have been the disentanglement of CF and BUF components, the role of projectile structure and the angular momentum involved. Further, there is a need to develop systematics for the break-up fusion reaction as well.

2. Experimental

In view of the above, a programme of measurement and analysis of (i) fusion excitation functions (EFs) (ii) forward recoil range distributions (FRRDs) and (ii) spin distributions (SDs), of reaction residues in a large number of projectile-target combinations, has been undertaken. The ion beams of interest (α-clustered ^{12}C and ^{16}O as well as non-α clustered ^{13}C, ^{14}N, ^{18}O and ^{19}F) with ≈ 4-7 MeV/A energies, have been obtained from the 15UD Pelletron accelerator facility of the IUAC, New Delhi. The stacked foil recoil catcher activation technique employing a high resolution (2 keV for

1.33 MeV γ-ray of ^{60}Co) HPGe γ-ray spectrometer has been used to determine the activities induced in the samples and the catcher foils, after irradiation. The residues populated via CF and/or BUF processes have been identified by their characteristic γ-lines and measured half-lives. The EFs and FRRDs have been obtained from the measured cross-sections of the residues in the target and catcher foils [3]. To study the role of ℓ-values in the successively opened BUF channels the particle-γ coincidence experiments using Compton suppressed Gamma Detector Array coupled to a Charged Particle Detector Array (hexagonal arrangement) set-up have been done and the spin distributions of residues populated via CF and/or BUF are determined. Prompt γ-rays in coincidence with fast charged particles (Z=1,2) have been recorded to achieve information about involved reaction processes on the basis of their experimentally observed spin populations during de-excitation [4].

3. Results and Discussion

The analysis of the measured EFs done within the framework of statistical model codes indicates that the α-emitting channels have significant contribution from the BUF processes for both the α- as well as non-α cluster projectiles. It has been found that the BUF probability depends not only on beam energy but also on the Coulomb factor ($Z_1.Z_2$) as well as on α-Q-value (Q_α) of the projectile. An increase in the Coulomb factor increases the BUF probability and as the Q_α value of the projectile becomes less negative the BUF contribution increases and vice versa. The FRRD measurements have been used to disentangle BUF and/or CF contributions in HI reactions. The deduced BUF fractions obtained from EF and FRRD measurements are found to be consistent with each other. For α-emitting channels identified from forward α-gated spectra, the intensity in the SD pattern increases up to a certain value of J_{obs} indicating a narrow spin population in the case of BUF reactions [4]. Further details of measurements, analysis and the systematics developed will be presented.

References

/1/ A. Diaz Torres, et al., Phys. Rev. Lett. 98 (2007) 152701.

/2/ M. Dasgupta, et al., Phys. Rev C 70 (2004) 024606.

/3/ M. Shariq Asnain, et al., Phys. Rev. C (2022) (Accepted).

/4/ P. P. Singh et al., Phys. Lett. B 671 (2009) 20.

Keynote and Invited Lectures

(Mini Symposium on Earth and Environmental Sciences)

What Single Hot Particles Tell Us: From Nuclear Forensics to Bioavailability

Clemens Walther[1], Darcy van Eerten[1], Laura Leifermann[1], Paul Hanemann[1], Manuel Raiwa[1], Tobias Weissenborn[1], Klaus Wendt[2]*

[1]Institute of Radioecology and Radiation Protection, Leibniz University Hannover, 30419 Hannover, Germany.
[2]Institute of Physics, Johannes Gutenberg-University Mainz, D-55099 Mainz, Germany.
*Email: walther@irs.uni-hannover.de

1. Introduction

When on April 26, 1986, the reactor of the Chernobyl nuclear power plant exploded, nuclear fuel was in part released as microscopic solid particles. Structurally intact hot particles pose a risk to humans mainly by the (unlikely) path of inhalation. However, over the decades, weathering may lead to considerable release of radionuclides that subsequently can enter the human food chain. Since hot particles differ strongly with respect to morphology, chemical composition and stability, investigations need to be performed on single particles, rather than on bulk samples.

2. Particle Identification and Experimental Method

We separate and extract the micrometre-sized particles from the environmental matrix in a scanning electron microscope (SEM) equipped with a micromanipulator. Subsequently, the particles are fixed by SEM glue on in-house made tungsten needles. Element composition is imaged by EDX measurements and radioactive isotopes are detected by gamma spectrometry. Subsequently, particles are transferred to our resonant laser-SNMS system (Secondary Neutral Mass spectrometry) developed at IRS Hannover.

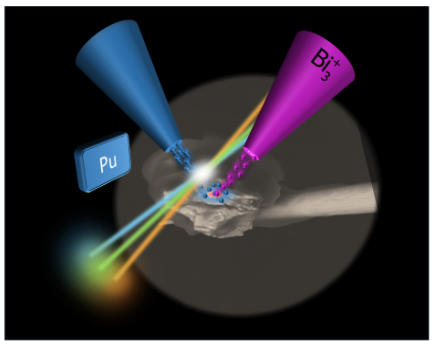

Figure 1: Single hot particle from the Chernobyl exclusion zone mounted on a tungsten needle. Sputtered Pu atoms are resonantly ionized and detected by time-of-flight mass-spectrometry

To achieve isotopic imaging at trace concentrations with a spatial resolution of below 100 nm the high element selectivity of resonance ionization was combined with the non-destructive analysis of a static TOF-SIMS instrument. A commercial TOF-MS (IONTOF 5) is coupled to a pulsed Ti:Sa laser system capable of performing two-, and three-step laser excitation on the sputtered secondary neutrals. In contrast to dynamic SIMS, the present system works quasi non-destructive [1].

3. Ultra-Trace Isotope Analysis and Imaging

We measure U, Pu, Sr, Cs and Tc isotopic compositions and perform spatially resolved full mapping of all elements on single µm-sized particles down to the sub fg scale (ca 10^5 atoms). Interfering isobaric elements, like Pu-238 and U-238, or Pu-241 and Am-241 are suppressed by up to five orders of magnitude [2]. In contrast to most mass-spectrometric techniques, only negligible mass is consumed, leaving the particle intact for further studies.

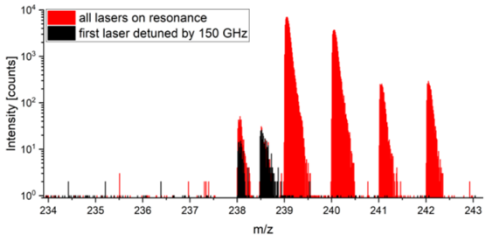

Figure 2: SNMS Spectrum of a single hot particle. Pu-238 is detected against a 105 times excess of U-238

4. Chemistry on Single Particles

Selected individual particles were sequentially leached in ammonium acetate solution, hydrochloric, oxalic, nitric acids and aqua regia. The solutions are then measured via gamma spectrometry and ICP-MS to analyze their uranium content and the amounts of leached fission and breeding products. Fuel particles from the Chernobyl accident are usually classified according to their appearance, dissolution rates and oxidation state: the further oxidized and brittle UO_{2+Z}, non-oxidized UO_2 and zirconium merged bearing U_X -Zr_Y-O_Z particles, of which we investigated at least one particle each. The first leaching steps did not attack the structure of the particles, and only small fractions of Am-241 and Cs-137 were leached under mild conditions, indicating a low bioavailability. Leaching behaviours were mostly in line with the predictions based on the visually assigned classes and oxidation states. From these data, conclusions on potential risks to human health and environment are drawn. The technique is applicable to almost all elements and opens up new scientific applications apart from the nuclear field.

References

/1/ M. Franzmann et al., J. Anal. At. Spectrom. 33 (2018) 730-737.

/2/ H. Bosco, et al., Sci. Adv. 7 (2021) 813.

Helium in The Universe, The World Stage and in India

*Debasis Ghose**

Formerly, Variable Energy Cyclotron Centre, 1/AF Bidhannagar, Kolkata 700064, India.
*Email: dghose43@gmail.com

Helium, the second lightest element, came about in the universe through a featureless dark dense sea of energy around 15 billion years ago [1,2]. Estimates indicate about 25% of the baryonic mass of the initial cosmos was a fireball having a temperature of about 20 million K consisting of the low mass stable elements hydrogen (H) and the rest principally helium (He^4), brought about through the transformation of hydrogen via the *pp* chain proton capture reaction sequence. Overall, it is estimated there is one helium atom for every eleven hydrogen atoms in the stellar universe [3].

Despite its overwhelming preponderance in the universe as a whole, ironically alongside the inert group of gases helium is classed as a 'rare gas' on earth. This flows from the fact that the atmospheric air which is the source of several commercial gases such as nitrogen, oxygen and argon is greatly depleted in helium showing up at an overall concentration of 5.2 ppm. Energy-wise the cost of extraction of a gas is inversely proportional to the square of its concentration in the feed gas. Therefore, atmospheric air, as a process gas, to achieve marketable volumes of helium is energetically hugely expensive. Large concentrations of helium are found in very old petroleum gas reserves associated with granitic bedrocks containing uranium and thorium. Therefore, large-scale commercialized sources of all helium worldwide are the 'helium-bearing' natural gas trapped at some favourable ancient (> 500 Ma) uranium-enriched underground hydrocarbon reserves that are also rich in nitrogen.

The earth has within its depths held onto a repository of solar helium accrued since the time of its formation. In India's Rajmahal volcanic basin in the eastern state of Jharkhand, millions of years of fluids incorporating gas compositions that have equilibrated to ancient helium, are stored in rock volumes in the region and are released continuously at variable rates through rock vesicles due to pressures and formation of grain-sized micro-cracks. Geologically

this region has a deep crustal structure that emerged out of a major volcanic activity, the Rajmahal volcanism, that erupted directly into the atmosphere for a duration of about 2 million years some 120 million years ago [4,5]. The roots of this eruption have created a more or less linear belt of hot springs with rough east–west alignment across Jharkhand. Here it is observed that there is a continuous outflow of soil gases bearing helium through concealed underground pathways into the atmosphere through a volcanically generated plumbing system about 40 km wide and 250 km long cutting roughly along the mid-rib of Jharkhand. Measurements carried out at numerous sites reveal the average helium permeation rate through soil cover into the atmosphere in this region to be typically about 3.6 litre/sq m surface/day or about 640×10^4 tons of helium gas per day across the overall area. This is a very large amount of helium gas loss. While natural gas has to date remained the most accessible helium resource, geothermal regions such as these provide an alternate pathway to open up commercial possibilities for sustained large-scale helium extraction. Helium extracted from these geothermal areas has the benefit that it is likely to last for geologically long time scales. It would provide an assured supply base for long durations.

References

/1/ P.J.E. Peebles, D.N. Schramm, E.L. Turner, et al., Nature 352 (1991) 769-776.

/2/ P.J.E. Peebles, Phys. Rev. Lett. 16 (1966) 410-413.

/3/ R.J. Tayler, Astr. Soc. 8 (1967) 313-333.

/4/ M. Mukhopadhyay. J. Geol. Soc. India. 56 (2000) 351-364.

/5/ D. Ghose, D.P. Chowdhury, B. Sinha. Curr. Sci. (2002) 993-996.

$^{87}Sr/^{86}Sr$ in Archaeological Cattle Bones from Coastal India

Supriyo Kumar Das[1], Bidisha Dey[2], Kaushik Gangopadhyay[3], Tomoyuki Shibata[2], Masako Yoshikawa[2]*

[1]Department of Geology, Presidency University, Kolkata, India.
[2]Earth and planetary system science program, Hiroshima University, Japan.
[3]Department of Archaeology, University of Calcutta, Kolkata, India.
*Email: sdas.geol@presiuniv.ac.in

1. Introduction

Strontium has three naturally occurring non-radiogenic (^{84}Sr, ^{86}Sr and ^{88}Sr) and one radiogenic (^{87}Sr) isotope. Strontium enters the body through food and water, and deposits as hydroxyapatite in animal bones by substituting calcium [1]. The strontium isotope ratio ($^{87}Sr/^{86}Sr$) in archaeological faunal remains has been used as a useful tool to determine pastoral migration and mobility [2]. The application of $^{87}Sr/^{86}Sr$ is based on the assumptions that an animal consumes only locally grown foods and that there is sufficient geologic homogeneity to reconstruct the $^{87}Sr/^{86}Sr$ range of a locale. The $^{87}Sr/^{86}Sr$ values of domesticated animals at Indian Harappan sites of Kotada Bhadli and Bagasra in Gujarat have been reported [3, 4, 5]. Using the average $^{87}Sr/^{86}Sr$ values (0.7093 to 0.7096), it is interpreted that cattle/buffalo have been raised locally and consumed at Kotada Bhadli [3], whereas cattle/buffalo were acquired from a region outside Bagasra [4]. Interestingly, the $^{87}Sr/^{86}Sr$ ratio of Indian eastern coastal archaeological sites is rare, where $^{87}Sr/^{86}Sr$-based interpretation is challenging due to possible diagenetic alteration of bones in the prevailing humid tropical climate. The research aims to analyse $^{87}Sr/^{86}Sr$ in cattle bones excavated from a protohistoric-historic coastal site known as Erenda (21°55'4.8"N, 87°34'42.4"E), which is located in the palaeo-delta of the Subarnarekha River in the East Medinipur District of West Bengal, India. The mound lies ~1.7 m above the MSL and covers an area of approximately 25 × 40 m^2. Geologically the site lies above Late Pleistocene-Early Holocene Sijua Formation. Human settlements at the site begin during the first millennium BCE [6]. The site was partly abandoned after 663 ± 92 BCE [6].

2. Experiment

Powdered bone samples, aged between 1810 ± 100 AD and 663 ± 92 BCE, were dissolved using HCl and loaded onto a 0.1 ml resin column containing Sr-spec resin (Eichrom). Strontium was recovered using 0.05M HNO_3 and loaded onto a single Re filament. $^{87}Sr/^{86}Sr$ were measured in positive ionisation mode (filament temperature ~1400 °C) using TIMS. $^{87}Sr/^{86}Sr$ isotopic ratio was corrected using $^{86}Sr/^{88}Sr$ (0.1194). One archaeological soil sample from the same horizon was also analysed.

3. Results and discussion

$^{87}Sr/^{86}Sr$ in Erenda bones ranges from 0.715561 to 0.715681. The $^{87}Sr/^{86}Sr$ ratio of bones is lighter than the archaeological soil (0.722706), nearby River Ganga water (0.7249 to 0.7282), groundwater (0.71619 to 0.7271) and seawater (0.709181) [7, 8, 9]. Unlike Harappan sites in Gujarat, the baseline value of bioavailable strontium is not available in Erenda [5]. Moreover, in coastal areas, the interpretation of radiogenic strontium isotope analysis is complicated due to the possible effect of sea salt on marine $^{87}Sr/^{86}Sr$ signature. It is likely that cattle have been raised locally and consumed vegetation/grass that shows marine influence in their $^{87}Sr/^{86}Sr$ values.

References

/1/ K.M. Frei. Danish J. Archaeol. 1 (2012) 113-122.

/2/ E.K. Thornton, S.D. DeFrance, J. Krigbaum, et al., Int. J. Osteoarchaeology 21 (2011) 544-567.

/3/ K.S. Chakraborty, S. Chakraborty, P.Le Roux, et al., J. Archaeol. Sci. Reports 21 (2018) 183-199.

/4/ B. Chase, D. Meiggs, P. Ajithprasad, et al., J. Archaeol. Sci. 50 (2014) 1-15.

/5/ B. Chase, D. Meiggs, P. Ajithprasad, et al., J. Archaeol. Sci. 92 (2018) 1-12.

/6/ S.K. Das, K. Gangopadhyay, A. Ghosh, et al., The Holocene 31 (2021) 1511-1524.

/7/ S. Krishnaswami, J.R. Trivedi, M.M. Sarin, et al., Earth Planetary Sci. Lett. 109 (1992) 243-253.

/8/ G.R. Tripathy, S.K. Singh, R. Bhushan, et al., Geochem. J. 45 (2011) 175-186.

/9/ T. Yoshimura, S. Wakaki, H. Kawahata, et al., Front. Earth Sci. 9 (2021) 592062.

Measurement of Naturally Occurring Radionuclides at the Archaeological Sites of Eastern India

Nabanita Naskar[1], Kaushik Gangopadhyay[2], Chandrima Shaha[2], Ahana Ghosh[3]*

[1]Diamond Harbour Women's University, South 24 Parganas -743368, India.
[2]University of Calcutta, 1 Reformatory Street, Kolkata-700027, India.
[3]Department of Humanities and Social Science, IIT, Gandhinagar, India.
*Email: g.nabanitanaskar94@gmail.com

1. Introduction

Estimation of Naturally occurring radionuclidic material (NORM) is rare in the field of archaeological exploration. Here, for the first time, the inventory of primitive radionuclides has been reported from two different archaeological sites of West Bengal (WB), Erenda (21.92°N, 87.58°E) located in East Medinipur district, and Bahiri (20.85°N, 87.79°E) located 22.5 km southeast of Erenda. The Erenda region is a part of the Belda-Contai upland which evolved as ancient deltas of the Subarnarekha and Kasai rivers whereas Bahiri is located within the sand dune ridges on the westernmost part of coastal Bengal, which is associated with the mid-late Holocene marine transgressive phase. Excavations revealed the existence of both 'public' and 'private' architectural remains.

2. Experiment

Soil and pottery samples were collected depth-wise from the excavated trenches at the sites of Erenda and Bahiri. The principal pottery of Erenda is black and red ware, along with red slipped ware. Redware and grey ware were the primary potteries from Bahiri. Fig. 1a and 1b present the excavated studied trench from Erenda and Bahiri. Samples were pre-treated following reference 1. After attaining secular equilibrium, the activities of primordial radioisotopes in the samples were measured using shielded HPGe detector having 80% relative efficiency and resolution of 1.65 keV at 1.33 MeV energy (make: CANBBERA). The photopeaks at 295.6, 351.7, 608.9 keV for ^{238}U, 338.3, 583.2, 911.2 keV for ^{232}Th and 1460.8 keV for ^{40}K were measured for 60000 s. Activities were calculated using the comparator method for which respective U, Th, K standards were prepared accordingly [2,3].

Fig 1a and 1b: Excavated Trench A1 at Erenda and Trench YB1 at Bahiri

3. Results and Discussion

In soil samples collected from Erenda, activities of ^{238}U, ^{232}Th and ^{40}K ranged between 25.7±2.4 to 44.4±2.9, 51.3±1.6 to 72.7±6.3 and 423.0±8.6 to 503.6±9.4 Bq kg^{-1}, respectively. In pottery samples from Erenda, ^{238}U, ^{232}Th, ^{40}K activities ranged between 36.6±2.2 to 46.9±0.5, 59.4±4.9 to 73.2±0.5 and 337.3±12.0 to 655.1±8.7 Bq kg^{-1}, respectively. Data showed lower content of ^{40}K in grey-wares. Obtained data for the soil samples collected from Bahiri, showed the range of ^{238}U, ^{232}Th and ^{40}K activities between 22.6±1.3 to 38.8±1.7, 59.7±4.4 to 95.2±6.9 and 391.5±8.6 to 860.5±12.5 Bq kg^{-1}, respectively. For pottery samples collected from the same context of Trench YB1, average ^{238}U, ^{232}Th and ^{40}K activities were 41, 75 and 875 Bq kg^{-1}. One significant observation was the consistently higher ^{40}K activity in both the soil and pottery samples of Bahiri, with respect to that of Erenda samples.

4. Conclusion

This study is the first report on natural radiation from two excavated sites in West Bengal, India. The obtained data reveal: (i) the measured activity of ^{232}Th is higher because of its insoluble nature and has not leached out during the time period (ii) ^{40}K activity decreased with the depth in Trench, indicating agricultural influence at the above digs (iii) availability of ^{238}U and ^{232}Th was rather uniform along the depth, supporting their geogenic origin. (iv) ^{40}K activity was elevated at the site of Bahiri.

Acknowledgement: NN acknowledges DST-INSPIRE Faculty Fellowship for the research grant.

References

/1/ P. Chaudhuri, N. Naskar, S. Lahiri, et al., J. Radioanal. Nucl. Chem. 311 (2017) 1947-1952.

/2/ N. Naskar, S. Lahiri, P. Chaudhuri, et al., J. Radioanal. Nucl. Chem. 314 (2017) 507-511.

/3/ N. Naskar, S. Lahiri, P. Chaudhuri, et al., J. Radioanal. Nucl. Chem. 316 (2018) 709-715.

Nuclear Techniques in Unravelling The Past

*Kaushik Gangopadhyay**

Department of Archaeology, University of Calcutta, Alipur Campus, 1, Reformatory Street, Kolkata 700027, India.
*E mail: k.gongo@gmail.com

1. Introduction

Radioisotopes have been used in archaeology since the discovery of the method in 1950 by Willard Libby. Particularly, the use of ^{14}C isotope has helped archaeologists to assign precise and absolute chronology to archaeological sites within the time range of 50 ka BP. Other than dating, radioisotopes could also be employed in the detailed characterization of archaeological artefacts, which helps in our study of provenance and ancient trade.

This paper includes case studies from India, which has employed radioisotopes in the study of the past. For the first time in the Indian context, the radioisotopic method has been used to calculate the total amount of Potassium in ancient glass and also in dating, for the first time, the earliest protohistoric site from eastern India. Also, new studies have been conducted which has successfully dated fossil remains from peninsular India. In this review paper, the author will make a comprehensive review of these and other research.

2. Discussions

The first paper to be discussed in this presentation [1] is on the analysis of glass beads from ancient Tamil Nadu using Compton Suppression Spectroscopy. The samples were analysed without using a reactor, accelerator or X-Ray source and the total ^{40}K was measured using a Gamma detector at the Saha Institute of Nuclear Physics, Kolkata. The implication of this study to understand the recipe for the production of glass beads from the archaeological sites of Manikollai and Arikamedu, Tamil Nadu, indicates the presence of both Potash-rich glasses from the sites of Manikollai and Arikamedu which could were manufactured locally. The second paper is on the recent radiometric dates (AMS) dates from coastal West Bengal. The site of Erenda, East Medinipur district, was dated using the AMS facility at IUAC. The result was to date the Chalcolithic period to 950 BCE, and from this level Black and Red

ware pottery, the signature pottery of the Chalcolithic period has been found [2]. Lastly, the recent dating of fossil bones from Manjra valley will be discussed. This region in Maharashtra has yielded fossils of the megafauna at the range of 24345 – 21423 BP, particularly elephants, large bovines and Hippopotamus. This research reflects on the climate and human-animal relation towards the end of the Pleistocene. Period [3].

Apart from radioisotopes, the XRF and XRD technique is also playing an important role in archaeological studies. These have taken into account mineralogical and elemental signatures in archaeological artefacts like pottery. Like the glass beads; pottery from archaeological contexts can be used to understand ancient trade. Important research from this perspective has also been carried out by (Das et al) where samples were collected and compared between Tamil Nadu and Bengal. The study shows that pottery was imported from Tamil Nadu to Bengal in the ancient period.

References

/1/ S. Lahiri, M. Maiti, K. Gangopadhyay. J. Radioanal. Nucl. Chem. 307 (2015) 226-228.

/2/ N. Naskar, K. Gangopadhyay, S. Lahiri, et al., Radiocarbon 63 (2021) 1645-1655.

/3/ S. Vijay, P. Kumar, P. Chakraborty, et al., Radiocarbon (2022) 1-9.

/4/ S. Das, S.Ghosh, K.Gangopadhyay, et al., Man & Environment, XLII (2017) 25-34.

The Radiological Hazards of Natural Radioactivity in The Punjab Plain, North-western India

Debabrata Das[1], Ritu Bala[1], Nabanita Naskar[2], Susanta Lahiri[2,3]*

[1]Department of Geology, Panjab University, Chandigah, India
[2]Diamond Harbour Women's University, Sarisha, India.
[3]Sidho Kanho Birsha University, Purulia, India.
*Email: debabratadas@pu.ac.in

1. Introduction

^{238}U, ^{232}Th and ^{40}K form the significant radioactivity component of soil. Change in their distribution pattern depends on various processes of weathering, soil characteristics and application of fertilizers [1]. Current study asses the radioactivity levels in the alluvial soil of Punjab with changes in land use. Soil in the region is deficient in nutrients and thus fertilizer of application is common practice. Fertilizers usually are found to have a high content of natural radionuclides [2-3]. Thus, a comparison has been made between agricultural and undisturbed sites. Radionuclide-level studies are important along the vertical soil profile and are missing in the region of interest.

2. Experiment

A total of 18 sites were covered with 13 agricultural and 5 undisturbed sites and samples were collected by using a manual hand auger from southwest Punjab (figure 1). Samples are named as AiDh or UiDh; i refers to the soil profile site and h (1–3) refers to the corresponding depth interval. A and U mark the agricultural and undisturbed areas respectively. Samples of known weights were tightly sealed in Petri plates. All these were kept aside for 30 days so that parent radionuclides and daughter products can attain secular equilibrium. ^{238}U, ^{232}Th and ^{40}K content were measured by gamma-ray spectrophotometer at Saha Institute of Nuclear Physics, Kolkata, India [4].

3. Results and Discussion

Radionuclide levels are found to be higher in the agricultural areas than the undisturbed, however, the variation observed is only up to the 600 cm depth interval. The values are comparable after this and show

the geogenic presence. Higher concentrations in agricultural land point to the influence of anthropogenic activities, particularly the use of fertilisers, on radionuclide concentration. With an average of 718.50 and 580.38 for agricultural and undisturbed areas, respectively (Table 1), ^{40}K is the radionuclide that contributes the most to the total activity of soil. This is because its concentration in the topsoil is relatively larger than that of the other radionuclides and can be a result of the extensive usage of NPK fertilisers. Thus, the original levels of ^{40}K in the agricultural sediment samples have risen due to the continuous addition of agrochemicals.

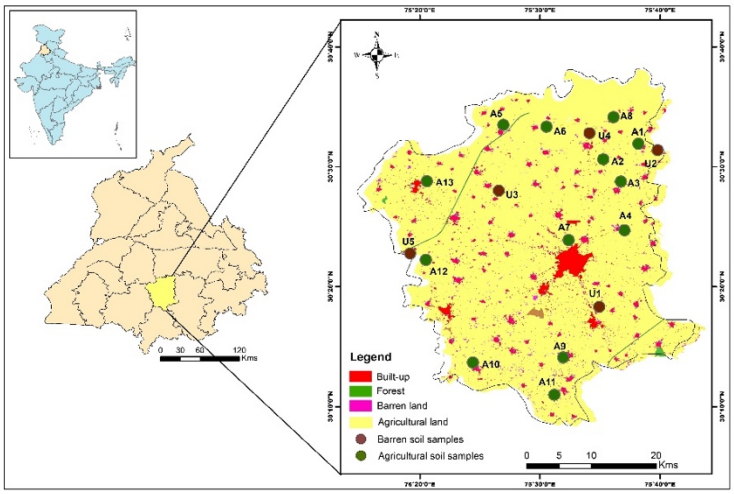

Figure 1: Location of the study area with sampling sites.

Table 1. Mean radioactivity concentration of radionuclides in agricultural and undisturbed areas

Land use	Depth (m bgl)		^{238}U	^{232}Th	^{40}K
Agriculture	D1	1-300	42.55	62.72	718.50
	D2	300-600	49.12	74.09	692.94
	D3	600-900	34.60	51.32	661.45
Undisturbed	D1	1-300	33.12	50.92	580.38
	D2	300-600	46.66	71.27	667.42
	D3	600-900	35.86	54.06	667.93

References

/1/ S. Priori, N. Bianconi, E.A.C. Costantini, Geoderma 226 (2014) 354-364.

/2/ A. Kumar, R.P. Chauhan, J. Radiat. Res. Appl. Sci. 7 (2014) 454-458.

/3/ N.N. Jibiri, K.P. Fasae, Radiat. Protect. Dosim. 148 (2012) 132-137.

/4/ N. Naskar, S. Lahiri, P. Chaudhuri, et al., J. Radioanal. Nucl. Chem. 312 (2017) 161-171.

Contributed Papers

(Main Symposium)

Synergistic Aqueous Biphasic Separation of ^{71,72}As from ∝-particle Irradiated Gallium Oxide Target using Catechins Extracted from Green Tea Leaves

Sayantani Mitra[1], Nabanita Naskar[2], Susanta Lahiri[2,3], Kalpita Ghosh[4], Punarbasu Chaudhuri[1]*

[1] Department of Environmental Science, University of Calcutta, 35, Ballygunge Circular Road, Kolkata, India.
[2]Diamond Harbour Women's University, Sarisha, South 24 Parganas, India.
[3]Department of Physics, Sidho Kanho Birsha University, Purulia, India.
[4]Department of Chemistry, Charuchandra College, Kolkata, India.
*Email: susanta.lahiri.sinp@gmail.com

1. Introduction

Recently the nature resourced chemicals (NRC), i.e., the chemicals derived from nature have drawn attention to the peer community [1]. Also, now-a-days aqueous biphasic system (ABS) is seldom used in developing benign chemical methods, as ABS does not use any organic solvent. In this paper, attempt has been made to develop a new ABS system comprising of Na-malonate and polyethylene glycol (PEG), to separate ^{71,72}As from α-particle irradiated gallium oxide target. Catechins, the natural polyphenolic compounds available plenty in green tea leaves, introduced in the ABS, acted as synergistic agent to improve the separation factor. It is noteworthy to mention that, among the radioisotopes of arsenics, ^{71}As and ^{72}As are promising imaging agents in diagnostic radiology.

2. Experiment

Catechin compounds were isolated from green tea leaves by solvent extraction using ethyl acetate followed by purification and characterization by TLC, UV-Vis, FTIR and RP-HPLC. Ga_2O_3 powder (135 mg) was irradiated with α particles of 46 MeV energy for 10 h at Variable Energy Cyclotron Centre, Kolkata, India. The irradiated powder was digested in a microwave digester in 1:1 HCl: HNO_3 acid medium. ABS comprised of 2M Na-malonate and PEGs (M.W 4000, 6000) were made. 3 mL 50% PEG solution was mixed with equal volume of salt solution and 0.1 mL radioactive stock solution. 30 mg catechins was added in the ABS with catechin before the addition of radioactive stock solution. The

system was then shaken for 10 min and settled for 5 min to achieve phase separation. Each phase was subjected to γ-spectrometric analysis by an HPGe detector. Bulk gallium was monitored by ^{67}Ga having a photopeak at 93.4 keV and NCA As was monitored by 175.4 keV photopeak of ^{71}As

3. Results and Discussion

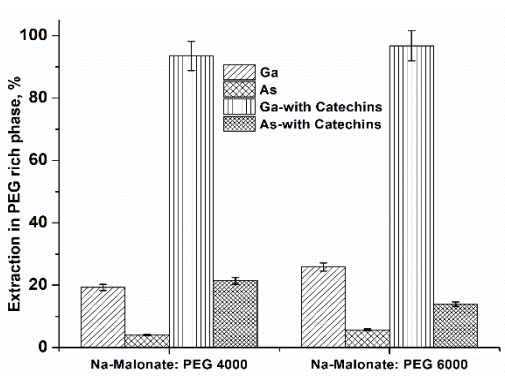

Figure 1a: Extraction in PEG phase

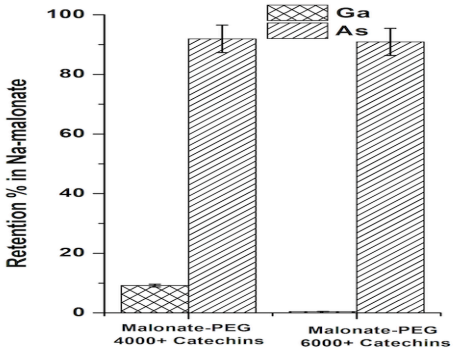

Figure 1b: Retention in salt phase after second extraction

Fig. 1a demonstrates the extraction of bulk gallium and NCA As radionuclides in the PEG-rich phase in the PEG-Na-malonate ABS system, without and with the addition of catechins in the system. It is clear that the catechin selectively binds with Ga and takes it to the PEG-rich phase. The phenolic OH groups present in catechin preferentially interact with Ga through complexation. Catechol derivatives are reported to be excellent chelators for metals having high charge-to-radius ratios such as Ga^{+3} or Fe^{+3}. Fig. 1b compares the activity of arsenic and bulk gallium retained in the Na-malonate phase. In PEG 6000-Na-malonate with catechins ABS system, more than 90% NCA As radionuclides were retained in the salt-rich phase with less than 0.2 % bulk gallium contamination after the second time extraction.

4. Conclusion

The above experiment demonstrates that the use of NRC is rewarding for developing simple, rapid as well as cost-effective methods. The NCA ^{71,72}As was retained in the salt-rich phase and therefore can directly be used for further applications.

Acknowledgements: Authors gratefully acknowledges Collaborative Research Scheme no UGC-DAE-CSR-KC/CRS/ 19/RC l0/ 0984 of UGC DAE Consortium for Scientific Research, Kolkata Centre.

References

/1/ S. Lahiri, D. Choudhury, K. Sen, J. Radioanal. Nucl. Chem. 318 (2018) 1543-1558.

Study of Hyperfine Interactions in Calcium Titanate Perovskite using TDPAC Spectroscopy

Ashwani Kumar[1,3], Manjulata Sahu[2*], B.S. Tomar[3*]*

[1]Radiochemistry Division, Bhabha Atomic Research Centre, Mumbai 400085, India.
[2]RadioAnalytical Chemistry Division, Bhabha Atomic Research Centre, Mumbai 400085, India.
[3]Homi Bhabha National Institute, Mumbai 400094, India.
*E-mail: kashwani@barc.gov.in, manju@barc.gov.in, tomarbs@hbni.ac.in

1. Introduction

Calcium Titanate (CTO), $CaTiO_3$, is the basic phase of the perovskite family. It is reported to be the most versatile ceramic host for high-level waste [1] and is one of the phases of SYNROC assemblage for immobilization of high-level radioactive waste from nuclear industry. CTO perovskite is also observed to be one of the promising candidates for various applications such as photocatalyst [2] and capacitor applications [3], which are dependent upon its electronic structure. Hence, it is important to study its electronic structure. CTO stabilizes in an orthorhombic lattice with Ti(IV) at the centre of oxygen octahedron. Time differential perturbed angular correlation (TDPAC) is one of the nuclear probe techniques to study the local structure in solids. In the present work, the chemical environment around the Ti-site of CTO has been studied using TDPAC spectroscopy.

2. Experiment

2.1. CTO Synthesis: CTO was synthesized by gel combustion method. $CaCO_3$ and titanyl acetyl acetonate were used as starting reactants. The gel combustion method has been described in reference [4]. XRD confirmed the single phase of orthorhombic calcium titanate.

2.2. Probe Doping: The probe was prepared as described elsewhere [5]. CTO powder was pressed into a cylindrical pellet (Ø8mm x 1mm). 10μL of ^{181}Hf solution was added drop by drop on the surface of the pellet and evaporated slowly using Infra-Red (IR) lamp. The pellet was annealed at 1250°C for 10 h.

2.3. Data Acquisition: Data was acquired using three LaBr(Ce) detector-based TDPAC spectroscopy setup. Detail of the setup is described in reference [4].

3. Results and Discussion

Figure 1 shows TDPAC spectrum of CTO along with its Fourier transform. The figure shows two broad oscillations which on fitting for G_{22} yielded two sites. Table 1 shows the hyperfine interaction parameters and EFG values. The study shows the probe atom (^{181}Hf) occupying two different sites with fractions 81% and 19%, having different interaction frequencies, and different electric field gradients (EFG). However, the asymmetry of the EFG was similar in the two sites.

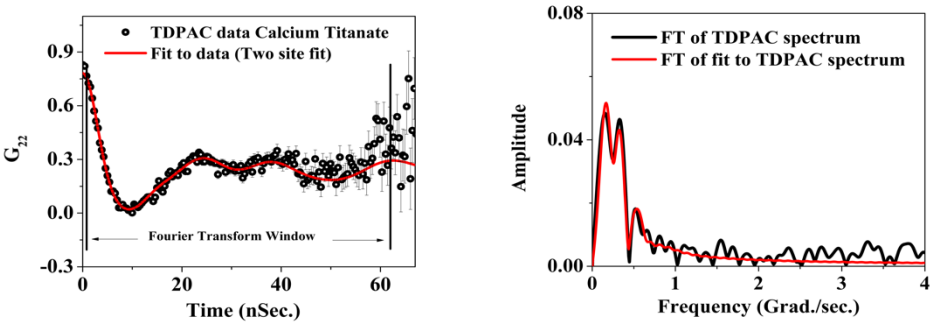

Figure 1: TDPAC spectrum of calcium titanate along with fit (L) and Fourier Transform (FT) to TDPAC spectrum and the fit (R)

Table 1. Hyperfine interaction parameters obtained from fit of TDPAC spectrum.

HFI parameters	Site-1	Site-2
ω_1 (Mrad/s)	203 ± 2	160 ± 2
η	0.47 ± 0.01	0.47 ± 0.03
δ	0.28 ± 0.01	0.06 ± 0.02
χ2 of fit	1.3	
EFG calc. (V/m^2)	3.12 (0.03) x 10^{21}	2.47 (0.03) x 10^{21}

4. Conclusion

Calcium titanate was synthesized by gel combustion route and doped with a TDPAC probe. TDPAC study infers that probe atoms occupying two sites have different electric field gradients but with similar asymmetry parameters.

References

/1/ A.S. Bhalla, R. Guo, R. Roy, Mater. Res. Innov. 4 (2000) 3-26.

/2/ M. Passi, B. Pal, Powder Technol. 388 (2021) 274-304.

/3/ A. Krause et al., Vac. Sci. Technol. B, Nanotech. Microelectron. 29 (2011) 01AC07.

/4/ A. Kumar et al., Mater. Sci. Mater. Electr. (2021) 1-11.

/5/ A. Kumar et al., Proc. Fourth Int. Conf. on ARCEBS, 5 (2018) 287-288.

Efficacy of Black Pepper Derived Alkaloid in Separation of ^{90}Nb from Natural Yttrium Target

Sayantani Mitra[1], Nabanita Naskar[2], Susanta Lahiri [2,3], Punarbasu Chaudhuri[1]*

[1] Department of Environmental Science, University of Calcutta, 35, Ballygunge Circular Road, Kolkata, India.
[2]Diamond Harbour Women's University, Sarisha, South 24 Parganas, India.
[3]Department of Physics, Sidho Kanho Birsha University, Purulia, India.
*Email: susanta.lahiri.sinp@gmail.com

1. Introduction

Chemicals obtained from nature have proven their superiority in radiochemical separation compared to organic reagents. One such example is piperine derived from black pepper, which exhibits a broad spectrum of bioactivities. Earlier piperine demonstrated excellent selectivity towards ^{198}Au [1] and ^{51}Cr [2] radioisotopes. In this paper, we have studied the efficacy of piperine in separating ^{90}Nb from α-particle irradiated yttrium target. ^{90}Nb is a positron emitter which has potential application in diagnostic nuclear medicine having a mean β^+ energy of 660 keV with high positron branching of 51%, a half-life of 14.6 h and can be effective for studying biological processes with slow distribution kinetics [3].

2. Experiment

Piperine was isolated from dried fruits of black pepper using ethanol and alcoholic KOH by Soxhlet extraction. The crude extract was purified using petroleum ether and benzene in cold conditions. The purity of the isolated product was checked by melting point, TLC and was characterized by UV-Vis and FTIR spectroscopy. A natural yttrium foil of thickness 3 mg cm^{-2} was irradiated with 34 MeV α- particles for ~10 h at VECC, Kolkata. Analysis of the spectra shows the presence of ^{90}Nb in the matrix which was produced through ^{nat}Y(α, 3n)^{90}Nb reaction. The irradiated yttrium foil was dissolved in a minimum volume of 1M HCl to prepare the radioactive stock solution. To monitor bulk Y, another yttrium foil of the same thickness was irradiated with 46 MeV α- particles which produced ^{87}Y, ^{90}Nb and ^{89}Zr in the matrix. ^{87}Y was separated by an already established method [4] and was spiked in the radioactive stock solution. A range of HCl solutions of varying concentrations was prepared for the SLX (solid-liquid

extraction) procedure. In each case, 100 mg of piperine was added to 3 mL of HCl and 0.1 mL of radioactive stock solution. After incubation for 10 minutes at room temperature (~30 ℃), it was shaken for 20 minutes, and centrifuged for 10 minutes. The piperine being insoluble in an aqueous solution was precipitated. The precipitate and supernatant were collected separately in a 2 mL Eppendorf and subjected to gamma spectrometry in an HPGe detector.

3. Results and Discussion

Figure 1 represents the SLX profile of NCA ^{90}Nb and bulk yttrium using 100 mg piperine and different concentration of HCl. From the separation profile, it is visible that the extraction of ^{90}Nb by piperine is somewhat dependent on the molarity of HCl, a sharp decline in extraction was observed at 1M HCl. The best separation was achieved at 10^{-3} M HCl, when more than 55% of the ^{90}Nb was extracted by piperine with less than 2% contamination of the bulk yttrium.

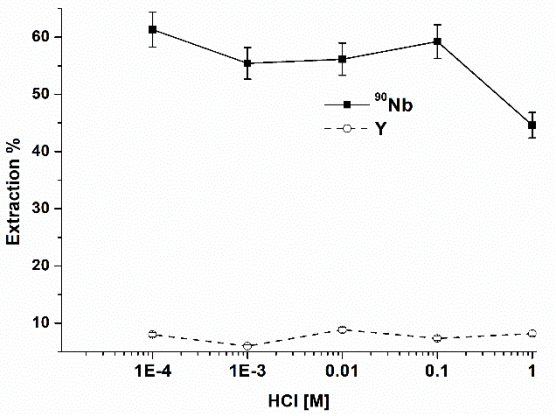

Figure 1: SLX profile of ^{90}Nb and bulk yttrium using piperine at different concentration of HCl

4. Conclusion

The developed method demonstrates the selectivity of piperine towards NCA ^{90}Nb. In this case, an affordable compromise has been made by allowing 2% contamination of the bulk. Contamination may further be reduced with changes in extraction conditions such as temperature, amount of piperine, etc.

Acknowledgements: SM gratefully acknowledges the fruitful discussion with Dr Kalpita Ghosh. Authors also acknowledge Collaborative Research Scheme no UGC-DAE-CSR-KC/CRS/ 19/RC l0/ 0984 of UGC DAE Consortium for Scientific Research, Kolkata Centre. NN acknowledges DST for the DST-INSPIRE fellowship. SL acknowledges CSIR for providing CSIR Emeritus fellowship.

References

/1/ K. Ghosh, S. Lahiri, J. Radioanal. Nucl. Chem. 274 (2007) 233-236

/2/ D. Nayak, K. Ghosh, S. Lahiri, Radioanal. Nucl. Chem. 280 (2009) 503-506

/3/ V. Radchenko, S. Busse, F. Roesch, Nucl. Med. Biol. 41 (2014) 721-727.

/4/ S. Lahiri, B. Mukhopadhyay, N.R. Das, J. Radioanal. Nucl. Chem. 218(2) (1997) 229-231.

Fission of Heavy Elements (HE) and Superheavy Elements (SHE)

*Tilak Kumar Ghosh**
(For the VECC- JINR Dubna Collaboration)

Variable Energy Cyclotron Centre,1/AF Bidhannagar, Kolkata - 700064, India.
Homi Bhabha National Institute, Training School Complex, Mumbai - 400085, India.
*Email: tilak@vecc.gov.in

The synthesis of superheavy elements (SHE), in pursuit of the 'island of stability' on the chart of the nuclei, is one of the foremost goals of today's nuclear physics research [1]. After the two fusing nuclei come into the contact configuration, (i) the di-nuclear system may evolve in shape to form a compact equilibrated heavy nucleus, or (ii) decay into fission-like events before forming a compound nucleus, known as quasi-fission. The competition between these two processes exhibits complex behaviour. The production of SHE requires an understanding of the mechanism of dynamical evolution that the system undergoes after contact. While quasi-fission is believed to be the culprit for the hindrance of the formation of the SHE, it is because of the nuclear shell effects that SHE exists. Under the umbrella of VECC-JINR Dubna Collaboration we have carried out several experiments [2-5] to understand the nuclear shell effects and the role of entrance channel properties on the mechanism of heavy element (HE) and superheavy element (SHE) formation.

The experiments to understand the influence of shell effect on the dynamics of the fusion-fission process and its evolution with excitation energy were carried out in the New Delhi pelletron and Kolkata cyclotron using the MWPC developed at VECC. Beams of ^{16,18}O, ^{19}F and ^{20}Ne were bombarded on several targets of pre-actinides and actinides nuclei producing the heavy elements ($Z < 104$) [4]. The challenge is to understand the asymmetric mass distribution for actinides [6]. These are explained by considering fragment shell properties, the 2nd peak was found to be near the doubly magic shell configuration which is manifested in the exit channel [6, 7]. Our measurement of mass – total kinetic energy distributions of the fragments in the fission of the ^{224}Th nuclei, populated at the similar excitation energy with different entrance channels having different magicity of the targets and projectiles, clearly demonstrate the role of the entrance channel shell effect in fusion-fission dynamics for mass-asymmetric reactions [5]. For the understanding of the fusion process, the role of the loosely bound projectile ^{9}Be in

the fission was investigated through the folding-angle, velocity, and mass distribution of binary fragments at the TIFR-LINAC in Mumbai [8-9]. Understanding the quasi-fission process for the HE elements may help to develop a picture of the reaction mechanism [10-12] around the nuclear chart.

All SHE elements beyond Z=113 discovered to date were synthesized with Ca beam [13-14]. The heaviest target that can be used in the synthesis of SHE experiment is (Z=98) Californium. Thus, for synthesis of new SHE beyond Z=118 requires a beam heavier than Z=20 (Calcium). To understand which projectile heavier than Ca is better for the synthesis of SHE, we have carried out experiments at the Dubna cyclotron facility using CORSET detectors. We investigated [2,3] the decrease of fusion probability in the reaction ^{52}Cr + ^{232}Th and ^{86}Kr+^{198}Pt compared to that in the reactions ^{48}Ca + ^{244}Pu. All the reactions lead to the formation of composite systems with Z = 114 (Flerovium). Cr and Kr-induced reactions were found to have a significant increase in quasi-fission events.

A quick overview of the study of fusion-fission physics related to the synthesis mechanism of HE [15-18] and SHE [2,3] along with new results [4,5] and our recent findings will be presented.

Acknowledgements: The author would like to thank the accelerator staffs and all his collaborators. Funding supports from DAE, DST and RFBR are acknowledged.

References:

/1/ D.J. Hinde, M. Dasgupta, E.C. Simpson, Rep. Prog. Phys. 118 (2021) 103856 and references therein
/2/ A. Sen, T.K. Ghosh, E.M. Kozulin, et al., Phys. Rev. C 105 (2022) 014627.
/3/ K. Kozulin, T.K. Ghosh, et al., Phys. Rev. C. 99 (2019) 014616.
/4/ K. Atreya, T.K. Ghosh, A. Nasirov, et al., (Under preparation).
/5/ A. Sen, T.K. Ghosh, et al., (Under review).
/6/ The Nuclear Fission Process, edited by C. Wagemans (CRC Press, Boca Raton, FL) 1991.
/7/ Wakhle et al., EPJ Web Conf. 35 (2012) 05008.
/8/ D. Paul, A. Sen, T.K. Ghosh, et al., Phys. Rev. C 104 (2021) 024604.
/9/ D. Paul, A. Sen, T.K. Ghosh, et al., Phys. Rev. C 102 (2020) 054604.
/10/ A.N. Andreyev, K. Nishio, K-H. Schmidt, Rep. Prog. Phys. 81 (2018) 016301 and references therein
/11/ N. Kumar, D.C. Biswas, T.K. Ghosh, et al., Phys. Rev. C 99 (2019) 041602.
/12/ Kavita, K.S. Golda, T.K. Ghosh, et al., Phys. Rev. C 100 (2019) 024626.
/13/ M. Itkis, E. Vardaci, et al., Nuclear Phys. A 944 (2015) 204 and references therein
/14/ E. Vardaci, et al., J. Phys. G: Nucl. Part. Phys. 46 (2019) 103002.
/15/ A. Chaudhuri, PhD thesis, HBNI (2019).
/16/ T.K. Ghosh, Cur. Sci. 116 (2019) 25.
/17/ S. Bhattacharya, C. Bhattacharya, P. Das, et al., Eur. Phys. J. A 54 (2018) 158.
/18/ A. Sen, T.K. Ghosh, et al., Phys. Rev. C 96 (2017) 064609.

The Study of Multiplicity Distributions for Prompt Neutrons Emitted in Spontaneous Fission of Trans-fermium Isotopes

R.S. Mukhin[1], A.V. Isaev[1], A.V. Andreev[1], M.L. Chelnokov[1], V.I. Chepigin[1], I.N. Izosimov[1], A.A. Kuznetsova[1], O.N. Malyshev[1,2], A.G. Popeko[1,2], Y.A. Popov[1,2], A. Rahmatinejad[1], B. Sailaubekov[1,3], T.M. Shneidman[1], E.A. Sokol[1], A.I. Svirikhin[1,2], M.S. Tezekbayeva[1,3], A.V. Yeremin[1,2]*

[1]Joint Institute for Nuclear Research, Dubna, Russia.
[2]Dubna State University, Dubna, Russia.
[3]Institute of Nuclear Physics, Almaty, Republic of Kazakhstan.
*Email: rmukhin@jinr.ru

1. Introduction

The spontaneous fission is one of the decay channels on a par with α- and β+-decays for heavy and super-heavy isotopes (Z > 100). The spontaneous fission is a complicated process that still could not be described by sufficiently reliable theory because of varying of possible final configurations of the system. There are a several theoretical models of the process (for example, semi-empirical [1] or fully-theoretical [2-3]) but none of them can describe well all known nucleus that could decay by spontaneous fission. Therefore, experimental studies of such processes are high-interesting and important.

2. Experiment

Due to the fact that most of isotopes of trans-fermium elements have an extremely short halve-live and extremely low formation cross-section (can be as low as 10^{-12} barn) that is impossible to carry out traditional offline experiments with chemical separation of nucleus of interest from the isotopes that were produced in competitive reactions. Because of that we have to use an online "in-beam" technique that involves the use of kinematic separator (velocity filter) SHELS [4] to clean up the nucleus of interest and direct them to the detection system SFiNx [5]. The SFiNx (single neutron registration efficiency ≈55%) consists of double-sided Si strip detector box surrounded by more than 100 ^{3}He-filled neutron counters. The main characteristic measured by setup is the multiplicity distribution of prompt neutrons

emitted in spontaneous fission of trans-fermium isotopes that were produced in complete fusion reactions with a few neutrons evaporation.

3. Results and Discussion

In a series of experiments prompt neutron multiplicity distributions were obtained for the following neutron-deficient isotopes: ^{246}Fm, ^{250}No, ^{252}No, ^{254}No, ^{256}Rf. In addition, the same characteristic was observed for ^{244}Cm, ^{248}Cm, ^{252}Cf (with using the sources). Since the registration efficiency of the SFiNx is far from 100% the measured distribution is heavily distorted in comparison with the original one and needs to be reconstructed. To reconstruct distributions, the Tikhonov regularization technique has been used [6].

After reconstruction, it is possible to roughly divide all distribution into two groups: symmetrical and asymmetrical. The asymmetry of the distribution of prompt neutrons emitted in spontaneous fission could point to the possible exotic mode of spontaneous fission.

In the report, such distribution in conjunction with spectra of total kinetic energies of fragments and theoretical predictions are shown. The technique to restore multiplicity distribution is discussed either.

References

/1/ K-H. Schmidt, et al., GEF model, © OECD (2014).

/2/ A.V. Andreev, et al., Eur. Phys. J. A 30 (2006) 579-589.

/3/ A.V. Isaev, et al., Eur. Phys. J. A 58 (2022) 108.

/4/ A.G. Popeko, et al., Nucl. Instrum. Methods Phys. Res. B 376 (2016) 140-143.

/5/ A.V. Isaev, et al., PEPAN Let. 19, (2022) 37-45.

/6/ R.S. Mukhin et al. PEPAN Let. 18, (2021) 439.

Preparation and Evaluation of a [^{64}Cu]Cu-Labeled Porphyrin Derivative: Investigating the Utility of Carrier-added Copper Towards Preparation of Porphyrin-based Multi-modal Agent

*Naveen Kumar[1,2], Mohini Guleria[1,2], Sandeep Shelar[3], Jeyachitra Amirdhanayagam[1], Tapas Das[1,2]**

[1]Radiopharmaceuticals Division, Bhabha Atomic Research Centre, Mumbai 400085, India.
[2]Homi Bhabha National Institute, Anushaktinagar, Mumbai 400085, India.
[3]Chemistry Division, Bhabha Atomic Research Centre, Mumbai 400085, India.
*E-mail: tdas@barc.gov.in

1. Introduction

Porphyrins have long been explored and are still studied for their natural tendency of exhibiting preferential accumulation in the neoplastic tissues [1]. This feature of porphyrin-based macrocyclic ligands has prompted their investigation for possible use in multi-modal utilities viz. fluorescence cell imaging, *in-vivo* optical imaging, photodynamic therapy (PDT) as well as in nuclear medicine.

2. Experiment

An unsymmetrically substituted porphyrin derivative, 5-carboxymethyleneoxyphenyl-10,15,20-tris(4-methoxyphenyl)porphyrin (UTriMA) was synthesized via a three-step reaction procedure. All the intermediates and final products were purified and characterized by standard techniques viz. UV-Vis, FT-IR, ^{1}H- and ^{13}C-NMR spectroscopy as well as mass spectrometry. A copper complex of UTriMA (Cu-UTriMA) was synthesized using non-radioactive metal and was characterized by UV-Vis spectroscopy and mass spectrometry. Both UTriMA and Cu-UTriMA were evaluated for their differential ability, if any, towards the generation of singlet oxygen using diphenylisobenzofuran (DPBF). Both UTriMA and its copper complex were evaluated for light-dependent toxicity by carrying out *in-vitro* studies in A549 (lung adenocarcinoma) and MCF7 (breast cancer) cells. Radiolabeling of UTriMA with ^{64}Cu was carried out by optimization of various reaction parameters viz. ligand concentration, time of incubation and specific activity of ^{64}Cu. Copper-64 was obtained via (n,γ) reaction

using natural copper (^{63}Cu) as a target. The specific activity of ^{64}Cu utilized in the present study was 20-25 mCi/mg (740-925 MBq/mg) which was low due to the presence of inactive isotopes of copper (^{63}Cu and ^{65}Cu). The percentage radiochemical purity of the radiolabeled complex was determined using RP-HPLC using a gradient elution system as shown in figures 1a and 1b.

3. Results and Discussion

The results of the present study demonstrated the suitability of low specific activity carrier-added ^{64}Cu towards the preparation of a radiolabeled in-house synthesized porphyrin derivative which could be prepared with a radiochemical purity of ~90 %. The ^{nat}Cu-porphyrin complex was found to exhibit a reduced ability to generate singlet oxygen compared to free-base porphyrin. This resulted in a reduction in the photocytotoxic potential of the former during *in vitro* studies in two different cancer cell lines, thereby weakening its candidature for dual-modality applications [2].

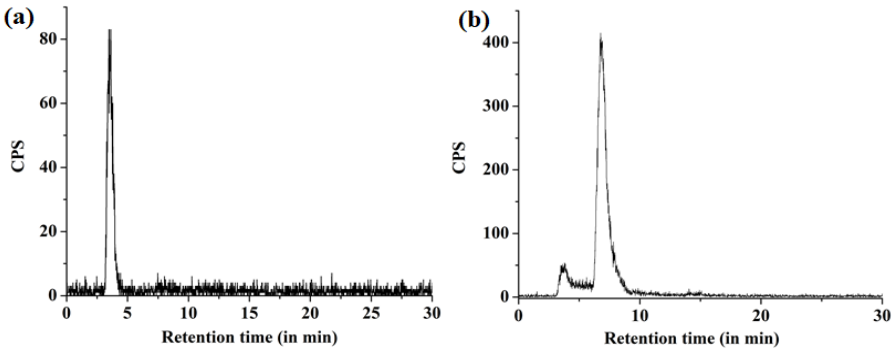

Figure 1**:** HPLC chromatograms of (a) free ^{64}Cu as $^{64}CuCl_2$ and (b) ^{64}Cu-labeled-UTriMA

4. Conclusion

Due to relatively inferior optical properties of porphyrin-copper complex, its utility as a dual modality agent may prove futile. However, such complexes may have potential as positron imaging tomography (PET) agent for scanning tumorous lesions.

Acknowledgements: The authors acknowledge Dr S. Kannan, Director, RC&IG, BARC for his support and encouragement and the colleagues from Radiochemical Section, Radiopharmaceuticals Division for providing ^{64}Cu.

References

/1/ M. Bhadwal, T. Das, H.D. Sarma, et al., Mol. Imaging Biol. 17 (2015), 111-118.

/2/ H. Ren, C. Liu, W. Yang, et al., Dyes Pigments 200 (2022) 110117.

Production and Separation of No-carrier Added ^{129}Cs from Alpha Induced Reactions on KI Target

Kousiki Ghosh[1], Nabanita Naskar[2], Susanta Lahiri[2,3]*

[1]Health Physics Division, Bhabha Atomic Research Centre, Trombay, Mumbai-400085, India.
[2]Diamond Harbour Women's University, Diamond Harbour Road, Sarisha, South 24 Parganas 743368, India.
[3]Sidho-Kanho-Birsha University, Ranchi Road, Purulia 723104, India.
*E-mail: kousiki@vecc.gov.in

1. Introduction

Production and separation of various important radionuclides produced from different light and heavy ion induced reactions on halide targets are being carried out for last few years in our laboratory [1-3]. In the present study KI was used as the target. Previously NaI was used as iodide target by researcher with long-lived ^{22,24}Na radio contaminants. Whereas here short-lived ^{44m}Sc is co-produced. ^{129}Cs was produced via ^{127}I(α, 2n)^{129}Cs reaction. ^{129}Cs is one of the potential radionuclides for heart imaging. Minute amount of co-produced ^{44m}Sc had been separated from ^{129}Cs.

2. Experiment

Irradiation details and separation technique: KI pellet targets of diameter 1 cm and thickness 1 mm were prepared at VECC target laboratory. These targets were irradiated with 36 MeV alpha particle with 300 nA beam current for 4 h. LLX separation technique was used to separate ^{129}Cs and ^{44m}Sc, using 18-crown 6 ether in nitrobenzene as organic and $HClO_4$ as aqueous phase.

3. Results and Discussion

Signatures of ^{129}Cs and trace amount of ^{44m}Sc radioisotopes were detected in the gamma spectrum of α-particle irradiated KI target. The nuclear properties and yield of different radioisotopes have been tabulated in Table 1. The extraction profiles of ^{129}Cs and ^{44m}Sc at varying $HClO_4$ and 18-Crown 6 concentrations, have been presented in Fig 1 and Fig 2 respectively. It was observed that NCA ^{44m}Sc remained quantitatively in the aqueous phase throughout the experiment while ^{129}Cs was extracted into 18-Crown 6 ether. The maximum extraction of ^{129}Cs has been achieved at 0.1 M $HClO_4$ and 0.1 M 18-

Crown 6 ether concentration. With ionic radii of 1.7 Å, Cs^+ is compatible with the cavity size (1.45±0.15 Å) of crown ether which leads to formation of stronger and stable complex with 18-Crown 6 ether molecules [4]

Table 1: Nuclear properties of different radioisotopes associated with the present study

Radiotracer ($T_{1/2}$)	E_γ, keV, (I_γ, %)	Probable contributing reaction	E_{th}, MeV	Yield, kBq
^{129}Cs (32.06 h)	371.9 (30.6), 411.5 (22.3), 548.94 (3.4)	^{127}I(α, 2n)^{129}Cs	15.68	558.1±64.2
^{44m}Sc (58.6 h)	271.13 (86.7)	^{41}K(α, n)^{44m}Sc	3.72	2.60±0.32

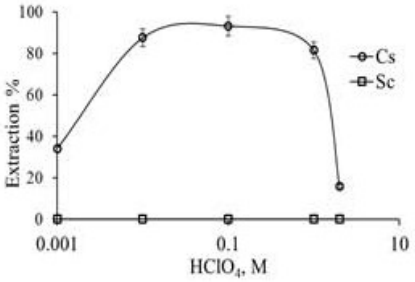

Fig 1: Extraction profile: varying $HClO_4$ conc.

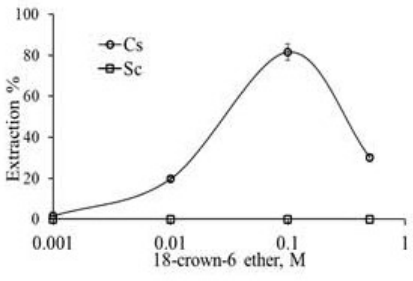

Fig 2: Extraction profile: varying 18-Crown 6 conc.

4. Conclusion

Production and separation of ^{129}Cs from alpha particle irradiated KI targets have been demonstrated. The limitation of this process is that the amount of ^{44m}Sc produced is not sufficient for practical application. Significant production of 558 kBq for ^{129}Cs has been obtained. Successful separation of ^{129}Cs from minute quantity of ^{44m}Sc has been achieved by LLX technique.

Acknowledgement: The cooperation from cyclotron staffs and target laboratory staffs of VECC is highly acknowledged. KG is thankful to Dr M S Kulkarni and Dr R Ravishankar for their constant support and encouragement. SL is thankful to CSIR for providing emeritus scientist project. NN is thankful to DST for providing DST-Inspire Faculty fellowship.

References

/1/ K. Ghosh, D. Choudhury, S. Lahiri, J Radioanal. Nucl. Chem. 321 (2019) 91.

/2/ K. Ghosh, D. Choudhury, S. Lahiri, Appl. Radiat. Isot. 178 (2021) 109966.

/3/ K. Ghosh, N. Naskar, S. Lahiri, J. Radioanal. Nucl. Chem., 331 (2022) 483.

/4/ K. Mukhopadhyay, D. Nayak, S. Lahiri, Radioact. Radiochem. 11 (2000) 19.

Model Calculation for α-induced Reactions of Theranostic Applications

Pankaj K. Giri, S. S. Ghugre, R. Raut*

UGC-DAE Consortium for Scientific Research, Kolkata Center, Kolkata-700106, India.
*Email: pankajcuj@gmail.com

1. Introduction

Some of the α-induced reactions provide pathways for the production of radioisotopes important in therapeutic and diagnostic applications. These isotopes may be of use in diagnostic techniques, such as ^{30}P, ^{38}K, ^{77}Br, ^{95,97}Ru, ^{147}Gd etc., used in PET and SPECT, or in radiotherapy, such as ^{211}At, ^{77}Br or isomers ^{193m}Pt, ^{195m}Pt and, ^{117m}Sn used for precision/targeted therapy. Objective of theoretical modelling of reactions that produce these isotopes is to reproduce the experimental cross section in the model calculations and, in the process, identify the different parameters that impact the results.

2. Methodology and Results

Here, the calculations have been carried out using the TALYS [1] framework owing to the comprehensive choice of models and adjustable parameters included therein. Some of the parameters/factor that impact the calculated cross-sections include optical model potential (OMP), level density (LD), gamma strength function (GSF) and pre-equilibrium (PE) modelling. Different sets of these parameters have been used to calculate the reaction cross-sections of interest and the results have been compared for overlap with the data available in the EXFOR [2] database. The nuclear reactions producing radioisotopes of medical use have been identified from the IAEA database [3] and/or the available literature. Some of these are ^{50}Cr(α,2n)^{52}Fe, ^{63}Cu(α,n)^{66}Ga, ^{72}Ge(α,3n)^{73}Se, ^{75}As(α,3n)^{76}Br, ^{85}Rb(α,3n)^{86}Y, ^{89}Y(α,3n)^{90}Nb, ^{108}Cd(α,2n)^{110}Sn, and ^{209}Bi(α, 2n)^{211}At etc. Figure 1 illustrates the plots for comparison between the calculated and the experimental cross-sections of the ^{50}Cr(α,2n)^{52}Fe and (α, 2n)^{211}At reactions. It has been generally noted that the α-OMP of Avrigeanu et al. [4] and GSF from Brink-Axel Lorentzian [1] have resulted in reasonable compliance of the calculated cross-sections with the experimental ones. As far as the LD model is concerned the Constant Temperature + Fermi gas model

(CTM) or the Back-shifted Fermi gas Model (BFM) or the Generalised Super fluid Model (GSM) or the Skyrme-Hartree-Fock-Bogoluybov have been used for different reactions. The exciton model (that includes numerical transition rates with energy-dependent matrix) was used for the pre-equilibrium processes. PACE-4 [5] calculated cross-sections are also shown for comparison. PACE-4 is a statistical model code based on Hauser-Feshbach formalism.

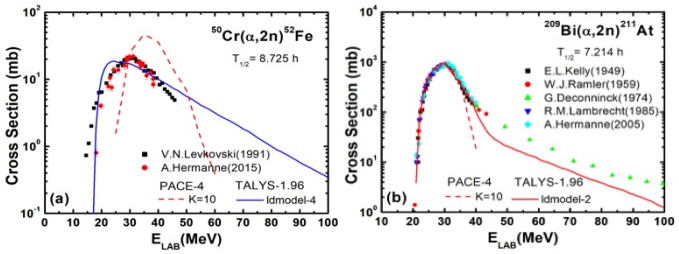

Figure 1: Excitation functions for the ^{52}Fe and ^{211}At radioisotopes along with theoretical prediction

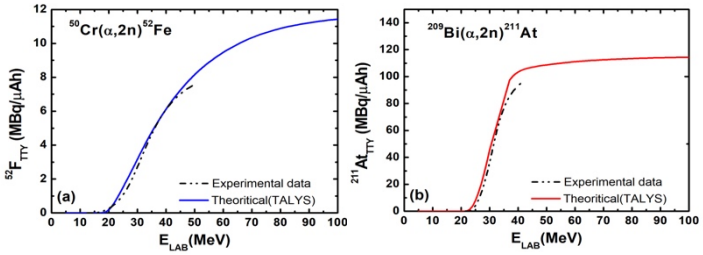

Figure 2: Thick target yield curves for the radioisotopes ^{52}Fe and ^{211}At. The experimental best fits are shown by dashed line, whereas the TALYS optimized model predicted excitation functions are represented by solid lines

The calculations have also been extended to estimate the thick target yield (TTY) of radioisotopes of interest. The calculated TTY have been compared with those estimated using the recommended cross-section data, as illustrated in Figure 2. Efforts are in progress to further optimize the parameters of the calculations and identify those that would be applicable to a wider variety of reactions.

Acknowledgements: This work has been carried out under the funding [CRG/2021/001011] received from SERB (DST), GOI.

References

/1/ A.J. Koning, et al., Proc. of the Internat. Conf. on Nucl. Data for Sc &Technol, (2008) 211-214.

/2/ N. Otuka, et al., Nucl. Data Sheets 120 (2014) 272; https://www-nds.iaea.org/exfor/

/3/ https://www-nds.iaea.org/relnsd/vcharthtml/MEDVChart.html

/4/ V. Avrigeanu, et al., Phys. Rev. C 90 (2014) 044612.

/5/ O.B. Tarasov, D. Bazin, NIM B 266 (2008) 4657; A. Gavron, Phys. Rev. C 21 (1980) 230.

Synthesis of *γ*-Irradiated CuS-Graphene Nanoparticles for Selective Detection of Cancer Biomarker CA-125

*Shalmali Basu[1], Kamalika Sen[1]**

[1]Department of Chemistry, University of Calcutta, 92, APC Road, Kolkata 700009, India.
*Email: kamalchem.roy@gmail.com; kschem@caluniv.ac.in

1. Introduction

Carbohydrate antigen 125 (CA 125) is a high molecular weight glycoprotein which is predominantly used for early-stage diagnosis of ovarian cancer [1]. Conventional methods for CA 125 detection like electrophoretic assay, immune-sensing, etc., are complex, time-labour-cost consuming processes [2]. Nanoparticles (NPs) are often used for sensing as they have a high surface area, surface charge, good surface chemistry, etc. Graphene has exceptional chemical, mechanical, electrical properties and is often used for modification of metal nanoparticles. Here we have synthesized copper sulphide nanoparticles (CuS-NP) using a polyphenol epigallocatechin gallate (EGCG), graphene nanoplatelets (Gr) and gamma irradiation (CuS-Gr-γ-NP) to explore it's *in vitro* sensing towards CA-125 in serum medium.

2. Experiment

CuS-Gr-NP was synthesized and then subjected to gamma radiation (total dose 30 kGy) (CuS-Gr-γ-NP). UV-visible absorption spectroscopy of CA 125 (5 U/mL) in presence of interfering biomolecules like dextrose, cholesterol (1 mM each), actrapid and huminsulin (40 mIU/mL each) was performed both in the presence and absence of the NPs (0.15 mg/mL) in serum medium to mimic the biological condition.

3. Results and discussion

TEM micrographs (Figure 1) show the average size of CuS-NP and CuS-Gr-NP are 10-12 nm and 18-20 nm respectively. γ-irradiation has reduced the size of CuS-Gr-γ-NP to a great extent (5-8 nm) and as a result, the effective surface area of CuS-Gr-γ-NP has increased for its better binding with CA-125.

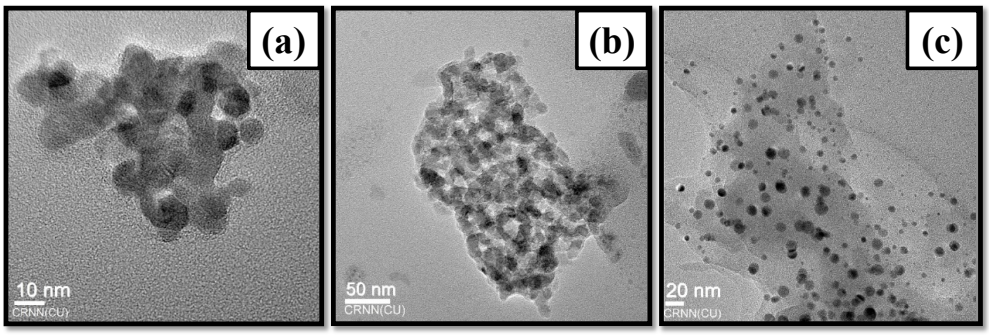

Figure 1: TEM of (a) CuS-NP, (b) CuS-Gr-NP, (c) CuS-G-γ-NP

Upon γ-irradiation, FTIR study shows radiolysis products of water interact with EGCG on the surface of CuS-Gr-γ-NP and thus van der Waal's interaction between CuS-NP and Gr is weakened. Peak at 1473 cm^{-1} appears due to -C-H stretching of EGCG disappearing upon incorporation in graphene. γ-irradiation causes this peak to reappear with lower intensity and lower energy due to thinning out of the EGCG layer and charge accumulation on NP surface (also supported by TEM images). Due to the charged nature and higher surface activity, CuS-Gr-γ-NP offers higher sensitivity for CA 125 (Table 1).

Table 1. LOD values of CA 125 at the different experimental conditions

NP variants	**Conditions**				
	LOD (U/mL)				
	None	**Dextrose (D)**	**Cholesterol**	**Actrapid (A)**	**Huminsulin (H)**
CA 125	0.070	0.031	0.056	0.057	0.049
CA-125+CuS	0.031	0.026	0.037	0.045	0.045
CA 125+CuS-Gr	0.024	0.027	0.032	0.040	0.035
CA-125+CuS-Gr-γ	0.019	0.015	0.007	0.029	0.029

Synthesized NPs were not sensitive to CA 19-9 and CEA confirming their good specificity for CA 125 sensing. CD spectroscopy shows CuS-Gr-γ-NP causes perturbation in the native conformation of CA 19-9 and CEA whereas the native structure of CA 125 remains somewhat unperturbed.

4. Conclusion

This study is a novel method for the detection of CA 125 in presence of several common physiological parameters that give rise to comorbidities. LOD value for CA 125 is lower for the graphene modified γ-irradiated NPs and even lower in presence of these disease-causing biomolecules.

References

/1/ N. Guo, Z. Peng, Z. Journal of Ovarian Research. 10 (2017) 1-7.

/2/ R. Aebersold, M. Mann. Nature. 422 (2003) 198-207.

Radiochemical Synthesis of ^{68}Ga-FAPI-4 Using In-house Developed Freeze-Dried Kit and Its Biological Evaluation

N. Sakhare[1], A. Mitra[1], L. Ram[1], S. Sana[1], A. Chakraborty[2], B. Sanjeevkumar[1], S. Sahu[2], A. Ghodke[1], R. Tiwari[1], A. Seema[1], A. Mathur[1], U. Pandey[1]*

[1]RPL, BRIT, Vashi, Navi Mumbai 400 703, India.
[2]RMC, BARC, Parel, Mumbai 400 012, India/
*Email: navin.sakhare@britatom.gov.in

1. Introduction

Fibroblast activation protein (FAP) is a Type II transmembrane serine protease. FAP is over-expressed on activated stromal fibroblasts and pericytes of most common human epithelial tumors such as lung, colon, pancreatic carcinomas etc. Among various FAP inhibitors (FAPI), ^{68}Ga labeled FAPI-4 a quinoline-based fibroblast activation protein (FAP) was found to have prolonged tumor retention on PET/CT imaging of cancer patients with solid tumors. Herein, we report the development of ready-to-use single vial freeze dried kit formulation of FAPI-4 for radiochemical synthesis of [^{68}Ga]Ga-FAPI-4. In this work, protocol for radiolabeling of in-house produced FAPI-4 freeze dried kit with [^{68}Ga]$GaCl_3$ was established. Efficacy of the in-house developed FAPI-4 freeze dried kit was established by performing quality control, *in-vitro* and *in-vivo* pharmacokinetic studies of the ^{68}Ga labeled product.

2. Experiment

2.1 Preparation of FAPI-4 freeze dried kit: Kit formulation was carried out in a clean room facility. A stock solution of FAPI-4 (1 mg/mL, MedChem Express, USA) was prepared by dissolving in ultrapure water. Aliquots of 50 µL (50 µg) of FAPI-4 were aseptically dispensed in sterile glass vial containing 0.43 N CH_3COONa (550 µL). The contents of the vial were lyophilized in freeze drier for 20 hours and sealed under vacuum. The freeze-dried vials were stored at -20°C until use. Stability of FAPI-4 freeze dried kit was evaluated for 3 months.

2.2 Radiolabeling of FAPI-4 freeze dried kit vial with [^{68}Ga]GaCl$_3$: One kit vial was thawed to ambient temperature. [^{68}Ga]GaCl$_3$ (~30 mCi) eluted in 4 mL of 0.05M HCl from a ^{68}Ge/^{68}Ga generator was added to it and mixed well. The reaction mixture was incubated at 95°C for 15 minutes.

2.3 Quality Control Studies of ^{68}Ga]Ga-FAPI-4: Radiochemical purity (RCP) was ascertained by radio-TLC (60A^o silica-gel, 0.1M sodium citrate buffer: pH-5.0) and radio-HPLC (Mode: gradient, Solvent: H_2O and CH_3CN with 0.1% TFA, UV: 220 nm & Flow rate: 1 mL/min) using reverse phase C18 column coupled with NaI(Tl) and UV detector. Stability of the [^{68}Ga]Ga-FAPI-4 was evaluated by radio-TLC and radio-HPLC up to 2h post-radiolabeling.

2.4 *In-vitro & In-vivo Pharmacokinetic Studies:* Human colorectal cell-line HT-29 expressing FAP was used for *in-vitro* evaluation. Cells were grown in McCoy's medium. HT29 cells were incubated with 1mL of internalization buffer (DMEM, 0.2% BSA) containing radioligand (~5x10^{-12} mol) for 15, 30, 60 & 120 min followed by washing with Phosphate Buffer Saline. Non-specific binding was assessed by co-incubation with cold FAPI-4. Biodistribution studies were performed in nude mice bearing tumor xenograft induced by HT29 cell lines and mice were sacrificed at 30 and 60 min post-injection of ^{68}Ga-FAPI-4.

3. Results and Discussion

3.1 Radiolabeling and Quality Control: Using one freeze dried FAPI-4 kit, ~18-20 mCi of [^{68}Ga]-FAPI-4 (4 patient doses) was prepared (n=3). [^{68}Ga]-FAPI-4 solution was observed to be clear and colorless, with pH between 4.0-6.0 RCP of [^{68}Ga]-FAPI-4 estimated by radio-TLC and radio-HPLC was >98% (n=3) with R_f: 0.0-0.1 and R_t: 13.5-14.5 minutes respectively in the radio-TLC and radio-HPLC system. [^{68}Ga]-FAPI-4 retained >98 % RCP up to 2h post-radiolabeling at ambient temperature (25^{o}C).

3.2 Cell Binding and Bio-distribution: [^{68}Ga]Ga-FAPI-4 showed good binding with HT29 cells (25-26%), reaching a plateau after 30 min. On incubation with 100 pico mole of cold FAPI-4, binding was reduced to 1.8-2.5% confirming the specificity of ^{68}Ga-FAPI-4. In the bio-distribution study, high uptake of ^{68}Ga-FAPI-4 was found in tumor (5.5 % ID/g) at 60 min post-injection with less retention in non-target organs.

[^{68}Ga]Ga-FAPI-4 could be formulated using in-house developed freeze-dried kit with RCP >98%. Neither pre-concentration of [^{68}Ga]GaCl$_3$ nor purification of final product was required in our optimized protocol. Results of pharmacokinetic studies demonstrate the potential of the kit-based [^{68}Ga]Ga-FAPI-4 for tumor imaging in patients.

Actinide Molecular Ion Beams At CERN-ISOLDE

Mia Au[1,2], Michail Athanasakis-Kaklamanakis[1,3], Jochen Ballof[4], Paul Fischer[5], Ulli Köster[6], Bruce Marsh[1], Maxime Mougeot[1,7], Lukas Nies[1,5], Jordan Reilly[8], Moritz Schlaich[9], Christoph Schweiger[1,10], Simon Stegemann[1], Frank Wienholtz[9], Wiktoria Wojtaczka[3], Christoph E. Düllmann[2,11,12], Sebastian Rothe[1]*

[1] CERN, CH-1211 Geneva 23, Switzerland.
[2]Johannes Gutenberg-Universität Mainz, 55099 Mainz, Germany.
[3]KU Leuven, B-3001 Leuven, Belgium.
[4]FRIB, Michigan State University, 48824 East Lansing, USA.
[5]Universität Greifswald, 17489 Greifswald, Germany.
[6]Institut Laue-Langevin, 38000 Grenoble, France.
[7]University of Jyväsklyä, 40014 Jyväsklyä, Finland.
[8]University of Manchester, M139PL Manchester, UK.
[9]Technische Universität Darmstadt, 64289 Darmstadt, Germany.
[10]Max-Planck-Institut für Kernphysik, 69221 Heidelberg, Germany.
[11]GSI Helmholtzzentrum für Schwerionenforschung, 64291 Darmstadt, Germany.
[12]Helmholtz Institute Mainz, 55099 Mainz, Germany.
*Email: mia.au@cern.ch

1. Introduction

Actinide elements have unique atomic and nuclear properties that lead to applications in astrophysics, environmental monitoring, energy production, and medicine. The lack of availability of many of these rare and radioactive isotopes currently limits their study and use. The ISOLDE facility at CERN [1] provides experiments with a wide range of isotopes across the nuclear chart, produced in nuclear reactions between accelerated protons and thick targets. This Isotope Separation On-Line (ISOL) method can be used to produce several of the light actinides.

Release-limited refractory elements have been successfully converted into volatile compounds to improve their extraction [2-6]. Delivering isotopes as molecular ions is also one technique employed to reduce isobaric contamination and improve beam purity. Beyond their uses for the extraction and purification of ion beams, molecules themselves provide opportunities towards development of new physics beyond the standard model [7,8]. Developing actinide molecular ion beams at ISOL facilities is thus of high interest within and beyond the scientific community

2. Experiment

Isotopes were produced at ISOLDE by the irradiation of porous uranium-238 carbide target with 1.4 GeV protons from CERN's Proton Synchrotron Booster. Reaction products then diffused and effused through the target matrix. Reactive tetrafluoro-methane (CF_4) gas was injected into the target unit to form fluoride molecules, which were then ionized using a hot plasma ion source. The ion beams were extracted and separated by mass-to-charge ratio. The composition of ion beams including atomic ions and molecular sidebands was further studied using several techniques. Mass separation and isobaric identification of the ion beams were done with the ISOLTRAP Multi-Reflection Time-of-Flight Mass Spectrometer (MR-ToF MS) [9]. Ion beams were sampled at the ISOLDE tape station [1,10] for online γ-ray spectroscopy and detection of β decays. Additionally, α- and γ-ray spectrometry were performed by implanting samples of the mass-separated ion beams into foils for off-line measurement.

3. Results and discussion

Mass spectrometry and decay spectroscopy indicate the presence of several isotopes of the light actinides actinium, neptunium, and plutonium as fluoride molecular ion beams in addition to the formation of uranium molecules from the target material. The results presented in this work add to the selection of actinides and heavy radioactive molecules available for experiments at ISOL facilities.

Acknowledgements: The authors gratefully acknowledge technical support from B. Crepieux, M. Owen, and ISOLDE operations. This project has received funding from the European Union's Horizon 2020 Research and Innovation Program under grant agreement number 861198 project 'LISA' (Laser Ionization and Spectroscopy of Actinides) Marie Sklodowska-Curie Innovative Training Network.

References

/1/ R. Catherall et al., Nucl. Inst. and Meth. B. 62 (1992) 535.
/2/ R. Eder et al., Nucl. Inst. and Meth. B. 62 (1992) 535.
/3/ R. Kirchner, Nucl. Inst. and Meth. B. 126 (1997) 135
/4/ H. Frånberg et al., Rev. Sci. Inst. 77 (2006) 03A708.
/5/ J. Ballof et al., Eur. Phys. J. A. 55 (2019) 65
/6/ U. Köster et al., Eur. Phys. J. Special Topics 150 (2007) 293.
/7/ M. Safronova et al., Rev. Mod. Phys. 90 (2018) 025008.
/8/ R. Garcia-Ruiz et al., Nature. 581 (2020) 396.
/9/ R. Wolf et al., Int. J. Mass Spec. 123 (2013) 349.
/10/ C. Neacşu et al., Nucl. Inst. and Meth. A 1026 (2022) 166213.

Thermodynamic Properties of ^{69}Zn Nucleus

Enakshi Senapati[1], S Mondal[2], S Bhattacharya[3], D Pandit[4], N. Dinh Dang[5], N. Ngoc Anh[6], L. T. Q Huong[7], R Santra[8], N. Q. Hung[8], B. Dey[9]*

[1]Department of Physics, Bankura University, Bankura 722155, India.
[2]Department of Physics, Bankura University, Bankura 722155, India.
[3]Department of Physics, Barasat Govt. College, Barasat, North 24 pgs 700124, India.
[4]Variable Energy Cyclotron Centre,1/AF-Bidhannagar, Kolkata 700064, India.
[5]RIKEN Nishina Centre for Accelerator-Based Science, RIKEN, 2-1 Hirosawa, Saitama, 351-0198, Japan.
[6]Dalat Nuclear Research Institute, Vietnam Atomic Research Institute, Dalat, Vietnam.
[7]Department of Natural Science and Technology, Khanh Hoa University, Nha Trang City, Vietnam.
[8]Institute of Fundamental and Applied Sciences, Duy Tan University, Ho Chi Minh City, Vietnam.
[9]Faculty of Natural Sciences, Duy Tan University, Danang City, Vietnam.
*Email: enakshisenapati2194@gmail.com

1. Introduction

Thermal motion of nuclei and their corresponding properties play a decisive role in nuclear physics. In a macroscopic conductor, the pairing phase transition is characterized by the sharp discontinuity in the heat capacity at the transition temperature [1]. In case of nucleus, as the nuclear radius is much smaller than the pair coherence length, large fluctuations are expected to suppress the sharp discontinuity, and leads to a shallow "kink" (looks like "S-shape") in the heat capacity at the transition temperature [2].

Till now, these kind of pairing phase transitions are observed mostly in the even-even nuclei [3,5] due to the breaking of nucleonic Cooper pairs at transition temperature. However, very recently, an S-shaped heat capacity has been observed in odd-odd deformed hot-rotating ^{184}Re nucleus, indicating the deformation-induced pairing as one of the possible reason [4]. A similar discontinuity in the heat capacity has also been found in even-odd ^{183,185}W nuclei [5]. Such observation has motivated us to carry out further investigation in odd-odd and even-odd systems in different mass regions, particularly in those nuclei which are important for nucleosynthesis, especially in slow (s) and rapid (r) neutron capture processes.

2. Experiment

We have investigated the pairing phase transition in an odd-even hot rotating ^{69}Zn nucleus by using the nuclear level density (NLD) data, which were experimentally extracted from the γ-gated particle spectra

[6]. The experimental NLDs have been compared with those obtained in the calculations within the microscopic exact pairing plus independent-particle model (EP+IPM) at finite temperature along with the results of other microscopic calculations such as Hartree-Fock BCS (HFBCS) and Hartree-Fock-Bogoliubov combinational (HFBC) method. It is found that the experimental NLDs can be well described by the EP+IPM using the recommended quadrupole deformation parameter β_2 rather than by HFBCS and HFBC [7].

3. Results & Discussions

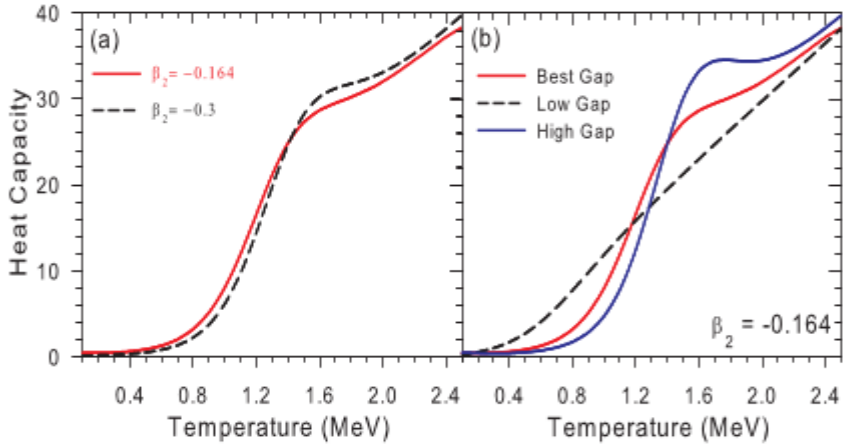

Figure 1: Heat capacities of ^{69}Zn as functions of temperature obtained by using the EP+IPM NLDs for $\beta_2 = -0.164$ and -0.3 MeV (a) as well as different values of pairing gap (b).

The heat capacity calculated using the EP+IPM NLD exhibits in Fig. 1(a) a sharp S-shape, which is not expected in such an even-odd system as reported earlier. Slightly adjusting the deformation parameter β_2 does not change much in this S-shape. However, in Fig. 1(b) increasing or decreasing the pairing gaps could enhance or destroy the S-shaped heat capacity. Therefore, the S-shaped heat capacity in an even-odd ^{69}Zn nucleus could be explained due to the deformation-induced pairing correlation [7].

References

/1/ B. Muhlschlegel, D. J. Scalapino, R. Denton, Phys. Rev. B 6 (1972) 1767.

/2/ S. Liu, Y. Alhassid, Phys. Rev. Lett. 87 (2001) 022501.

/3/ R. Chankova et al., Phys. Rev. C 73 (2006) 034311.

/4/ B. Dey et al., Phys. Lett. B 789 (2019) 634.

/5/ K. Kaneko, M. Hasegawa, Phys. Rev. C 72 (2005) 024307.

/6/ R. Santra et al., Phys. Lett. B 806 (2020) 135487.

/7/ E. Senapati, S. Mondal, communicated.

Preparation of The Radiolabeled Tracer to Quantify C-reactive Protein – A Cardiac Marker

Tanhaji S Ghodke[1], *Shalaka Paradkar*[2], *Karunakara N*[1], *Vijay Kadwad*[2], *K Bhasker* Shenoy[1]*

[1]Department of Applied Zoology/CARRT, Mangalore University, Mangalore 574199, India.
[2] Radiopharmaceutical Division, Board of Radiation and Isotope Technology, Vashi complex Vashi, Navi Mumbai 400057, India.
*Email: kshenoyb@gmail.com

1. Introduction

Radioimmunoassays are used to measure trace concentrations of hormones/protein to ensure the physiological condition of patients [1]. In radioimmunoassay, ^{125}I ($T_{1/2}$=60 d), labelled to tyrosine/ histidine amino acid residues of analyte/antibody, is used as radiotracer [2]. C-Reactive Protein (CRP) is a well-known cardiovascular marker utilized for the early prediction of cardiac diseases. CRP is a pentameric protein present in serum, synthesized by lever. The present work reports the preparation of a radiotracer to develop an Immunoradiometric assay (IRMA) procedure to quantify CRP in human serum.

2. Experiment

The paired monoclonal antibody was procured from Biotech (R&D), and the CRP for standards preparation was from Sigma. The chloramine-T oxidation method was adopted for the radiolabeling of a monoclonal antibody [3]. The reaction mixture was purified by column chromatography using the Sephadex G-75. Column preparation was done before iodination, super-saturated BSA was used to saturate the column. Reaction for radiolabeling was initiated by adding 20 µg of anti CRP monoclonal antibody with isotope Na-I^{125} 225 µCi and oxidized by chloramine-T (10 mg/mL). This was incubated for 60 seconds; the oxidation reaction was stopped by the addition of metabisulphite (10 mg/mL) and the reaction was terminated by the addition of KI (10 mg/mL). Contents were immediately added to the column. Phosphate buffer (0.05 M) was used as the elution buffer. 1 mL elute was collected in each tube which contained 1 mL of 1% BSA buffer. Activity of collected fraction was measured for 10 s using gamma counter. Two peaks were observed of which the highest peak was labelled mAb with I^{125}. Paper

electrophoresis was done to calculate the specific activity of radiolabeled tracer. Similarly, Radio Chemical Purity (RCP) was checked by using paper electrophoresis.

Radioiodination yield = Total CPM of the labelled protein peak in pooled fraction/ total CPM*100

Radiochemical purity = Total CPM of the labelled antibody peak strip number/ total CPM*100

3. Results and Discussion

Radioiodination procedure standardization is major step in the development of IRMA, where antibody is used for radiolabeling. In iodination procedures, the chloramine-T method with minor changes is adopted [3]. Fig 1 shows the counting of pooled fraction with fraction number on X-axis, and the gamma count (for 10 s) on Y-axis. Fraction number 6-9 had labelled mAb and the other second peak was only free iodide. Specific activity was found to be 840 µCi/µg of radiolabeled antibody with a radioiodination yield of 74.70%. Tracer was prepared by addition of the fraction number 6-8 and the initial CPM was set to be $1x10^5$ per 100 µL. Fig 2 represents the purity of labelled molecules (87%). These labelled mAb will be used for development of IRMA.

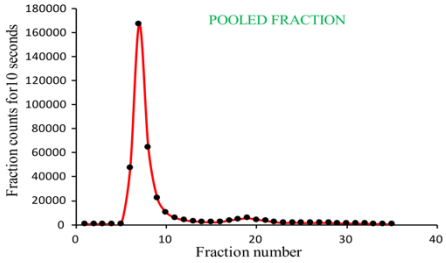

Fig 1: Radio-iodination yield for anti-CRP mAb

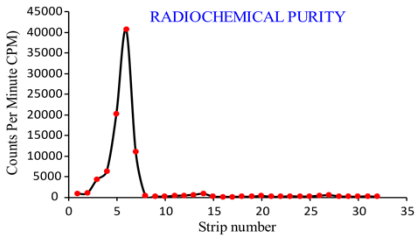

Fig 2: Radio Chemical Purity (RCP) of labelled mAb

Radiolabeling to the monoclonal antibody was optimized, radioiodination yield was 74.70%; RCP was found to be 86% and specific activity was calculated and found to be 840 µCi/µg. Radiolabeled mAb can be adopted to standardize the IRMA procedure.

Acknowledgement: Support and assistance from BRIT, RRCAT and Dept of Applied Zoology, Mangalore University is highly acknowledged.

References

/1/ Ridker, M. Paul, Circulation 107 (2003) 363-369.

/2/ R.S. Yalow, S.A. Berson, J. Clin. Invest. 39 (1960) 1157-1175.

/3/ W.M. Hunter, F.C. Greenwood, Nature 194 (1962) 495-496.

Development of A Time-of-flight Mass Spectrometer with A Laser Desorption/Ionization Source

Keerthana Kamalakannan[1,2], Noël Servagent[2], Anne Piscitelli[2], Ferid Haddad[1,2], Vincent Metivier[2], Arnaud Cadiou[2], Stéphane Martinez[2], Mériadeg Guillamet[2], Louis-Marie Rigalleau[2], Nathalie Michel[2]*

[1] Groupement d'Intérêt Public ARRONAX, 44800 – Saint Herblain, France.
[2] Laboratoire SUBATECH, IMT Atlantique, Université de Nantes, CNRS/IN2P3, Nantes, France.
*Email: keerthana.kamalakannan@subatech.in2p3.fr

1. Introduction

The SMILES (Séparation en Masse couplée à l'Ionisation Laser pour des applications Environnementales et en Santé) project is focused on the development of mass separators: one using a magnetic dipole and the other, a time-of-flight mass spectrometer (TOF-MS). In both cases, lasers will be employed to desorb and ionize the isotopes of interest. This current study is focused on the development of a TOF-MS for which SIMION software has been proven useful in designing the TOF-MS and in studying the ion trajectories in electric and magnetic fields [1, 2]. One of the uses of this TOF-MS will be to analyse the contaminants present in environmental samples.

2. Experiment

1.1. *Ion source:* A laser desorption-ionization source will be used to produce ions. A 532 nm wavelength laser inclined at an angle of 45° to the surface will be employed to desorb the atoms from the sample while a 266 nm wavelength laser will be used to ionize these free atoms.

1.2. *Simulations:* A typical TOF-MS consists of an acceleration region, a field-free region and a detection region. After being produced with the laser beams, the ions are accelerated toward a field-free region before reaching the detector. A collinear model was designed to study the functioning of TOF-MS where all the components are arranged on the same line. A space-time graph not only helped us in understanding the system but also helped us choose the right geometry. Moreover, the simulations helped

us in choosing the right parameters to have better mass resolution and efficiency of detection. Based on the simulations, a focalization system was introduced after the acceleration region.

3. Result and discussion

Elements like Cu, Er, Ra and U are studied, as they are major anthropogenic and/or radioactive pollutants. Figure 1 shows the ^{235}U and ^{236}U ion impact simulation on the detector and Figure 2 shows the associated TOF. The resolution of detection, in this case, is 468 at 36% valley. Table 1 shows the analytical calculation and simulated values of Δt, the difference in TOF between the two isotopes.

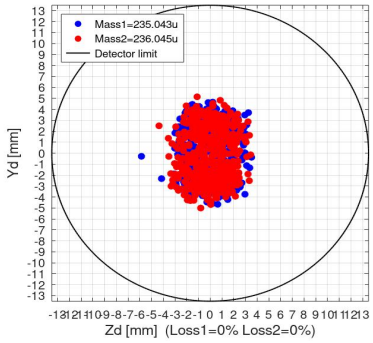

Figure 1: ^{235}U-^{236}U ion impact on detector

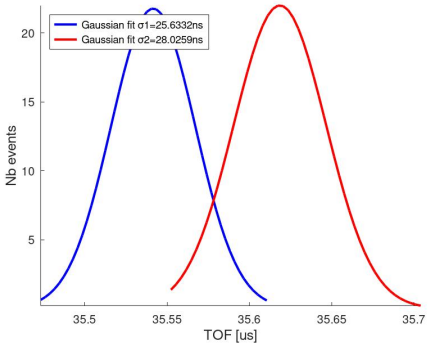

Figure 2: TOF of ^{235}U-^{236}U ions (loss = 0%)

Table 1: Modelled and simulated values of Δt values with respect to mass

Element	Modelled Δt_m [ns]	Simulated Δt_m [ns]	Error in Δt_m %
Cu63-65	298.96	290.7	2.7
Er167-168	92.48	88.94	3.8
Ra226-228	159.24	154.7	2.8
U235-236	78.07	76.94	1.4

4. Conclusion

The collinear model gives us the relation between the TOF of ions to their mass and their initial velocity. From the SIMION simulations, a two-step voltage extraction method will be employed in the acceleration region as well as a focalization system after the acceleration region to improve the TOF resolution and to avoid ion loss out of the detector. Finally, the simulated and the modelled values are in agreement with each other with a small deviation.

References

/1/ K. Blaum, C. Geppert, H.-J. Kluge, et al., Nucl. Inst. Meth. Phys. Res. B. 204 (2003) 331-335.

/2/ J.L. Henares, N. Lecesne, L. Hijazi, et al., Nucl. Inst. Meth. Phys. Res. A. 830 (2016) 520-525.

IAEA Compact Neutron Generators for Demonstrating Industrial Radiotracers Production

*Haifa Ben Abdelouahed**, *Natko Skukan, Kalliopi Kanaki, Danas Ridikas*

Nuclear Science and Instrumentation Laboratory, Division of Physical and Chemical Sciences, Department of Nuclear Sciences and Applications, International Atomic Energy Agency
*Email: h.ben-abdelouahed@iaea.org

1. Introduction

The Nuclear Science and Instrumentation Laboratory (NSIL) [1] of the Physics Section, the Division of Physical and Chemical Sciences [2], expanded its capabilities in neutron analytical techniques and capacity building through the establishment of a neutron science facility in the premises of the IAEA Seibersdorf Laboratories [3], Austria. The facility is based on two compact neutron generators, one Deuterium-Deuterium (DD) generator and one Deuterium-Tritium (DT) generator. These generators are to be used for training purposes, research and development activities as well as services according to the IAEA programmatic and Member States' needs. Demonstrating radiotracers production in small quantities for training purposes is one of the targeted applications of the NSIL compact neutron generators. It is a pertinent alternative to improve the availability of appropriate tracers for various types of tracing operations that could lead eventually to further development of tracer technology and expansion of radiotracer applications in industry and environment.

Although most industrial radiotracers are produced either in fission reactors or high-energy accelerators, some references [4] [5] have shown that compact neutron generators can also provide useful quantities of radioisotopes via the (n,γ), (n,2n), and (n,p) reactions. However, for such purposes, neutron fluxes shall be in the range of 10^8 to 10^{10} $ns^{-1}cm^{-2}$. This work presents the preliminary calculations (shown in Table 1), optimization and measurements that can further motivate the efficient utilization of a moderate flux neutron generator for this type of application. Based on these calculations, the DT NSIL neutron generator that emits neutrons up to 2×10^8 n/s in 4π is already operational and is planned to be tested to activate some chemical elements with high thermal reaction cross-section (such as Chlorine, Manganese, Cobalt, Bromine, Indium, and Europium) for production of radiotracers with nuclear characteristics (half-life, radiation type and energy) relevant for industrial applications [6].

Table 1. FISPACT-II predictions of tracer activation using the IAEA D-T compact neutron generator emitting 2×10^8 n/s in 4π at a distance of 3.8 cm (after 2h of 10-gram activation)

Element	**Chlorine**	**Manganese**	**Cobalt**	**Bromine**	**Indium**	**Europium**
Reaction	$^{37}Cl(n,\gamma)^{38}Cl$	$^{55}Mn(n,\gamma)^{56}Mn$	$^{59}Co(n,\gamma)^{60}Co$	$^{81}Br(n,\gamma)^{82}Br$	$^{115}In(n,\gamma)^{116m}In$	$^{151}Eu(n,\gamma)^{152m}Eu$
Half-life	37.18 min	2.58 h	5.27 y	35.34 h	54 min	9.3 h
Main Gamma energies (keV)	2168 1642	847 1811	1173 1332	776 554	1294 1097	841 963
Activity (Bq)	3.748E+03	1.427E+05	2.482E+01 ^{60}Co 5.552E+05 ^{60m}Co	7.922E+02	2.367E+06	2.411E+06

References

/1/ Nuclear Science and Instrumentation Laboratory (NSIL) | IAEA

/2/ Division of Physical and Chemical Sciences | IAEA

/3/ Seibersdorf laboratories | IAEA

/4/ K.-N. Leung, J. K. Leung, G. Melville, Appl. Radiat. Isot. 137C, (2018) 23.

/5/ Ka-Ngo Leung, Nucl. Technol. 206 (2020) 1607-1614.

/6/ IAEA Technical Report, Radiotracers and Labelling Compounds for Applications in Industry and Environment, Technical Consultant Report 16-19 June (2004), DOI: 10.13140/RG.2.2.15357.36321.

Design and CFD Simulation of Radiotracer Test Loop for National Radiotracer Laboratory of Iran

Hossein Sayyar[2], Ali Taheri[1,2], Javad Karimi-Sabet[1,2*], Pouneh Tayyebi[1], Seyed Pezhman Shirmardi[1,2]*

[1]Nuclear Science and Technology Research Institute, Tehran, Iran.
[2]Radiation Application Development Company, National Radiotracer Lab, Tehran, Iran.
*Email: jvkarimi@nstri.ir, atahery@aeoi.org.ir

1. Introduction

Radiotracer techniques have been widely established in different industries for troubleshooting, monitoring and visualization of process parameters. Most of these industries employ multiphase flow systems which require careful and efficient design, optimization and management. It is necessary to have complete information about process parameters, e.g., phase distribution, residence time, flow rate, flow pattern, etc. [1,2]. In this regard, radiotracer methods alongside theoretical calculations and CFD (Computational Fluid Dynamics) simulations can provide accurate characterizing [3]. As the responsible organization in this field, we decided to establish a national laboratory in the field of radiotracers to integrate all related activities. While starting to equip the laboratory with detection and DAQ systems, one of the most important missions is to design and build a radiotracer test loop. Using this test loop, it is possible to test the instrument, validate the simulation results, and launch research projects. In this work, a test loop is designed and simulated using ANSYS modelling.

2. Experiment

A schematic view of the designed test loop is shown in Figure 1. A 2-D model of the separator, using ANSYS (SpaceClaim), with a diameter of 1.7 m, a length of 3.2 m and a weir thickness of 13 mm (length of 1 m) was modelled. Also, a multi-phase flow with air as the primary phase and water and oil as the secondary phases at the inlet was considered. Furthermore, radiotracer phase was modelled as a liquid with the density higher than oil and lower than water injected into the inlet flow (0.5 s). The volume fractions of water and oil phases were considered 0.2 and 0.1 at the inlet, respectively. The Eulerian

multiphase flow model was introduced in the solver. The velocities of all phases at the inlet were set to 0.8 m/s. A transient analysis of 5 s with a time step of 0.003 s was carried out.

3. Results and discussion

The radiotracer volume fraction at the inlet is illustrated in Figure 2, and no radiotracer is present at the outlet after 5 s which was expected to be true in the case of a real separator. The contour plots of velocity and volume fraction of water (a) and oil (b) phases after 5 s are depicted in Figure 3.

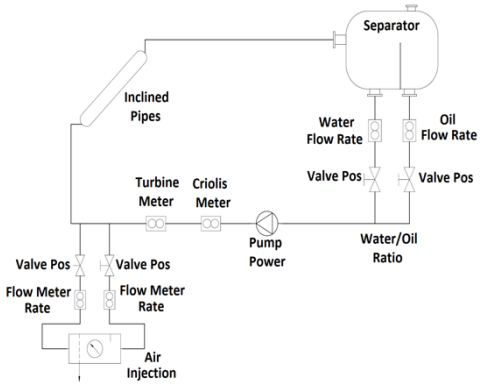

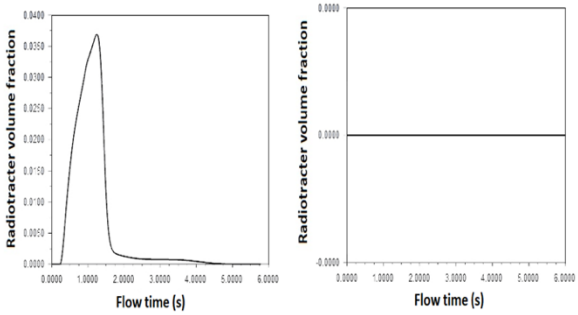

Figure 1: a schematic view of the designed test loop

Figure 2: (a) radiotracer volume fraction rate at the inlet and (b) radiotracer volume fraction rate at the outlet

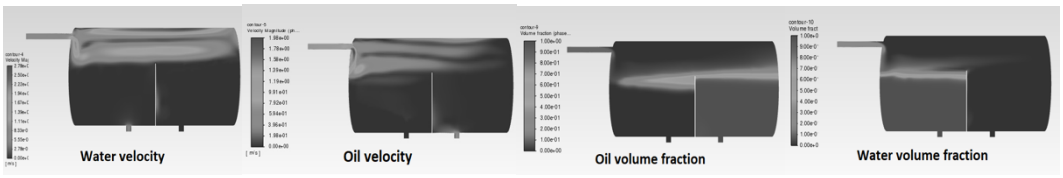

Figure 3: velocity and volume fraction of water and oil phases after 5 s

According to the simulation, no radiotracer is present at the outlet after 5 s. The figures show that no sign of radiotracer is detected at the outlet which is expected to be true in the case of a real separator.

References

/1/ H.J. Pant, Appl. Radiat. Isot. 182 (2022) 110076.

/2/ R.G. Peyvandi, A. Taheri, Appl. Radiat. Isot. 107 (2016) 335-339.

/3/ IAEA-TECDOC-1262, Radiotracer technology as applied to industry, 1997-2000.

/4/ N. H. Yusoff, et al., NTC: 2015, Malaysia.

Progress Toward Observing γ-rays Emitted from ^{229m}Th by Doping Fluoride Crystals with ^{229}Pa

Yudai Shigekawa, Wang Yang, Yin Xiaojie, Akihiro Nambu, Hiromitsu Haba*

RIKEN Nishina Center for Accelerator-Based Science, RIKEN, Wako, Saitama 351-0198, Japan.
*Email: yudai.shigekawa@riken.jp

1. Introduction

The first excited state of ^{229}Th, ^{229m}Th, has an extremely low excitation energy of ~8.3 eV (149 nm) [1], which may allow laser excitation from the ground to the isomeric state and lead to an ultraprecise nuclear clock. Nuclear clocks require narrow bandwidth of the excited state, and thus the internal conversion (IC) process of ^{229m}Th with a half-life of ~7 μs [2] must be inhibited to deexcite ^{229m}Th via the γ-ray emission with a long half-life [3]. To inhibit the IC process of ^{229m}Th, electron binding energy of ^{229m}Th should be much higher than 8.3 eV. ^{229m}Th doped into fluoride crystals is a candidate to realize such chemical environments. M. Verlinde *et al* suggested a method to dope ^{229m}Th into fluoride crystals by implanting ^{229}Ac ions into them [4], and recently reported the observation of the γ rays from ^{229m}Th [5]. They reported the isomer energy and the half-life of ^{229m}Th in MgF_2 to be 8.338(24) eV and 670(102) s, respectively. For confirming the γ-ray emission from ^{229m}Th by a different scheme and determining the radiative half-life, we are aiming to dope a fluoride crystal with ^{229m}Th by doping with ^{229}Pa, which decays to ^{229m}Th by electron capture with negligibly small recoil energy. Doping with ^{229}Pa is realized by implanting high-energy ^{229}Pa ions into a fluoride crystal and then annealing it. In this study, we developed a photon measurement apparatus for observing the γ rays of ^{229m}Th emitted from a ^{229}Pa-doped crystal and a method for ionizing Pa and implanting it into a crystal.

2. Experiment

We developed a photon measurement apparatus shown in Fig. 1. A photomultiplier (PMT1) for measuring γ rays of ^{229m}Th can be cooled to −25 °C by a Peltier cooler for noise reduction. In order to reduce background photons originating from high-energy radiations produced by the decays of ^{229}Pa and other radioactive impurities, we placed a band-pass filter that passes only 151±20 nm photons and

another photomultiplier (PMT2) that detects scintillation photons produced by high-energy radiations in a fluoride crystal. For evaluating the background photons emitted from ^{229}Pa samples, we produced ^{229}Pa by irradiating ^{232}Th foils (total thickness 138 mg/cm^2) with 1 μA of 30-MeV proton for 10 h. ^{229}Pa was chemically separated by anion exchange chromatography with a chemical yield of 91(3)%. Purified ^{229}Pa solution was dropped on a CaF_2 crystal and then evaporated. The CaF_2 crystal containing 48 kBq of ^{229}Pa, 2.5 kBq of ^{232}Pa, and 6.6 kBq of ^{230}Pa was subjected to the photon measurement. We examined the efficiency of ionizing Pa by the surface-ionization technique [6] and implanting it into a fluoride crystal using ^{233}Pa separated from ^{237}Np. ^{233}Pa solution was dropped and evaporated on a Re filament coated with colloidal graphite, and then the filament was heated to 2000 °C by applying a current of 5.5 A. Produced ^{233}Pa ions were accelerated to −15 kV and implanted into a CaF_2 crystal.

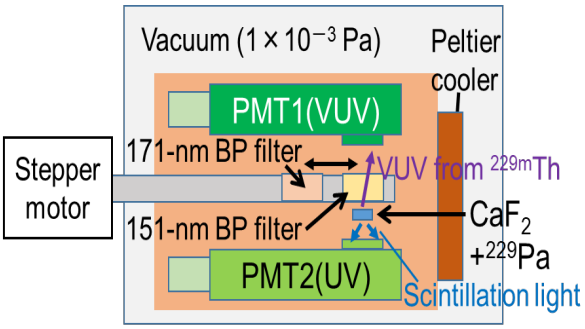

Figure 1: Schematic view of the photon measurement apparatus.

3. Result and discussion

The count rate of the background photons for PMT1 was ~9 s^{-1}, which was reduced to 1/3 using scintillation photons detected with PMT2. We estimated that doping a CaF_2 crystal with 100 kBq of ^{229}Pa allows us to observe the γ rays of ^{229m}Th and determine the radiative half-life with ~25% precision. Meanwhile, the overall efficiency for ionization and implantation of ^{233}Pa was 0.53 (1)%. Hence, producing 19 MBq of ^{229}Pa allows to prepare a CaF_2 crystal containing 100 kBq of ^{229}Pa.

References

/1/ B. Seiferle et al., Nature 573 (2019) 243.

/2/ B. Seiferle et al., Phys. Rev. Lett. 118 (2017) 042501.

/3/ Y. Shigekawa et al., Phys. Rev. C 104 (2021) 024306.

/4/ M. Verlinde et al., Phys. Rev. C 100 (2019) 024315.

/5/ S. Kraemer et al., arXiv:2209.10276 [nucl-ex] (2022).

/6/ D. A. Pickett et al., Anal. Chem. 66 (1994) 1044.

Prognostic Role of Staging & Interim 18F-FDG PET/CT for Predicting Initial Bone Marrow Involvement, Delayed Disease Relapse and Histopathological Transformation in Follicular Lymphoma: A Retrospective Cohort Study

Sayan Das[1], Jayanta Das[2], Raju Gupta[2]*

[1]School of Medical Science & Technology, IIT Kharagpur, India.
[2]Department of Nuclear Medicine, Tata Medical Centre, Kolkata, India.
Email: sdchemistry2017@kgpian.iitkgp.ac.in

1. Introduction

Follicular lymphoma (FL) is the second most common type of non-Hodgkin lymphoma (NHL) and accounts for up to 30% of all lymphomas. Initial bone marrow involvement, disease relapse & histological transformation (HT) of follicular lymphoma to a more aggressive lymphoma are some serious events affecting the final disease outcome. 18F-Fluro-deoxyglucose Positron Emission Tomography –Computer Tomography (18F-FDG PET/CT) whole body scan done before initiation of any therapy (as staging scan) is accepted as a standard imaging procedure to assess the initial stage of FL. Interim 18F-FDG PET/CT scan is done after administration of 3 cycles of chemotherapy to evaluate the early response to the treatment. In previous studies, interim PET/CT scans could variably predict long-term clinical outcomes of FL based on treatment response. The 18F-FDG-PET/CT scan was also highlighted as a non-invasive diagnostic tool for the detection of relapse & bone marrow involvement. However, early prediction of HT based on findings of 18F-FDG PET/CT scan is not yet established in literature. The objective of the present study is to evaluate the role of the staging and interim 18F-FDG PET/CT scan to detect bone marrow involvement and predict disease relapse with or without HT based on the standardized uptake value (SUVmax) of lesions. SUVmax is a semi-quantitative measurement of the glycolytic activity of any lesion suspected to be disease under consideration. This study also investigated the Disease Free Survival (DFS) of FL based on the 5- point Deauville Score (5PDS) response criteria of interim 18F-FDG-PET/CT scan.

2. Experiment

This retrospective study was done on histopathologically proven FL patients, aged above 18 years. It included a total of 60 patients out of which 33 male (55%) and 27(45%) female patients are there. The age range of the cohort was 25 to 79 years and the median age was 58 years. Staging and interim 18F-FDG PET/CT scans were done in all patients as per standard protocol. Interim PET/CT scans were done after 3 cycles of chemotherapy in all patients. All lesions were measured by SUVmax. All patients were followed up till the completion of 6 cycles of chemotherapy. Bone marrow involvement and HT were confirmed by histopathological examination.

3. Results

SUVmax of staging 18F-FDG PET/CT scan have no correlation with HT & disease relapse. Staging 18F-FDG PET/CT scan has poor sensitivity for detection of bone marrow involvement and hence cannot replace initial bone marrow biopsy. 5PDS of interim 18F-FDG PET/CT scan is significantly associated with a disease relapse as well as DFS. Therefore, treatment modification may be considered based on an interim 18F-FDG PET/CT scan.

A further prospective study with a larger patient population and uniform treatment protocol is needed for the final conclusion.

References:

/1/ P.E. Kinahan, J.W. Fletcher, Seminars in ultrasound, CT, and MR. 31 (2010) 496-505.

/2/ M. Xie, L. Wang, Q. Jiang Q, et al., Cancer Cell Int. 21 (2021) 394.

/3/ K.M. Boughan, P.F Caimi, Curr. Oncology Reports. 21 (2019) 63.

/4/ L. Xerri, S. Dirnhofer, L. Quintanilla-Martinez, et al., Virchows Archiv. 468 (2016) 127-39.

Determination of Boron in Borated Samples using Charged Particle Activation Analysis

J. Datta[1], S. Dasgupta[1], K.K. Swain[2]*

[1]Analytical Chemistry Division, Bhabha Atomic Research Centre, VECC, Kolkata-700064, India.
[2]Analytical Chemistry Division, Bhabha Atomic Research Centre, Trombay, Mumbai – 400085, India.
*Email: sdasgupta@vecc.gov.in

1. Introduction

The nuclear industry made substantial use of borated rubber (BRU), borated high-density polyethylene (BHDPE), borated concrete rubber and borated polyethylene (BPE) for shielding purposes. Shielding from fast as well as slow neutron is offered by BRU, BPE utilising the elastic collisions with hydrogen and ultimately capture by $^{10}B(n,\alpha)^{7}Li$ reaction, due to the high thermal neutron capture cross-section of boron (Boron $_{elemental}$ = 764 barn and ^{10}B = 3,837 barn). Nuclear reactors, nuclear battleships, medical vaults, X-Ray Facilities are few examples of its use [1]. On the other hand, borosilicate glass (BSG) is developed for vitrification of nuclear waste. Therefore, accurate determination of B content using an appropriate analytical technique such as conventional, spectroscopic and nuclear methods [2, 3] is important. In this work, we have used instrumental charged particle activation analysis (CPAA) technique due to its favorable features of being non-destructive in nature so that chances of loss of boron during sample preparation, handling and even during irradiation are very low.

2. Experiment

The glass samples were cut into ~10×10 mm size for irradiation. The BPE and BRU samples were cut into pieces of ~10×10 mm size and were then wrapped in Al-foils. This was done as a precautionary measure from accidental melting due to heating and further contamination of the sample holder as a whole. Red mud samples were ground using an agate mortar-pestle into smooth powder and then were pelletized using hydraulic pelletizer into 10 mm dia. pellets. Tantalum boride (TaB) pellets were also prepared and used as standards of B. The standards and samples of TaB, BSG, BRU, BPE and red mud were irradiated using 7 MeV proton beam at 250-300 nA current at the Room Temperature Cyclotron,

VECC, Kolkata. BSG2 and red mud samples were irradiated for 2-3 hours. All other samples, along with the standard were irradiated for 15-30 minutes. The samples were cooled using LCW circulation in the sample holder during irradiation, to prevent thermal stress. All irradiated samples were cooled for 3-4 days to bring down the matrix activity before radioactive counting was taken up.

3. Results and Discussion

For B analysis, $^{10}B(p,\alpha)^{7}Be$ ($T_{1/2}$ = 53.29 days) nuclear reaction was used. The 477.6 keV γ-energy of the ^{7}Be was monitored for quantification of B using HPGe detector (Relative efficiency: 40%; Resolution: 1.9 keV @1332 keV) coupled to 8k channel analyzer. The Comparator Method [3] was used for determining the concentration of B in the respective samples. We observed that the significant amount of Fe, Cr, Ca, Ti, etc., present in these samples, mask the photo peak of ^{7}Be when using a 13 MeV proton beam. Keeping in mind the interfering elements, their probable nuclear reactions at different energies etc., we optimized the irradiation parameters to maximize the yield of our desired isotope with minimum inference from elements present in their respective matrices. It has been observed that 7 MeV proton beam significantly reduces the background near the peak of our interest (478 keV) region. The reported experimental uncertainty is computed by error propagation formula (using errors in all involved parameters to obtain the reported value) and the detection limit is based on 3σ value of observed counting statistics. These results will be compared with other suitable analytical techniques.

Table 1. Content of Boron (%) in borated samples by CPAA

Sample	Mark	B (%)	DL (%)
Borated PolyEthylene	BPE	1.45±0.07	0.14
Borated Rubber	BRU(B7)	0.77±0.04	0.08
Borated Rubber	BRU(A8)	10.98±1.15	0.43
Borosilicate glass	BSG1	18.65±1.05	0.20
Borosilicate glass	BSG2	0.27±0.02	0.05
Red mud	RM	0.155±0.011	0.031

4. Conclusion

The determinations of B in a variety of borated samples were measured using instrumental charged particle activation analysis for a wide range of boron concentration. It has been found that 7 MeV proton beam is more suitable in comparison to 13 MeV proton beam.

References

/1/ D. V. Subramanian, et al, Indian J. Pure Appl. Phys. 56 (2018) 583-586.

/2/ S. Chhillar, R. Acharya, S. Sodaye, et al., Anal. Chem. 86 (2014) 11167-11173.

/3/ S. Dasgupta, J. Datta, K. K. Swain, J. Radioanal. Nucl. Chem. 328 (2021) 33-38.

A Novel Concept of Laser-assisted Electronic State Chromatography towards Studies of Superheavy Elements

Biswajit Jana[1,2,3], Michael Block[1,2,3], Eunkang Kim[1,2,3], Steven Nothhelfer[1,2,3], Sebastian Raeder[2,3], Harry Ramanantoanina[1,2,3], Elisabeth Rickert[1,2,3], Elisa Romero Romero[1,2,3], Jonas Schneider[1], Philipp Sikora[1], Mustapha Laatiaoui[1,2,3]*

[1] Department of Nuclear Chemistry, Johannes Gutenberg University, Mainz, Germany
[2] Helmholtz-Institut Mainz, Germany
[3] GSI Helmholtzzentrum für Schwerionenforschung, Darmstadt, Germany
*Email: bjana@uni-mainz.de

1. Introduction

Exploring the atomic structure of Superheavy Elements (SHE) with atomic numbers Z>100 equally fascinates and challenges experimental scientists. These SHE have to be produced artificially in a heavy-ion-induced nuclear fusion-evaporation process. To investigate these elements, extremely sensitive and fast techniques are mandatory due to very low production rates of few ions per hour or even per day and they have very short half-lives. Recently, a novel concept, Laser Resonance Chromatography (LRC) [1] technique, has been conceived to study the atomic structure of SHE for example lawrencium (Lr, Z= 103). In the LRC technique, the measurement is carried out on the ion species avoiding the neutralization that is required for laser resonance ionization with existing techniques such as RADRIS (Radioactive decay detected Resonance Ionization Spectroscopy) and IGRIS (Ion Guide detected Resonance Ionization Spectroscopy). Electronic state-resolved chromatography is explored to measure the change of population in the ions' ground state through laser resonant excitation of the ions to their higher excited levels.

To demonstrate the LRC technique, an experimental setup has been designed, developed and commissioned [2]. Initial experiments are carried out to characterize the quadrupole mass spectrometer and the ions' transportation through various sub-systems such as stopping cell, ion guide and ion buncher. In this presentation, I will introduce the LRC technique and present the initial experiments carried out in the LRC setup on transition metal elements such as Cr^+ and Fe^+.

Funding: This project has received funding from the European Research Council (ERC) under the European Union's Horizon 2020 Research and Innovation Programme (Grant Agreement No. 819957).

References

/1/ M. Laatiaoui et. al., Phys. Rev. Lett. 125 (2020) 023002.

/2/ E. R. Romero et. al., Atoms, 19 (2022) 87.

Coulomb Diffraction Interference in ^{23}Al Breakup Reaction at 40-100 MeV/n Beam Energies

*Surender, Ravinder Kumar**

Deenbandhu Chhotu Ram University of Science and Technology Murthal Sonepat, Haryana -131039, India.
*Email: drravinderkumar.phy@dcrustm.org

1. Introduction

The study of exotic nuclei is directly connected with astrophysics. The breakup reactions have been frequently used to explore their nuclear structure. As far as neutron halos are concerned breakup mechanisms are well understood, but in case of proton halo breakup reactions, the situations are more complicated, because of additional valence proton interaction with core and target. Few year before, the interference among the Coulomb and diffraction mechanisms during breakup reaction especially in proton halo cases were studied and reported to effects the breakup observables [1-3]. Recently ^{23}Al, proton-rich nuclei has been studied because of it's key role in astrophysical nuclear reactions [4]. In present work, we have studied ^{23}Al breakup reaction and specially investigated the role of Coulomb diffraction dissociation interference on the single proton breakup cross section and core longitudinal momentum distribution (LMD) width. We have investigated this effect for three different targets, i.e. ^{12}C, ^{58}Ni and ^{208}Pb, at four frequently used incident beam energies i.e., 40, 60, 80 and 100 MeV/n.

2. Theoretical Formalism

The longitudinal momentum distribution (LMD) of the core fragment in the diffraction breakup mechanism is calculated using the Eikonal approximation, whereas Coulomb breakup is calculated using sudden approximation, taking Coulomb potential to all orders, as discussed in detail in references [1-3]. The proton-rich nucleus, ^{23}Al is assumed to have core plus single proton ground state configuration [$0^{+}\otimes 1d_{5/2}$], whose radial wave function is calculated by numerically solving the Schrodinger wave equation for Woods-Saxon nuclear potential. The depth of Woods-Saxon potential (V_0=36.12 MeV) is fitted to reproduce the separation energy (S_p=0.141 MeV [4]) of valence proton with range (r_0=1.25 fm) and diffuseness (a_0= 0.7 fm) parameters, as used in reference [4].

3. Results and Discussion

The calculated LMD full width at half maxima (FWHM) and single proton breakup cross section corresponding to diffraction, Coulomb and diffraction calculated with Coulomb mechanism are shown for different incident beam energies i.e., 40, 60, 80 and 100 MeV/n for ^{12}C target in Table 1. The same calculations with ^{58}Ni and ^{208}Pb have also been carried out and will be discussed in details in the conference.

Table 1. Calculated single proton breakup cross-section and FWHM of LMD for ^{23}Al projectile on ^{12}C target at different incident beam energies corresponding to diffraction, Coulomb, Coulomb with diffraction mechanisms along with their percentage interference effects.

Beam Energy →	**40 MeV/n**		**60 MeV/n**		**80 MeV/n**		**100 MeV/n**	
Breakup Mechanism	σ_{-p} (mb)	FWHM (MeV/c)	σ_{-p} (mb)	FWHM (MeV/c)	σ_{-p} (mb)	FWHM (MeV/c)	σ_{-p} (mb)	FWHM (MeV/c)
Diffraction	10.37	164.24	16.45	178.30	13.65	177.59	9.46	178.50
Coulomb	5.27	121.33	4.30	128.76	3.92	135.40	3.50	139.14
Coul+Diff(simple sum)	15.64	145.64	20.75	163.07	17.57	164.65	12.96	164.71
Coul+Diff(Cal. toget.)	16.42	144.54	20.01	160.64	16.20	162.20	11.59	161.97
% Interference	+4.99	-0.75	-3.57	-1.49	-7.80	-1.48	-10.57	-1.66

4. Conclusion

The effects of Coulomb and diffraction dissociation interference have been investigated in single proton breakup reaction from ^{23}Al nucleus. The effect is analyzed for single proton breakup cross section and FWHM width of LMD of core fragment in ^{12}C, ^{58}Ni and ^{208}Pb target cases. The study is performed for most generally used incident beam energy range i.e., 40-100 MeV/n. We found that for ^{12}C target Coulomb diffraction interference is destructive which reduces the breakup cross section up to 10% and also reduces the LMD width by -1.6% with increase in incident beam energy (except the case of 40 MeV/n). However for ^{58}Ni and ^{208}Pb targets it is found always constructive, which enhances the breakup cross section by +20% and up to +10% with beam energy while the variation in LMD width is +6% to +0.7% for ^{58}Ni and almost +5% for ^{208}Pb. So we found that Coulomb diffraction interference affects the observables significantly and depends on the target as well as incident energies.

5. References

/1/ R. Kumar, A. Bonaccorso, Phy. Rev. C 86 (2012) 061601(R).

/2/ R. Kumar, A. Bonaccorso, Phy. Rev. C 84 (2011) 014613.

/3/ A. Bonaccorso, D.M. Brink, C.A. Bertulani, Phys. Rev. C 69 (2004) 024615.

/4/ A. Banu et.al., Phys. Rev. C 84(1) (2011) 015803.

Assessment of Fertilizer Phosphorus Recovery for Wheat in an Inceptisol Using ^{32}P Radiotracer Technique

Manoj Shrivastava, Ashish Khandelwal, Renu Singh, Bhupinder Singh*

Division of Environment Science, Indian Agricultural Research Institute, New Delhi 110012, India.
*Email: manojshrivastava31@gmail.com

1. Introduction

Phosphorus is an essential nutrient for both plants and animals. In general, the apparent recovery of applied P by different crops in Indian soils is ~15 to 20%. Wheat (*Triticum* sp.) is one of the major staple foods for 35% of the world's population [1]. The choice of the right kind of phosphatic fertilizer source may likely improve the efficiency of phosphate utilization. This study was undertaken to evaluate the agronomic efficiency of two phosphatic fertilizers, namely, single super phosphate (SSP), and diammonium phosphate (DAP) in relation to P utilization by wheat in inceptisol using the ^{32}P radiotracer technique.

2. Experiment

A net house pot culture experiment was conducted to assess the efficacy of different phosphorus (P) fertilizers for wheat (*Triticum aestivum* cv HD 3086) using the ^{32}P radiotracer. Two fertilizer sources of P viz. diammonium phosphate (DAP) and single superphosphate (SSP) were labelled with ^{32}P (Carrier free $H_3{}^{32}PO_4$) and applied at three rates (12.5, 25 and 50 mg P_2O_5 per kg soil). Wheat was grown in pots containing 2 kg of soil (Inceptisol) for 42 days. Total P in the digest was determined using the vanadomolybdate yellow colour method after wet digestion with a 5:1 mixture of HNO_3 and $HClO_4$ and the uptake of P was estimated. ^{32}P in the digest was estimated by measuring Cerenkov radiation using a liquid scintillation analyzer. E_{max} for ^{32}P is 1.710 MeV and the Cerenkov counting efficiency of the counter was found to be 51.4%. Isotopic parameters were computed, namely, percent P derived from fertilizer (%Pdff), A-value (available P from the soil), percent fertilizer P utilization, and the equivalent ratio [2]. The a-value concept was developed by Fried and Dean [3]. Plants growing in soil is getting

nutrients from two sources i.e., native nutrients present in soil and nutrient provided by the external source. The plant will absorb from each of these in proportion to the respective amounts available. The amount of available nutrients in the soil to be determined in terms of standard fertilizer is known as 'A' value.

3. Results and Discussion

The results indicated that the dry matter yield (DMY) of the wheat shoot, P uptake, percent P derived from fertilizer (%Pdff) and A-value of the soil increased with increasing fertilizer rate. Among the fertilizer sources, DAP was found to be superior in enhancing the DMY of wheat, P uptake, and %FPU as compared to SSP. The %Pdff was found to be significantly higher in DAP treatments in comparison to SSP (fig. 1) and the reverse was true in the case of the A-value of the soil. The A-value was higher in SSP (132-215 mg P pot^{-1}) than in DAP (54-104 mg P pot^{-1}) treatment.

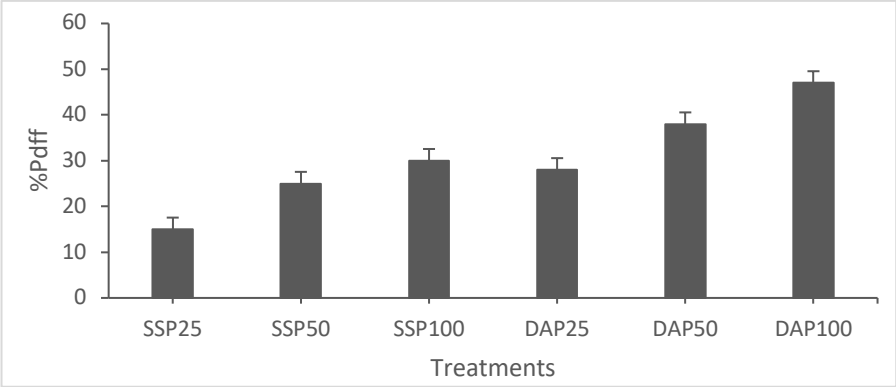

Fig 1: Phosphorus derived from fertilizer (%Pdff) as influenced by different fertilizer rates and sources

The experiment using ^{32}P labelled fertilizer can provide valuable information on P fertilization to the wheat crop. This study indicates that DAP was more efficient than SSP for wheat crops in an inceptisol.

Acknowledgement: BRIT, Department of Atomic Energy, Government of India, is acknowledged for providing radiolabeled fertilizers.

References

/1/ P.R. Shewry, J. Experimental Botany 60 (2009) 1537-1553.

/2/ M. Srivastava, S.F. D'Souza, J. Radioanal. Nucl. Chem. 274 (2007) 397-401.

/3/ M. Fried, L.A. Dean, Soil Sc. 73 (1952) 263-271.

Correlation of Intrinsic Fusion Barriers and Evaporation Residue Cross-Sections of Z = 114, 117-118

Dalip Singh Verma, Vivek, Pooja Chauhan*

Central University of Himachal Pradesh, Dharamshala, Kangra (H.P.)-176215, India.
*E-mail: dsverma@cuhimachal.ac.in

1. Introduction

The knowledge of suitable projectile-target combination and incident energy is of utmost importance for the synthesis of superheavy elements. The most suitable energy for the synthesis can be obtained from the variation of intrinsic fusion barrier with incident energy. The minimum value of the intrinsic fusion barrier at a given energy corresponds to the maximum of the fusion probability. The intrinsic fusion barrier is defined as the difference between the maximum of the fragmentation potential in the fragment masses region smaller than the projectile mass and potential at projectile mass [1]. Here, the fragmentation potential is calculated within the framework of quantum mechanical fragmentation theory. The theory is worked out in terms of the collective coordinate of mass (η)/charge (η_Z) asymmetry, relative separation of the fragments (R), neck length parameter, multi-pole deformations, and orientations. The fragments are considered in hot optimum orientations and deformations are taken up to hexadecupole order [2]. The variation of the intrinsic fusion barriers with incident energy has been analyzed for four ^{48}Ca-induced reactions and it's correlation with the measured evaporation cross-section has been explored.

2. Experiment

The fragmentation potential at a fixed relative separation R (= X_1+X_2, where X_i is the projection of radius vector along collision axis of interacting nuclei) and temperature T is

$$V(\eta, R, \ell, T) = \sum_{i=1}^{2} B_i(A_i, Z_i, \beta_{\lambda i}, T) + V_P(R, A_i, \beta_{\lambda i}, \theta_i, T) + V_C(R, Z_i, \beta_{\lambda i}, \theta_i, T) + V_\ell(R, A_i, \beta_{\lambda i}, \theta_i, T) \quad (1)$$

The binding energy $B_i(A_i, Z_i, \beta_{\lambda i}, T)$ are expressed as the sum of T-dependent liquid drop energy of [3],

an extension of Seeger's mass formula [4], and shell corrections of [5]. The bulk and asymmetry constants of Seeger's mass formula are adjusted by different authors to reproduce the experimental and/or theoretical ground state excess, see details in ref. [6]. Other terms V_P, V_C and V_ℓ are nuclear proximity, Coulomb and centrifugal potentials, respectively. For a given η, the ηz-coordinate is fixed by minimizing the potential V (η, R, ℓ, T) for Z_i (i=1, 2). The temperature is related to excitation energy of the compound nucleus as $E^*_{CN} = (A/10)T^2 - T$, where A=A_1+A_2. The intrinsic fusion barrier is calculated from the fragmentation potential as $B^*_{fus} = V^{\max}(R, A_2, T, \ell) - V(R, A_2(= A_P)T, \ell)$.

3. Results and Discussion

Fig. 1 shows that a range of the smaller values of the intrinsic fusion barrier corresponds to a range of the higher values of the measured evaporation residue cross-section (σ_{ER}) for all cases [7], see the shaded region. This means a relatively smaller intrinsic fusion barrier is a favour for process of fusion or synthesis of superheavy elements.

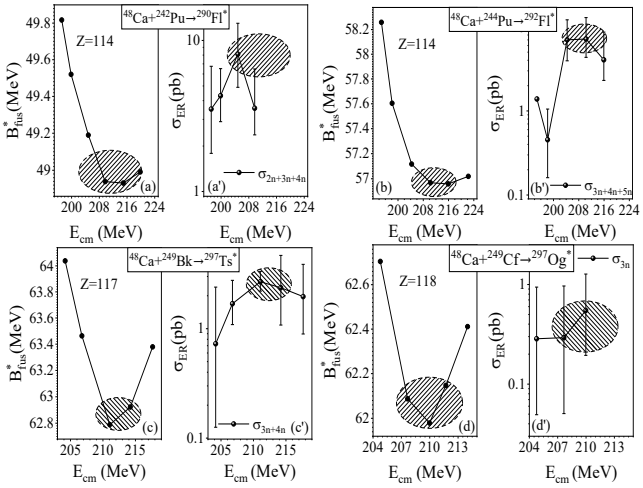

Figure 1: Intrinsic fusion barrier and the measured evaporation residue cross-section [7] as a function of incident energy for ^{48}Ca induced reactions

4. Conclusion

The most suitable energy for the synthesis of superheavy elements is the incident energy which corresponds to the relatively smaller values of the intrinsic fusion barriers.

References

/1/ G. Giardina, S. Hofmann, A.I. Muminov, et al., Eur. Phys. J. A 8, (2000) 205-216.

/2/ R.K. Gupta, M. Balasubramaniam, R. Kumar, et al., J. Phys. G: Nucl. Part. Phys. 31 (2005) 631-644.

/3/ N.J. Davidson, S.S. Hsiao, J. Markram, et al., Nucl Phys A 570 (1994) 61-68.

/4/ P.A. Seeger, Nucl. Phys. 25 (1961) 1-135.

/5/ W.D. Myers, W. . Swiatecki, Nucl. Phys. 81 (1966) 1-60.

/6/ D.S. Verma, Kushmakshi, J. Radioanal. Nucl. Chem. 322 (2019) 139-146.

/7/ Y.T. Oganessian, V.K. Utyonkov, Nucl. Phys. A 944 (2015) 62-98.

Role of Incomplete Fusion in Production of ^{155}Tb

Nitin Sharma[1], Dharmendra Singh[1], Amritraj Mahato[1], Pankaj K. Giri[1], Sneha B. Linda[1], Harish Kumar[2], Suhail A. Tali[2], M. Afzal Ansari[2], I. Ahmed[3], S. Kumar[3], Yashraj[3], R. Kumar[3], K.S. Golda[3], S. Muralithar[3], R. P. Singh[3], P. Sugathan[3]*

[1]Department of Physics, Central University of Jharkhand, Ranchi - 835222, India.
[2]Deptartment of Physics, Aligarh Muslim University, Aligarh- 202002, India.
[3]Inter University Accelerator Centre, Aruna Asaf Ali Marg, New Delhi - 110067, India.
*Email: dsinghcuj@gmail.com

1. Introduction

The study of Terbium (Tb) isotopes has become an active area of research and is referred to as the "Swiss knife" in the literature because of its four valuable radioisotopes, ^{149}Tb, ^{152}Tb, ^{155}Tb, and ^{161}Tb [1]. Specifically, ^{155}Tb is an interesting radionuclide having characteristic γ -rays of 87 keV (32%) and 105 keV (25%), negligible high energy γ-emissions, and relatively long half-life of 5.3 days, making it suitable for single photon emission computed tomography (SPECT) imaging with potential use in the diagnosis of oncological disease [2]. The production of ^{155}Tb suitable for medical applications is still a challenge [1,3]. ^{155}Tb radionuclide can be produced by light-charged particle activation, Heavy Ion (HI) activation and spallation reactions. Light-charged particle activation and spallation reactions provide good yields of ^{155}Tb but have high content of radionuclidic impurities [3]. Very limited data is available using HI reactions for the production of ^{155}Tb. In this context, the present study has been done with ^{16}O + ^{146}Nd system at 102 MeV beam energy. In this energy region, the compound nucleus formation takes place followed by complete fusion (CF) and incomplete fusion (ICF) reaction mechanism, so this route for the production of ^{155}Tb may provide an alternate way to obtain it.

2. Experiment

The experiment was performed at Inter University Accelerator Centre (IUAC), New Delhi. The pelletron accelerator was used to obtain $^{16}O^{7+}$ beam and experiment was carried out in general purpose scattering chamber (GPSC) by our group. The ^{146}Nd targets were prepared using vacuum evaporation technique. A target stack consisted of seven ^{12}C capped ^{146}Nd targets, backed by ^{27}Al foil. The thickness of ^{12}C,

^{146}Nd, and ^{27}Al was ≈ 10 μg/cm^2, ≈400-600 μg/cm^2 and ≈0.77-1.62mg/cm^2 respectively. Energy loss calculation for each stack was done using SRIM software. The target bombardment was carried out for ≈10 hr 35 min. After the end of the bombardment, the activities induced in each ^{27}Al catcher were recorded individually using a pre-calibrated high-resolution high-purity germanium (HPGe) γ -ray spectrometer coupled to a CAMAC-based personal computer employing CANDLE software.

3. Results and discussion

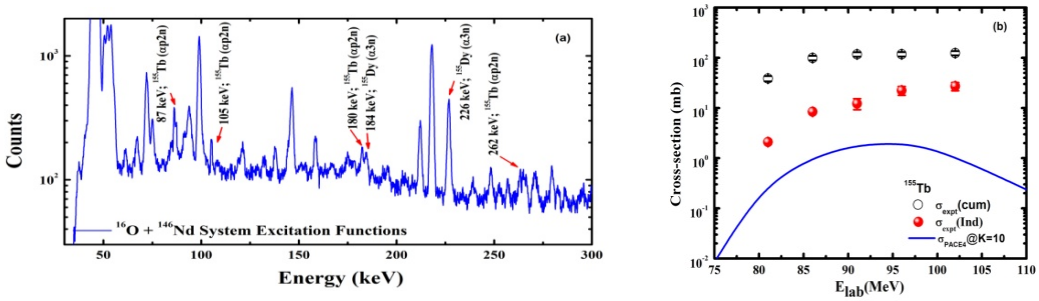

Fig. 2(a) Typical γ-ray spectra for ^{16}O+^{146}Nd system at energy 102 MeV, (b) Excitation function of ^{155}Tb, hollow and solid dots represent cumulative and independent cross-section and the line represents PACE-4 predictions

The γ-ray spectra obtained and the excitation functions of residue ^{155}Tb (αp2n) populated via ^{16}O + ^{146}Nd system have been shown in Fig.1(a) and (b), respectively. The cross-section of the ^{155}Tb (αp2n) residue has been compared with the theoretical model code PACE4. It has been found that the cross-section of the residue ^{155}Tb is enhanced as compared to the PACE4 predictions. As PACE4 only takes into account the CF hence, the observed enhancements are attributed to ICF. Moreover, there has been a contribution from ^{155}Dy ($t_{1/2}$ = 9.9 hours) which will not create much problem in extracting ^{155}Tb due to huge difference in their half-lives. Other residues populated in the ^{16}O and^{146}Nd reaction are ^{158}Er, ^{157}Er, ^{157}Ho, ^{156}Ho, ^{155}Dy, ^{155}Tb, ^{153}Tb, ^{153}Dy and ^{152}Dy. The advantage of this process can be that all the residues populating in the reaction have very short half-lives ranging from a few minutes to few hours except ^{153}Tb (2.34 days). The calculations of thick target yield (TTY) and activity measurements can provide more information.

References

/1/ N. Naskar, S. Lahiri, Front. Med. 8 (2021) 675014.

/2/ C. Müller, K. Zhernosekov, U. Köster, et al. J. Nuclear. Med. 53 (2012) 1951-9.

/3/ C. Favaretto, Z. Talip, F. Borgna, et al., EJNMMI Radiophar. Chem. 6 (2021) 37.

Simulation on The Production of Evaporation Residues from The Interaction of High Energy ^{14}N Beam on ^{181}Ta Target

Sumana Mukherjee[1], Susanta Lahiri[1,2], Chiranjib Barman[1]*

[1]Department of Physics, Sidho-Kanho-Birsha University, Purulia 723104, India.
[2]Diamond Harbour Women's University, Diamond Harbour Road, Sarisha, South 24 Parganas 743368, India.
*Email: susanta.lahiri.sinp@gmail.com

1. Introduction

The prime thrust of nuclear physics community in the international scenario is to use high energy high flux secondary radioactive ion beams which will ultimately enable researchers to reach the unreachable corner of the radionuclide chart and to discover exotic neutron-rich or -deficient radionuclides. To achieve this goal converter targets are proposed which are basically high Z target materials, like liquid Hg, Pb-Bi eutectic (LBE), Pb-Li eutectic (LLE), and also the high Z refractory elements like Ta or W. In 2014, in CERN-ISOLDE users meeting it was proposed that beside the use of converter targets for basic and fundamental science research, it could be large source of useful radioisotopes, many of them may be used clinically and may be non-conventional PET isotopes [1]. Therefore, it is of utmost importance, to know the total inventory of radioisotopes produced from the interactions of high energy beams on high Z materials. The only such studies were recently carried out to make total inventory of radioisotopes from the interaction of 1.4 GeV proton beams on LBE target [2,3]. However, till date no such works have been carried out on the interaction of high energy heavy ion beams with high Z material.

On the other hand, Variable Energy Cyclotron Centre (VECC), Kolkata is now equipped with Superconducting Cyclotron (SCC). Recently they have extracted 252 MeV $^{14}N^{4+}$ beam [4]. The Aim of this paper is to simulate the total residual radioisotopes arising from the interaction of 252 MeV $^{14}N^{4+}$ beam on ^{181}Ta target.

There are different nuclear model codes to determine the excitation function theoretically such as, ALICE, PACE, EMPIRE, TALYS etc. We have used the Monte Carlo code PACE4 [5] to predict

the cross sections of the evaporation residues of the nuclear reactions ^{14}N (252 MeV) + Ta target. A total of 20000 cascades were selected for each simulation keeping all other parameters default.

2. Result and Discussion

Figure 1 shows a plot of the mass numbers vs the cross section of the residual nucleus as predicted by the PACE4 code. The code predicts total 98 residual nucleus with the mass numbers ranging between 162<A<183. Amongst these, only 17 isotopes have mass ≥180. Rest masses are less than 180. Spallation produces radioisotopes with mass number slightly less than the target mass number. Therefore, most of the nucleus has been produced probably by spallation mechanism. The residual nucleuses having mass close to ^{181}Ta have been observed with low production cross-sections, probably produced by the inelastic reactions. Amongst the produced evaporation residues, ^{176}Os has the maximum production cross section of 158 mb. Interestingly no residual nucleus has been suggested by PACE4 in the mass range 90-105, which shows that there is no signature of fission.

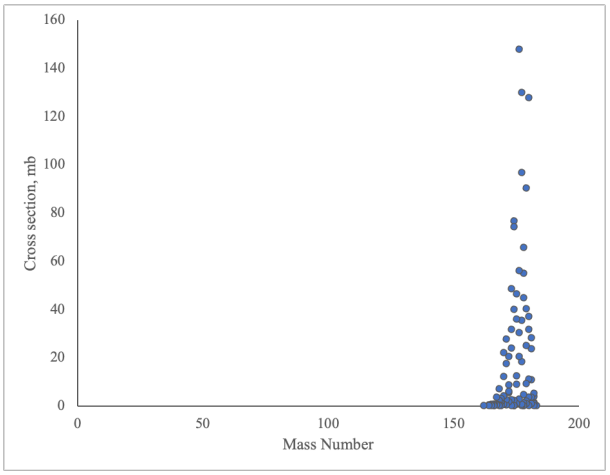

Fig-1: Variation of Cross section with mass number

3. Conclusion

PACE4 code has some inherent limitations, most important is thar PACE4 considers only equilibrium emission (EQ) and it does not consider for pre-equilibrium emission (PEQ) or direct (DIR) reactions. If in this case PEQ and DIR reactions predominate, then an under estimation of the theoretical cross section values will be observed. Therefore, it is important to simulate by other Monte Carlo codes like FLUKA, ALICE, TALYS, etc., which will help to understand the underlying reaction mechanism more precisely.

References

/1/ S. Lahiri, M. Maiti, ISOLDE workshop and Users Meeting, Nov. 18-20, CERN, Geneva, Switzerland (2009).

/2/ M. Maiti, K. Ghosh, T. M. Mendonça, et al., J. Radioanal. Nucl. Chem. 302 (2014) 1003-1011.

/3/ D. Choudhury, S. Lahiri, N. Naskar, et al., Eur. Phys. J. A. 56 (2020) 204.

/4/ https://www.vecc.gov.in/writereaddata/upload/files/Major%20Achievement_K500%20SCC_01012021.pdf.

/5/ A. Gavron, Phys. Rev. C 21 (1980) 230-236.

Prediction of Nature Resourced Chemicals-Metal Conjugates by Theoretical Computational Study

Puja Samanta[1], Sayanti Show[1], Pujarini Banerjee[1], Raj Kumar Nandi[1], Nabanita Naskar[1], Susanta Lahiri[1,2]*

[1] Diamond Harbour Women's University, Sarisha, South 24 Parganas 743368, India.
[2]Sidho-Kanho-Birsha University, Ranchi Road, Purulia 723104, India.
* Email: pujarini.banerjee87@gmail.com

1. Introduction

The interest in chemicals derived from natural resources has recently been renewed, especially after the introduction of green chemistry. Various important chemical processes were developed using such natural resources, for example, an eco-friendly method was developed to separate positron emitter ^{88}Zr from proton irradiated yttrium target using potato peel as a bioreagent [1]. In these types of works, biomasses were used without paying attention to particular components which are responsible for the desired chemical processes. Recently the nature resourced chemistry has been introduced which deals with the development of chemical processes with chemicals or reagents of natural origin. It excludes the use of total bio-organism like algae, yeast, etc., without knowing or isolating particular chemicals responsible for a particular process [2]. An example of nature resourced chemical (NRC) is the use of piperine derived from black pepper, which is a specific reagent for gold [3].

In this paper, we have selected one such NRC, curcumin, which is available in plenty in turmeric powder and studied the possibility of the formation of ^{99m}Tc-curcumin complex. If ^{99m}Tc conjugates with the selected NRC, then the radiopharmaceuticals can directly be injected into human body, which will also act as a free-radical scavenger during the introduction of radioisotopes in the human body.

2. Predictions of electronic structure theory

Electronic structure theory has over the past several decades proved to be an indispensable tool in understanding the equilibrium structures of molecules and their interactions with their surroundings. A vital part of the present study is to identify the viability of the ^{99m}Tc-curcumin complex. To this end, computations have been carried out using the Gaussian 09 Program package [4] to first identify the

minima on the potential energy surface of curcumin, and then to identify possible binding sites on the optimized curcumin with ^{99m}Tc. Calculations have been performed with the widely used DFT functional B3LYP in conjunction with the LanL2DZ basis set. Both di-keto and mono-enol forms of curcumin have been considered, out of which the former is predicted to be 8.7 kcal/mol lower in energy at the B3LYP/LanL2DZ level of theory. The figure below depicts the optimized structures of curcumin complexed with ^{99m}Tc in one of its most favored oxidation states +5. It is clear that the carbonyl oxygen on both the di-keto and mono-enol groups on curcumin are favored binding sites for Tc^{+5}. The high predicted magnitudes of the binding energies (2250.7 and 2312.8 kcal/mol for the diketo and mono-enol forms, respectively) of the complexes, as well as the short Tc-O bond lengths (2.00 and 1.92 Å, respectively), are indicative of strong Tc^{+5}-curcumin binding, which provides theoretical support for the use of curcumin as a nature resourced chemical.

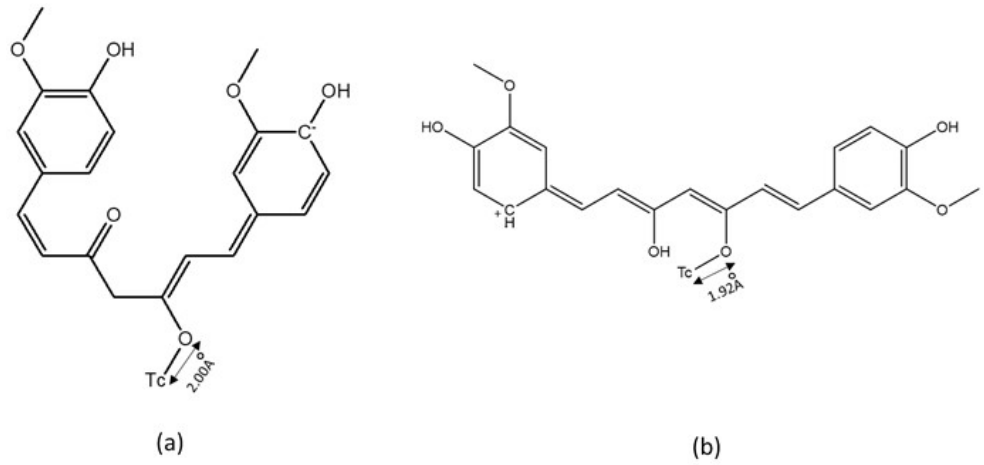

Figure1: Optimized structure of curcumin in di-keto form (a) and keto-enol form (b) with Tc^{5+} predicted at B3LYP/LanL2DZ level of theory

Acknowledgements: NN acknowledges DST-INSPIRE fellowship. SS and SL acknowledge CSIR-ES for providing necessary fellowship.

References

/1/ N. Naskar, D. Choudhury, S. Basu, et al., J. Radioanal. Nucl. Chem. 322 (2019) 231-235.

/2/ S. Lahiri, D. Choudhury, K. Sen, J. Radioanal. Nucl. Chem. 318 (2018) 1543-1558.

/3/ K. Ghosh, S. Lahiri, J. Radioanal. Nucl. Chem. 274 (2007) 233-236

/4/ Frish et al, Gaussian 09, Revision C.02, Gaussian, Inc., Wallingford CT, 2016.

Neutron Irradiation and Soxhlet Leaching Studies on The Strontium Substituted Sodium Iron Titanate

Manish Chand, B. Robert Selvan, A.S. Suneesh, N. Ramanathan, S. Sriram, S. Vijayalakshmi, V. Jayaraman*

Materials Chemistry and Metal Fuel Cycle Group, Indira Gandhi Centre for Atomic Research, Kalpakkam, India.
*E-mail: mchand@igcar.gov.in

1. Introduction

The leach resistance of a solid matrix can be understood by the Soxhlet experiment, in which the solid matrix is subjected to heat treatment in the presence of an aqueous medium and the metal ion's leaching tendency is analyzed by different spectroscopic techniques such as atomic absorption spectroscopy or flame emission spectroscopy etc. However, the scope of the above analytical methods is restricted to respective detection limits. In this context, a highly sensitive radiotracer, produced by neutron activation would be a suitable alternative technique for exploring the leaching behavior of the elements present in the matrix using the soxhlet method. This paper demonstrates the development of a neutron activation-cum-soxhlet based analysis of the leaching behavior of constituents present in the strontium-substituted sodium iron titanate matrix.

2. Experiment

The sodium iron titanate was synthesized by the hydrolysis of tetraethyl orthotitanate (47 mmol, 10 mL) and ferric chloride (5 mL of 1.87 mmol) using NaOH (0.67 M solution, 100 mL) solution. Strontium-substituted sodium iron titanate was prepared by the equilibration of strontium solution with sodium iron titanate powder [1]. Sr substituted (2.5 atom %) sodium iron titanate pellet was prepared from the corresponding powder sample and the pellet was further calcined at 1273K. The calcined pellet (about 150 mg) was packed in clean polyethylene sheets and irradiated at pneumatic fast transfer system (PFTS) position of the KAMINI reactor at 15 kW reactor power with a neutron flux of 10^{11} n cm^{-2} s^{-1} for 2 h. After sufficient cooling time, the sample was assayed by gamma spectrometry using 50% co-axial High Purity Germanium (HPGe) detector. The irradiated sample was subjected to dynamic leaching at 90 °C using the soxhlet method for 28 days towards the leaching study of the constituents present in the

strontium substituted sodium iron titanate (Sr, Na, Fe, Ti). During leaching, sample of 5 mL from the leachate solution was collected in a glass vial at different time intervals for 28 days and the total volume was maintained at 500 mL by adding Millipore water. After 28 days, the entire leachate solution was pre-concentrated to 5 mL and the pellet was packed again in the fresh polythene cover. All the leachate samples and pellets were assayed by HPGe detector in reproducible geometry and the activity was determined for the constituent elements.

3. Results and Discussion

The activity of various activation products produced by the nuclear reaction (n,γ), (n, p) and (n,α) of the constituent elements and impurities were calculated using HPGe detector. The full energy peak efficiency corresponding to each activation product was determined using the known radioactive point source i.e., ^{152}Eu. The activities of the activation products in strontium substituted sodium iron titanate pellet before and after leaching were recorded. The activities of ^{85}Sr, ^{59}Fe, ^{54}Mn, ^{51}Cr before leaching studies were found to be 0.82±0.01, 3.60±0.04, 0.20±0.00, 3.72±0.07 nCi respectively and after 28 days of leaching activities of the same radioisotopes were found 0.84±0.01, 3.66±0.06, 0.20±0.00, 3.70±0.08 nCi respectively. The activities of the various activation products at the end of irradiation in the pellet before and after the leaching study were found the same. The activity of the activation products in the various leachate solutions and pre-concentrated solutions was also calculated and was found to be in the background level. These observations conclude the negligible leaching of the constituent elements and confirm the rigid nature of the matrix. Therefore, the results of the present study confirm the suitability of the neutron activation technique in establishing the leaching behavior of the elements present in strontium-substituted sodium iron titanate.

4. Conclusion

The leaching study implied that neutron activation-cum-soxhlet leaching study is a suitable method to establish the leaching tendency of elements present in strontium-substituted sodium iron titanate matrix. The negligible leaching rate of the elements present in the matrix was confirmed by neutron-activation-cum-soxhlet leaching studies. The leaching corresponding to sodium could not be performed due to short live Na-24 (14.9 h), for the same the inactive experiment is in progress.

References

/1/ P. Amesh, et al., Sep. Purification Technol. 238 (2020) 116393.

Development of External (in Air) Particle-Induced Gamma-ray Emission Method for Non-Destructive Quantification of Low Z Elements in Reactor Materials

Sk Wasim Raja[1,3]*, R. Acharya[2,3]

[1]Radiochemistry Division (BARC), Variable Energy Cyclotron Centre, Kolkata-700 064, India.
[2]Radiochemistry Division, Bhabha Atomic Research Centre, Mumbai-400 085, India.
[3]Homi Bhabha National Institute, Mumbai-400 094, India.
*Email: sw.raja@vecc.gov.in

1. Introduction

Particle Induced Gamma-ray Emission method is based on the detection of prompt gamma rays when the target is bombarded with low-energy proton beams from accelerator [1]. This method is especially suitable for the quantification of low Z elements like Li, Be, B, F, Na, Al, Si etc. We have developed an external PIGE method at FOTIA, BARC where a proton beam is extracted in air through a thin Ta window [2] and applied it successfully for the characterization of nuclear reactor materials. This paper gives a brief of our developmental work on the external PIGE facility at FOTIA and its important applications for the characterization of nuclear reactor materials.

2. External PIGE facility

We have developed an external (in the air) PIGE facility at FOlded Tandem Ion accelerator (FOTIA), BARC in the PIGE/PIXE beam line for the rapid analysis of non-standard geometry samples in a greener way. For external PIGE, the proton beam was extracted in air through 25 μm Ta window and proton beam energy on target was ~3.5 MeV for the in-vacuum beam energy of 5 MeV [2]. Here beam current fluctuations was monitored either using 136 keV of ^{181}Ta(p,p'γ)^{181}Ta from Ta window material or 2313 keV of ^{14}N(p,p'γ)^{14}N from nitrogen present in air. The External PIGE method has several advantages over conventional vacuum chamber PIGE direct analysis of as received samples, high sample throughput, convenience, truly non-destructive and greener method.

3. Applications of external PIGE method to nuclear reactor materials

The external PIGE method has been successfully applied for quantification of low Z elements like B, Si, Al, Ti etc. in reactor materials (boron-based ceramics, alloys etc.) and isotopic composition of B (IC, $^{10}B/^{11}B$ atom ratio) in ceramic control rod materials (B_4C and other ceramics) in direct powder samples

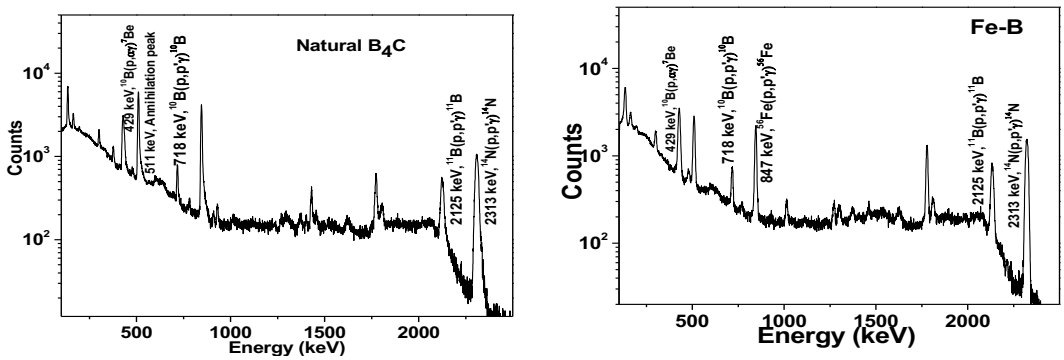

Figure 1: PIGE spectra of B_4C (left) and ferro-boron alloy (right) samples

without any sample pretreatment. Non-destructive simultaneous determination of Fe and B in ferro boron alloys were done using this external PIGE method by simply wrapping the samples in thin Mylar foil and irradiation with 3.5 MeV proton beam of current ~10-15 nA for 10-15 minutes and the characteristic prompt gamma rays were detected online with HPGe detector system. Typical PIGE spectra of boron carbide and Fe-B alloys are shown in Fig.1 with their characteristic prompt gamma rays. Details of the PIGE method development and its applications will be presented in the symposium.

4. Conclusion

The External PIGE method has successfully been applied for the determination of isotopic composition of B and its total mass fraction in different ceramic/refractory neutron absorbers, low Z elements like Fe and B in ferro-boron alloys etc. using direct samples wrapped in thin Mylar foil (as received samples). The developed method is found to be convenient, rapid, truly non-destructive and greener method for the analysis of reactor materials.

References

/1/ S. W. Raja, R. Acharya, P. K. Pujari, J. Radioanal. Nucl. Chem. 313 (2020) 1359.

/2/ S. W. Raja et al., Anal. Chim. Acta. 1202 (2022) 339686.

Effect of Wine Bottle Parameter on Absorption Effects in Coulomb Excitation Experiments

Monika Goyal[1], Rajiv Kumar[2], Rajesh Kharab[3]*

[1]Department of Physics, DAV University, Jalandhar-144012, India.
[2]Department of Physics, Govt. College for Girls, Taraori, Karnal -132001, India.
[3]Department of Physics, Kurukshetra University, Kurukshetra-136119, India.
*Email: kumarrajivsharma@gmail.com

1. Introduction

Coulomb excitation is a process in which a nucleus is excited by electromagnetic interaction of another nucleus [1-3]. The rigorous theoretical understanding of the electromagnetic interaction makes the Coulomb excitation process as one of the widely used tools for probing the properties of exotic nuclei [1]. However, such applications necessitate ascertaining the purity of the Coulomb excitation process. In case of experiments that are performed at beam energies above the Coulomb barrier, the projectile breaches the barrier and hence it is likely to be under the influence of strong nuclear interactions that violates the purity of the Coulomb excitation process. The undesirable effects caused by the strong nuclear interaction are known as absorption effects [2]. In the analysis of intermediate energy Coulomb excitation data, the absorption effects can be accounted through the concept of survival probability $|S(b)|^2$of the projectile as a function of impact parameter b [2].The value of$b$is always kept equal to or larger than sum of nuclear radii of the projectile(P) and the target(T) i.e.$b_{min} \geq R_P + R_T$. For all values of $b \geq b_{min}$ the absorption effect are considered to be vanishingly small. One of the crucial ingredients to evaluate the survival probability $|S(b)|^2$ is matter density distribution of the projectile. Out of several types of matter dependent density distribution, two parameter Fermi (2pF) and three parameter Fermi (3pF) density distribution is commonly used [3]. In the matter density distribution there are some free parameters which decide the shape of the distribution. Various nuclear properties like alpha decay half-lives, absorption effects and Coulomb excitation cross section have been found to be depending upon these free parameters namely wine-bottle parameter $(w_i)$and surface diffuseness parameter(a_i) [4].The 2pF and 3pF matter density distribution is distinguished by the parameter w_i. Therefore, it is interesting

to investigate the variation of $|S(b)|^2$ and absorption effects as a function of the parameter w_i. In present work, a recently studied projectile target system $^{46}Cr+^{197}Au$ [5] is chosen as a representative case.

2. Theoretical Formalism

The expression for the 2pF matter density distribution is $\rho(r) = \frac{\rho_0}{\left(1+\exp\left(\frac{r-R_i}{a_i}\right)\right)}$ (Eq. 1)

The expression for the 3pF matter density distribution is given by [3] $\rho(r) = \frac{\rho_0\left(1+\frac{w_i r^2}{R_i^2}\right)}{\left(1+\exp\left(\frac{r-R_i}{a_i}\right)\right)}$.(Eq. 2)

here ρ_0, R_i,$a_i$and w_i are central density, radius, surface diffuseness and wine bottle parameter respectively and suffix $i$standsfor projectile or target nucleus. The parameters R_i, a_i and w_i are determined for a given A_i using the equations mentioned in references [3]. It is pertinent to mention here that for the calculations of the survival probability, Coulomb excitation cross section, the absorption effects the code DWEIKO was used [6] but with 2pF and 3pF matter density distribution.

3. Results and discussion

The 2pF and 3pF type matter density distributions when plotted for ^{46}Cr are found to be different from each other. For a fixed value of a_i the Fermi density distribution extends spatially in the peripheral region as the value of $w_i$increases from $-0.19$to 0.0. Thus the variation in $w_i$lead to spatial extension of the matter density distribution of the projectile. We have plotted only the peripheral regions and also impact parameters b, against various density distributions. All these calculations will be discussed.

4. Conclusion

In conclusion the negative value of wine bottle parameterw_i have been found to be affecting the survival probability, Coulomb excitation cross section and the absorption effects significantly.

References

/1/ T. Glasmacher, *Lecture Notes in Physics,* edited by A. Khalili, E. Roeckl*,* Vol. 764 (Springer, Heidelberg, Germany, 2009).

/2/ R. Kumar, R. Kharab, H.C. Sharma, Phys. Rev. C 81 (2010) 037602.

/3/ S. Jain, M. Sharma, R. Kumar, Nucl. Phys. A 997 (2020) 121699.

/4/ M. Ismail et al., Nuclear Physics A 947 (2016) 64.

/5/ A. Boso, et al., Phys. Lett. B 797 (2019) 134835.

/6/ C.A. Bertulani, C.M. Campbell, T. Glasmacher, Comput. Phys. Commun. 152 (2003) 317.

Investigation of High Spin States and Shears Band Structure of ^{204}At

D. Kanjilal[1], S. K. Dey[2], S. Saha[3], M. Das[3], C. C. Dey[3], S. Ray[4], A. Bisoi[5], S. Nag[6], R. Palit[7], S. Saha[7]*

[1]Department of Physics, Raiganj Surendranath Mahavidyalaya, Raiganj, West Bengal 733134, India.
[2]Present address: KEK, Japan.
[3]Saha Institute of Nuclear Physics, I/AF Bidhannagar, Kolkata 700064, India.
[4]Amity Institute of Nuclear Science and Technology, Amity University, Noida, India.
[5]Indian Institute of Engineering Science and Technology, Shibpur, Howrah 711103, India.
[6]Indian Institute of Technology (Banaras Hindu University), Varanasi 221005, India.
[7]Tata Institute of Fundamental Research, Mumbai 400005, India.
*Email: debasmita.kanjilal@gmail.com

1. Introduction

Today's nuclear physics is pushing to the limits of our knowledge to the extremes of nuclear existence, away from line of stability. The synthesis and study of new elements (high Z) is one of the challenging prospects in nuclear research. Apart from a scientific challenge, it is also an experimental one. Heavy and Superheavy nuclei with Z above 82 and N less than or above 126 provide a unique laboratory to study nuclear structure and dynamics under the influence of large Coulomb forces and large mass. They are predicted to exhibit several interesting phenomena, such as abundance of isomers, shears bands, shape coexistence, octupole correlations. Exploring them is also important for the prediction of the end point of the *r*-process nucleosynthesis [1]. These heavy nuclei have very small liquid-drop fission barrier and are therefore stabilised only by quantum shell effects near the shell closure. Stability beyond the "doubly magic" ^{208}Pb decreases rapidly. That's why populating them via standard heavy ion-induced fusion-evaporation reaction is itself a challenge as fission dominates over the formation of evaporation residue (ER) resulting in reduction of ER yield and overwhelming unwanted background. Hence, fewer experimental data exist especially for odd-proton odd-neutron nuclei, as these are the least stable. For the synthesis of heavy-super heavy nuclides, it is very important to select reaction partners and the beam energies accurately and also to have good knowledge about the fission barrier. Theoretical shell model calculations are virtually impossible for these nuclei. To date, only a few shears bands were found in nuclei with small deformation for Z=84 and above, like ^{205}Rn [2], ^{206}Fr, ^{204}At [3], all having N =119 and

recently in ^{201,203}At [4, 5] isotopes. In almost all cases, these shear bands are created based on the interplay of a few high-spin protons involving $h_{9/2}$ and $i_{13/2}$ orbitals and the neutron holes in the $i_{13/2}$ sub shell. In our recent paper [6], we have attempted to establish the level scheme of doubly odd ^{204}At (Z= 85, N=119), which was partly known. The shears band observed earlier, has been evaluated in more detail and established to be in reasonable agreement on the basis of the shears mechanism with principal axis cranking (SPAC) model [7].

2. Experiment and Results

The experiment was done in TIFR, Mumbai using Indian National Gamma Array (INGA), at the Pelletron Linac facility via the $^{12}C + ^{197}Au$ fusion evaporation reaction. All the relevant details of experiment and the results have been published recently [6]. The level scheme of doubly odd ^{204}At, which was partly known from earlier studies, was extended upto ~8 MeV and ~25 ħ. Magnetic dipole band structure over the spin parity range: ~16^+ - 23^+, has been confirmed and explored in more detail, including the missing cross-over E2 transitions. Band-crossing along the shears band resulting from change of particle-hole configuration was observed and compared with the similar phenomena in the neighbouring ^{202}Bi, ^{205}Rn isotones and ^{203}At isotope. Lower spin part of the band is accounted for by $\pi(1h_{9/2})^2\pi(1i_{13/2})(\times)\nu(1i^{-1}_{13/2})$ configuration while post band-crossing configuration arise from breaking of two more particle-hole pairs leading to $\pi(1h_{9/2})^4\pi(1i_{13/2})(\times)\nu(1i^{-1}_{13/2})$. The experimental B(M1)/B(E2) for the shears band obtained from SPAC are compared with results from experiment using the measured intensities of the M1 and corresponding cross-over E2 transitions. For SPAC minimization at each spin, parameters are adjusted to be in reasonable agreement with the experimental results. Based on comparison of the measured values for transitions along the band with the SPAC, the shears band of ^{204}At was firmly established along with the level scheme.

References

/1/ I. V. Panov et al, A & A 513, A61 (2010).

/2/ J.R. Novak et al., Phys. Rev. C **59**, R2989 (1999).

/3/ D.J. Hartley et al., Phys. Rev. C **78**, 054319 (2008).

/4/ K. Auranen et al., Phys. Rev. C **91**, 024324 (2015).

/5/ K. Auranen et al., Phys. Rev. C **97**, 024301 (2018).

/6/ D. Kanjilal et al., Eur. Phys. J. A 58, 159 (2022).

/7/ A. A. Pasternak et al., Acta Phys. Pol. B 40, 647 (2009).

Thermal Evolution of Pyrochlore Phase in $La_2Zr_2O_7$ Pyrochlore: Local Probing by Time Differential Perturbed Angular Correlation Spectroscopy

D. Banerjee[1], Santosh K. Gupta[2], Kakoli Banerjee[3]*

[1]Radiochemistry Division (BARC), Variable Energy Cyclotron Centre, Kolkata-700064, India.
[2]Radiochemistry Division, Bhabha Atomic Research Centre, Trombay, Mumbai-400085, India.
[3]Prabhu Jagatbandhu College, Andul-Mouri, Howrah-711302, India.
*Email: dbanerjee@vecc.gov.in

1. Introduction

The immobilization of radioactive waste with long half-lives has always been a challenging research area in the nuclear industry. For this purpose, ceramic compounds have high chemical and radiation stability over glass matrices [1–2]. Among such potential ceramic compounds, pyrochlore has high stability even in non-stoichiometric chemical compositions and is considered as a promising host matrix [3]. Pyrochlores have the general formula: $A_2B_2O_7$ (A: Rare earth and B: Transition metals) and they possess high radiation tolerance due to the facile transition from an ordered to a disordered phase. Among Pyrochlores, Zirconates and Hafnates show great potential to be candidates for nuclear waste immobilization matrices [4]. Among the various pyrochlore compounds, $La_2Zr_2O_7$ (LZO) is a promising candidate. As the physical properties of LZO pyrochlore strongly depend on its phase stability, structural and functional applications involving LZO require information on fluorite to pyrochlore phase transition. The aim of the present work is to understand the evolution of pyrochlore phase with temperature by local probing with Time Differential Perturbed γ–γ Angular Correlation (TDPAC) Spectroscopy.

2. Experiment

LZO pyrochlore in the present work has been synthesized from Zirconium Oxychloride and Lanthanum Nitrate precursors by coprecipitation method and subsequent annealing over a temperature range of 1073-1423K for 8 h in air. TDPAC measurement was carried out with $^{181}Hf/^{181}Ta$ probe present at ppm level in the sample. All the measurements were carried out at room temperature.

3. Results and Discussion

The TDPAC spectra for LZO samples annealed at different temperatures are shown in Fig. 1.

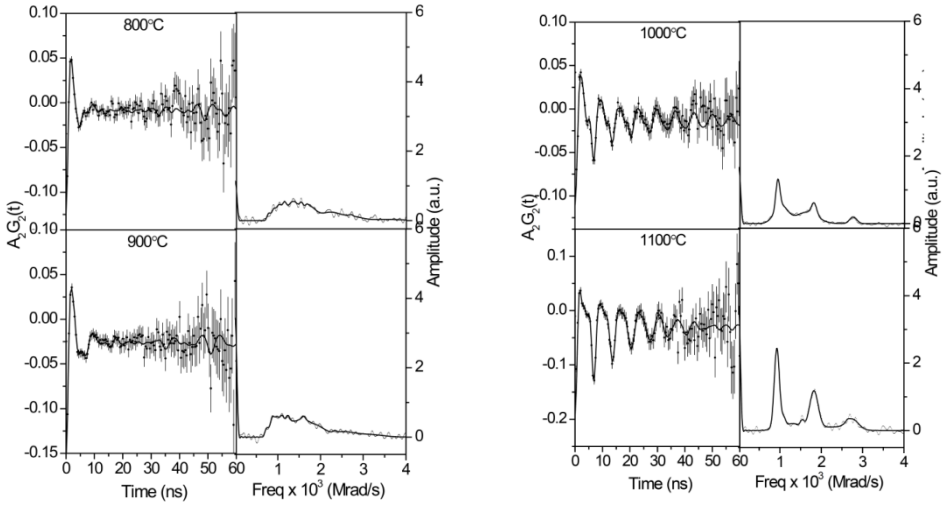

Figure 1: TDPAC Spectra for $La_2Zr_2O_7$. Left: $A_2G_2(t)$ and Right: Fourier transform

The gradual evolution of oscillatory pattern corresponding to the pyrochlore phase is clearly visible in the above figure. The powder XRD pattern of the LZO pyrochlore annealed at 1273K show the peaks for pyrochlore phase and TDPAC parameters for the phase could be well supported by DFT calculation [5]. The local structure around Zr-atom indicates that the pyrochlore phase formation starts only at 1223K and the relative population of pyrochlore phase gradually increases. XRD and other complimentary measurements for samples annealed at different temperatures will be presented during the conference.

References

/1/ K.E. Sickafus, L. Minervini, R.W. Grimes, et al., Science 289 (2000) 748-751.

/2/ J. Zhang, J. Lian, F. Zhang, et al., J. Phys. Chem. C. 114 (2010) 11810-11815.

/3/ S.N. Achary, S.K. Sali, N.K. Kulkarni, et al., Chem. Mater. 21 (2009) 5848-5859.

/4/ V. Trummel, S.K. Gupta, M. Pokhrel, et al., J. Luminescence 207 (2019) 1-13.

/5/ D. Banerjee, S.K. Gupta, B. Modak, et al., Abstract accepted in 9th Interdisciplinary Symposium on Materials Chemistry (ISMC-2022).

Production of TiO_2 Microspheres for Radiological and Environmental Applications

D. Maji[1], S. Balakrishnan[1], V. Jayaraman[1], K. Ananthasivan[2]*

[1]Materials Chemistry & Metal Fuel Cycle Group, [2]Reprocessing Group,
Indira Gandhi Centre for Atomic Research, Kalpakkam-603102, India.
*E-mail: dmaji@igcar.gov.in

1. Introduction

TiO_2 microspheres have captured large attention in environmental science due to it's application in removal of toxic metals from water [1]. TiO_2 microspheres could also be used as ion exchange material to remove plutonium from the waste solutions produced in nuclear reprocessing plants [2, 3] for nuclear waste management. However, in most of the studies, the focus is on the exploration of its potential in applications [1-3]. Detailed investigations on the preparation of TiO_2 microspheres have not been reported so far. Hence, an investigation of the production of the TiO_2 microspheres by the internal gelation process and optimization of the process parameters is carried out in this work.

2. Experimental

2.1. Materials and preparation of gelled spheres: Aqueous solutions of $TiOCl_2$ (~4 M), hexamethylenetetramine (HMTA) and urea (~3 M), were used as stock solutions. Feed solutions were prepared by mixing the stock solution at 273 K for different compositions. The cooled feed solution was dispersed through a vibratory capillary nozzle into hot silicone oil (363 K), circulating through the internal gelation system (Figure 1) in the form of droplets. The feed droplets get transformed into soft gel spheres due to gelation. The gelled spheres (commonly termed as microspheres) were washed with CCl_4 followed by 8% NH_4OH and isopropanol. These microspheres were dried in air at 298 K for 24 h and at 473 K for 8 h, respectively. The dried microspheres were then calcined at 923 K for 4 h in air. The dry, as well as calcined microspheres, were characterized for crystal structure and crystallite size by XRD, bulk density as well as residual carbon.

3. Results and Discussion

Figure 1 shows the schematic of the experimental set-up and the process of gelation. The detailed optimization of feed composition has been established and the most suitable feed composition was determined. Figure 2 shows photographs of the dried and calcined microspheres. Bulk density of 1.0505 ± 0.0016 g/cc, residual carbon of 215 ppm and crystallite sizes of 20.6 nm were observed for the calcined microspheres. The presence of anatase titanium dioxide is affirmed by XRD.

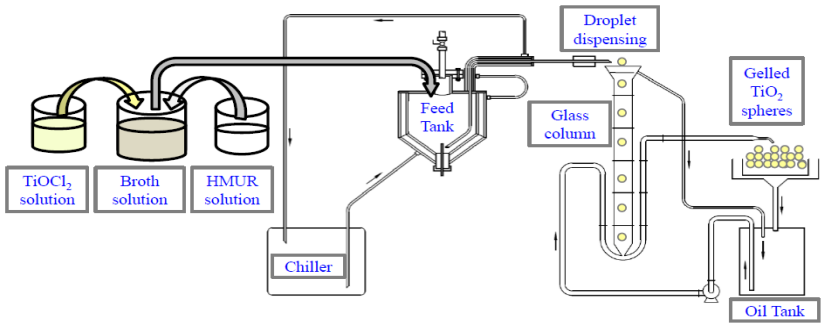

Fig 1: Schematic diagram of experimental set-up and gelation process

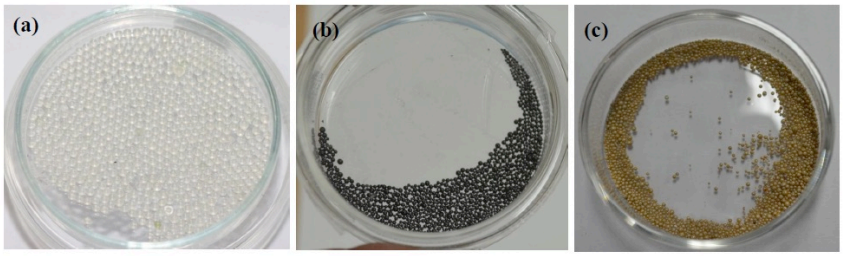

Fig 2: Photograph of TiO_2 gelled spheres: (a) Soft gel; (b) Dried and (c) Calcined

4. Conclusion

TiO_2 microspheres have been produced by optimizing different process parameters for the separation of heavy metals related to radiological and environmental applications. These microspheres were characterized for crystal structure and crystallite sizes were determined from XRD data.

Acknowledgement: Support from the sol-gel team of AFSS and the mechanical team from CFED is acknowledged.

References

/1/ D. Charu, R. Naina, M. Kumar, et al., J. Radioanal. Nucl. Chem. 294 (2012) 131-136.

/2/ I.C. Pius, M.M. Charyulu, B. Venkataramani, et al., J. Radioanal. Nucl. Chem. 199 (1995) 1-7.

/3/ I.C. Pius, R.D. Bhanushali, Y. R. Bamankar, et al., J. Radioanal. Nucl. Chem. 261 (2004) 547-550.

Demonstration of Quantitative Extraction of Radioactive Kr and Xe Fission Gases through Liquid Sodium

G.V.S. Ashok Kumar, M. Bootharajan, J.S. Brahmaji Rao, N. Ramanathan, K. Sundararajan, V. Jayaraman*

Materials Chemistry and Metal Fuel Cycle Group, IGCAR, Kalpakkam – 603102. India.
*Email: gvs@igcar.gov.in

1. Introduction

The Prototype Fast Breeder Reactor (PFBR) is a 500 MW(e), 1250 MW(t) pool-type liquid sodium cooled fast reactor using uranium plutonium mixed oxide [(U,Pu)O2] as the fuel. The reactor is equipped with several stringent safeguard procedures for its continuous operation. Failed fuel location module is one of the safe operating methodologies used to identify the fuel subassembly (FSA) having fuel pins with clad failure. Identification of a failed FSA due to the dry rupture of its fuel pin in PFBR was standardized by studying the interaction of fission gases (Kr & Xe) with liquid sodium and their detection by high-resolution gamma spectrometry using HPGe detector. The initial experiments were performed with inactive Kr/Xe gases using Ar as a carrier gas and the detection of these gases was carried out using Gas Chromatography. The results are found to be that interaction of these gases with liquid sodium is negligible. However, to improve the results with respect to detection limits and to simulate the actual experimental conditions, studies with radioactive fission gases were carried out.

2. Experiment

The radioactive fission gases were collected from a Madras Atomic Power Station (MAPS) by passing the cover gas through a silica gel trap to absorb the moisture in the cover gas, followed by the absorption of fission gases onto the charcoal source trap maintained at cryogenic temperatures. The charcoal source trap was connected to the experimental setup consisting of silica gel trap-2 for removal of traces of moisture, if any before releasing the fission gases into the sodium, purge gas originating compartment (PGOC) with pre-calibrated line volume and prototype sodium module (PTSM) with liquid sodium (Fig.

1). Outlet of PTSM was connected to a sodium trap to remove the vapours of sodium followed by a charcoal bed (CB) for the collection, identification and quantification of fission gases. A known volume of fission gases was taken into the PGOC and introduced into the PTSM, which was maintained at 360 ^{o}C. The fission gases were subsequently collected into the CB maintained at liquid nitrogen temperature with Ar purge into the PTSM. The activities of fission gases in CB were measured by High Purity Germanium (HPGe) detector.

3. Results and Discussion

The CB was assayed initially without the introduction of fission gases to register the blank gamma spectrum. The gamma spectra of blank CB and CB with fission gases are shown in Fig.2. As CB is non-standard in matrix and geometry, full-energy peak efficiency calibration was carried out using EFFTRAN - A Monte Carlo efficiency transfer code for gamma spectrometry, which uses geometry and dimensions of detector and sample. The arrived efficiency calibration was used to quantify the ^{135}Xe ($t_{1/2}$ = 9.1 h), ^{133m}Xe ($t_{1/2}$ = 2.198 d) and ^{85m}Kr ($t_{1/2}$ = 4.48 h). The results showed that a quantitative recovery (> 95%) of the fission gases was observed with the detection limits of sub picogram (pg) levels. The present study affirms and demonstrates the plausibility of identification of dry rupture of the fuel pin in the FSA as the detection methodology used could identify the fission gases in sub pg levels.

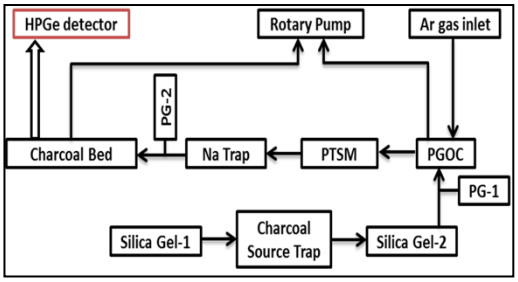

Figure 1: Schematic block diagram of the experimental set-up

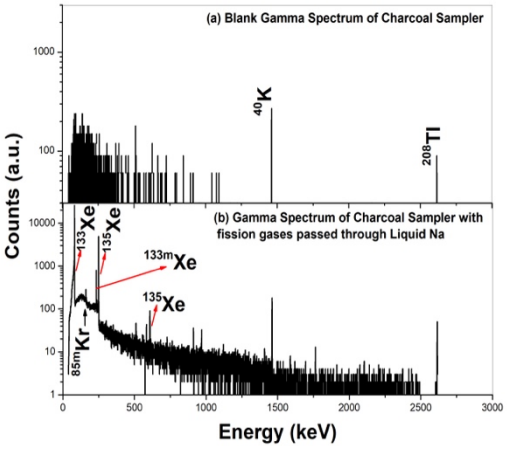

Figure 2: Gamma spectrum of (a) blank CB and (b) CB with fission gases passed through Liquid Na

References

/1/ N. Ramanathan, M. Bootharajan, G.V.S. Ashok Kumar, et al., J. Nucl. Mat. 558 (2022) 153326.

Assay of Platinum in Pt/SiO_2 Catalyst using EDXRF and INAA

*J.S. Brahmaji Rao[1], S. Ramakrishna Reddy[2], R. Senthilvadivu[1], G.V.S. Ashok Kumar[1], K. Sundararajan[1]**

[1]Materials Chemistry and Metal Fuel Cycle Group, [2]Reprocessing Group,
Indira Gandhi Centre for Atomic Research, Kalpakkam 603102, India.
*Email: sundar@igcar.gov.in

1. Introduction

Silica-supported platinum (Pt/SiO_2) catalysts prepared and characterized using various techniques are gaining popularity for many applications [1,2]. In nuclear plants, Pt/SiO_2 would be used as a catalyst during the reduction of U(VI) to U(IV) and also destroy the hydrazine during reprocessing of nuclear fuels. Analysis of such samples by conventional wet chemical methods such as AAS and ICP-OES is cumbersome which demands quantitative dissolution. Therefore, in the present study, non-destructive analytical techniques viz. Instrumental Neutron Activation Analysis (INAA) and EDXRF were investigated for the assay of platinum in catalyst materials.

2. Experiment

EDXRF and INAA methods were used for the non-destructive analysis of catalyst materials procured for the applications in IGCAR. The samples were first qualitatively analyzed using EDXRF technique using a low power Rh-target X-ray tube. The samples were excited with voltage and current of 15 kV, 300 μA respectively in air ambience for about 300 sec. In the case of INAA, a known amount of two catalyst powder samples were taken on cellophane paper and sealed in cleaned polythene covers. The solution of platinum as a reference standard was also taken on filter paper and dried. The samples and standard were heat sealed and irradiated for 2 h at the pneumatic fast transfer system position of KAMINI reactor at 20 kW power. After overnight cooling, the samples were counted using high-resolution gamma spectrometry by a 30% p-type high pure germanium detector coupled to ITEC 8 k MCA module and Inter Winner software.

3. Results and Discussion

The EDXRF spectrum of the sample (Fig.1) indicated the presence of Si and Pt. However, the quantification of these elements was not carried out due to the non-availability of matrix-matched standards. Hence, the matrix independent method of analysis, INAA was used to analyse the samples for the Pt content. The relative method of INAA was employed to calculate the concentration of platinum and the same is presented in Table.1. The assay indicated that the amount of Pt present in the sample was used to evaluate the quality of the catalyst material.

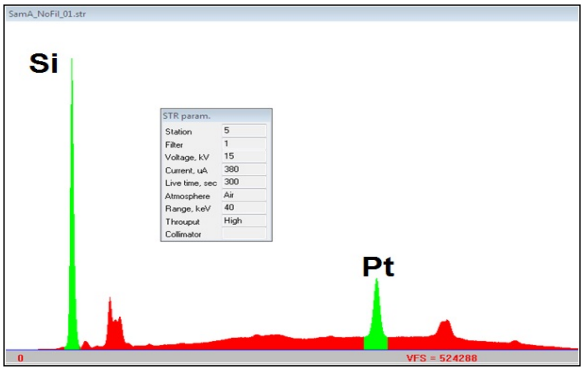

Figure 1: EDXRF spectrum of Pt/SiO_2 catalyst

Table 1: The results of Pt by INAA

Sample ID	Pt (%)
A	1.166 ± 0.130
B	1.151 ± 0.142

4. Conclusion

Non-destructive analytical technique, INAA can be used to estimate the platinum accurately in the catalyst samples. The study also ascertains the assay of an accurate amount of Pt in catalyst for accountability of precious platinum used in the experiments.

References

/1/ R. Zahaf et al., Aerosol Air Quality Res. 15 (2015) 2409-2421.

/2/ R. Verma et al., BARC Report, BARC/2014/E/018 (2015).

Standardization of Digestion Method for Efficient Recovery of Sr Radioisotopes from Hydroxyapatite Matrix and Soft Tissues

Debasish Saha, J Vithya, A. Arul Kumari, K Sundararajan*

ACSD, MC&MFCG, Indira Gandhi Centre for Atomic Energy, HBNI, Kalpakkam, 603102, India.
*Email: dsaha@igcar.gov.in

1. Introduction

Therapeutic radiopharmaceutical $^{89}SrCl_2$ is produced at IGCAR, Kalpakkam via $^{89}Y(n,p)^{89}Sr$ reaction using India's only fast reactor i.e. FBTR [1-2]. The QC data of IGCAR produced $^{89}SrCl_2$ radiopharmaceutical matches with the recommendations of US, EU and International Pharmacopeia. To obtain regulatory clearance from Radiopharmaceutical Committee (RPC), DAE for its regular production for metastatic bone cancer patients, in addition to above QC data, biodistribution data on animal is also required. Biodistribution shall be performed by injecting a small fraction of $^{89}SrCl_2$ in laboratory rats e.g. Wistar rats or Swiss mice. In this paper, we have demonstrated the digestion of hydroxyapatite matrix with soft tissues and recovery of $^{85+89}Sr$ tracer post digestion.

2. Experiment

Bone mineral is mostly (85%) in the form of hydroxyapatite (HA, $Ca_{10}(PO_4)_6(OH)_2$), with calcium carbonate (10%), calcium fluoride (2–3%) and magnesium fluoride (2–3%). Femur bone with flesh of locally grown broiler chicken (Gallus gallus domesticus), obtained from a slaughter house was divided into three almost equal pieces and was used for this study. In this study, we have used bone along with flesh hereafter referred as 'hydroxyapatite matrix and soft tissues'. Initially, digestion was standardised without the addition of tracer in 'hydroxyapatite matrix and soft tissues' to check the feasibility of the digestion. Broiler chicken bone matrix was used instead of mice/rat, because of i) easy availability ii) higher bone weight and iii) higher bone density. A mixture of H_2SO_4 and H_2O_2 was used, which upon reaction forms per-oxy-mono-sulphuric acid (H_2SO_5), which is highly oxidising species in nature [3].

About 10g of 'hydroxyapatite matrix and soft tissues' was digested using 75 mL of conc. H_2SO_4 and with gradual addition of H_2O_2 . Vigorous reaction took place when the ratio became 3:1. Without any external heat source, the temperature of the solution raised up to 100-120^oC, due to exothermic nature of the reaction. This whole process took only 4-5 minutes for complete dissolution.

A 100µL fraction of $^{85+89}Sr$ tracer (M/ BRIT, Mumbai) was injected into the flesh portion of 'hydroxyapatite matrix and soft tissues' with a surgical syringe. Digestion experiment was carried out in the similar lines as above. The experiment with tracers was repeated twice. After completion of the experiments, solution was cooled, a fraction of sample was withdrawn and was assayed by gamma spectrometry using HPGe (M/s Baltic, Latvia) and Cerenkov counting using LSC (M/s Perkin Elmer).

3. Results and Discussion

Piranha solution is oxidizing and corrosive mixtures of H_2SO_4, H_2SO_5, and H_2O_2. Since H_2O_2 was added step by step, highly hygroscopic H_2SO_4, reacts with organic matter violently and forms black carbon, which on further addition of H_2O_2 gets oxidised to CO_2. The major element of bone, Ca forms calcium sulphate, which is soluble in the medium. The assay of the samples using 514 keV γ ray due to ^{85}Sr suggests, 98.0 (±1.5) % recovery of ^{85}Sr radioisotope post digestion, whereas Cerenkov counting shows, the recovery of ^{89}Sr is 92.4 (±1.7) %, may be due to quenching in the sample.

4. Conclusion

It is absolutely necessary to standardise the digestion method and to know the extent of recovery. Hence, this important study was performed using a mixture of a γ (^{85}Sr) and β^- (^{89}Sr) emitting radioisotopes. The % recovery of ^{85}Sr in post digestion shows almost quantitative recovery of the radioisotope, whereas same sample by cerenkov assay of ^{89}Sr shows slightly less recovery. It is well known phenomena that, the assay of gamma does not get perturbed by medium much compared to the assay of beta emitters by a scintillation counters. The excellent recovery data by the gamma counting shows this digestion method can be used for further experiments with respect to actual biodistribution of $^{89}SrCl_2$ radiopharmaceuticals to animals.

References

/1/ D. Saha, et al. Radiochim. Acta. 101 (2013) 667-673.

/2/ D. Saha, J. Vithya, R. Kumar, Indust. Eng. Chem. Res. 61 (2022) 3817-3830.

/3/ H. G. Schmidt, ACS Chem. Health Safety 29 (2021) 54-61.

Recovery of NCA ^{60}Co Radioactive Source from SS 316 Irradiated in FBTR

J Vithya, Debasish Saha, S Annapoorni, S Vijayalakshmi, K Sundararajan*

ACSD, MC&MFCG, Indira Gandhi Centre for Atomic Energy, HBNI, Kalpakkam 603102, India.
*Email: dsaha@igcar.gov.in

1. Introduction

^{60}Co has its application in radiotherapy due to its strong gamma energy. ^{60}Co can be produced in Fast Breeder Test Reactor (FBTR) by ^{60}Ni(n, p)^{60}Co reaction. No carrier added (NCA) ^{60}Co produced via this reaction shall have specific activity of ~10^3 Ci/g, compared and is much higher than the thermal reactor produced ^{60}Co. Due to the long half-life of 5.3 years, a long irradiation time is better but availability of reactor with continuous operation is a limiting factor. In this scenario we wanted to explore the feasibility of separation of ^{60}Co produced from structural material used in FBTR i.e. SS316, which contains 10-14% Ni.

2. Experiment

The fraction of alloy specimen was obtained from FBTR irradiated fuel subassembly, which was irradiated in 3rd ring of FBTR core centre. The subassembly got irradiated during reactor operating conditions between 1985-2011. The contact dose of the specimen was 1700 μSv/h. The dissolution of FBTR irradiated SS316 alloy (0.36g) was carried out in 20 mL 1:1 HCl and HNO_3 mixture. Due to very similar chemical properties of transition elements present in SS316, rarely selective methods of separation are available. Hence multistage separation method is always preferred. Selective separation of Fe(III) was standardised in HCl medium using solvent extraction method and di-isopropyl ether (DIPE) as extracting agent. The basic extractant Aliquat 336 (methyl-tricaprl-ammonium chloride, $R_4N^+Cl^-$) /SCN in xylene is known for the extraction of anionic complexes. Separation of Co from various other elements was carried out using solvent extraction method and by Aliquat 336 as extractant. The radioactive ^{60}Co source so obtained after two stages of solvent extraction (Fig.1) was assayed by Radioactive Ion Chromatography (IC) technique and Gamma Spectrometry using HPGe detector.

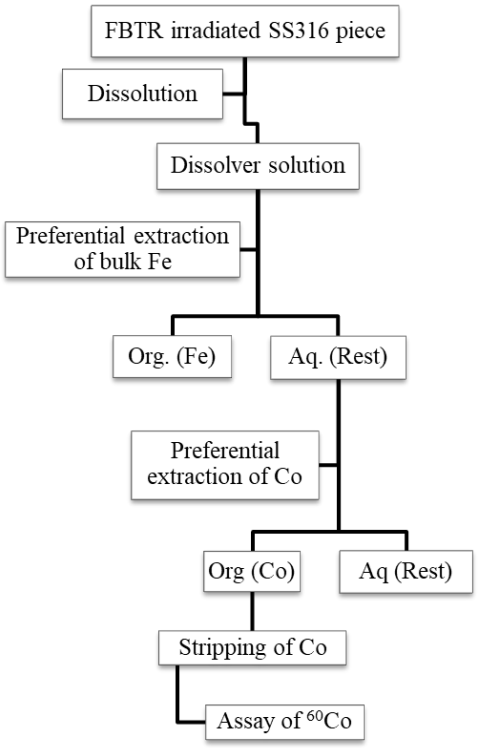

Fig. 1: Flow chart for the preferential separation of ^{60}Co from FBTR irradiated SS316 alloy

3. Results and Discussion

Complete dissolution was obtained within 30 minutes. Fe(III) gets preferentially extracted as $FeCl_4^-$ leaving rest of the elements in the aqueous phase [1]. The AAS profile of the separation with simulated solution confirms preferential extraction of Fe to the organic phase leaving rest of the elements in the aqueous phase [2]. It was found that Co, got preferentially extracted to organic phase by Aliquat 336, since it forms a stable octahedral complex with Co(II), i.e., $[R_4N(Co)(SCN)_6]$. The extraction was carried out keeping the aqueous phase in same concentration after Fe extraction. With two extractions steps quantitative extraction was achieved. Stripping was done using dilute (pH 3) acid solution, since the complex formed is unstable at these conditions.

The impurity concentration of the purified radioactive ^{60}Co fraction (Fig.1) was found less than the LOD level (≤10 ppb) of the IC UV VIS detector. The gamma spectrum does not show the presence of any other gamma emitters. The ^{60}Co yield was found 4.2 mCi/g of SS316 at the end of irradiation. Assuming an average wt. of a subassembly as 15kg, the yield of ^{60}Co shall be 63 Ci/ subassembly. The yield of ^{60}Co is sufficiently high for its usage as a brachytherapy source as well as a standard source. With the present 40MW$_{th}$ FBTR, the yield is expected to be higher than the obtained activity

Acknowledgement: We thank Dr R Divakar and his colleagues of RML, MMG, IGCAR for providing FBTR irradiated SS316 alloy and R. Umamaheswari, ACSD for analysis of few samples by AAS.

References

/1/ R. W. Dodson, J. F. Gerard, H. S. Ernest, J. Am. Chem. Soc. 58 (1936) 2573-2577.

/2/ A. A. Nayl, J. Hazardous Materials 173 (2010): 223-230.

Batch and Column Adsorption of Ag(I) and Zn(II) from Aqueous Solutions using Radiotracer Technique

Sabrina A. Shaikh, *Hemlata K. Bagla**

Department of Nuclear and Radiochemistry, Kishinchand Chellaram College, Mumbai- 400020, India.
*Email: hemlata.bagla@kccollege.edu.in

1. Introduction

Heavy metals above allowable limits often negatively affect humans, other organisms and the environment. Retardation, neurotoxicity, fragile bones, and other conditions have all been linked to chronic and acute toxicity from exposure to metal ions like Ag(I) and Zn(II). Exposure to silver in the air should not exceed 0.01 mg/m3, whereas toxicity levels of zinc have been reported when greater than 50 mg. The present research focuses on removing and recovering these metallic ions from aqueous solutions by employing the adsorption process. It is one of the most efficient, feasible, and economically intriguing techniques for the removal of toxic heavy metals from wastewater.

2. Experiment

Batch adsorption and subsequent desorption of Ag(I) and Zn(II) were carried out using the radiotracer technique, with each process optimized at a contact time of 5 min. The effect of various cations on the sorption process was studied and desorption parameters were adjusted to achieve the recovery of metal ions. Dry Cowdung Powder (DCP) and Humic Acid (HA) were used directly without being subjected to any pre-treatment [1]. Characterization was carried out by FTIR and Brunauer-Emmett-Teller (BET) techniques. The experimental data was examined using standard modeling methods and the treated solutions were analyzed by NaI(Tl) gamma-ray spectrometer. Additionally, a composite material of DCP and HA was prepared in the form of beads to carry out the column adsorption experiment.

3. Results and Discussions

The results reported that the Freundlich isotherm and the pseudo-second-order model are more in line with the experimental data, suggesting that the adsorption process of Ag(I) and Zn(II) is driven by

chemisorption and occurs in multilayers. The binary study showed that there is no competition for active sites between the ions. Column adsorption was carried out using a 5mL bed, with a flow rate of 30 mL/hr, and 6-bed volumes/hr. Within the first 30 min, 86±3% and 88±3% of Ag and Zn were adsorbed using a composite material of DCP/HA columns respectively. As illustrated in Fig 1 and Fig 2, the FT-IR spectra of untreated DCP and HA demonstrate peaks of O-H stretch, C-H (symmetric), C-H (antisymmetric), C=O stretch, C-H bend, C-O stretch, and aromatic C-H bend. Post adsorption, some shifts in the peaks were detected, indicating the possible interaction of these functional groups with Zn(II). Table 1 lists the percentage efficiency for the batch adsorption and desorption process.

Table.1 Adsorption and desorption efficiency of Ag(I) and Zn(II) by DCP and HA

	DCP	HA
% Adsorption of Ag(I)	94 ± 2	76 ± 2
% Desorption of Ag(I)	91±3*	90 ± 3*

	DCP	HA
% Adsorption of Zn(II)	94 ± 2	61 ± 2
% Desorption of Zn(II)	96±3**	95 ± 3**

**1M Citric Acid* ***1M Hydrochloric acid*

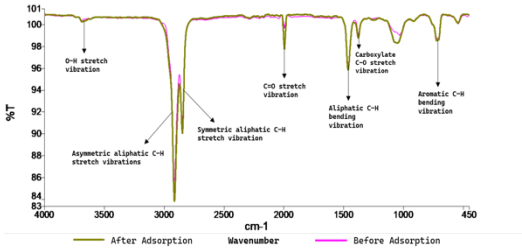

Fig 1: FTIR graph of DCP before and after adsorption of Zn(II)

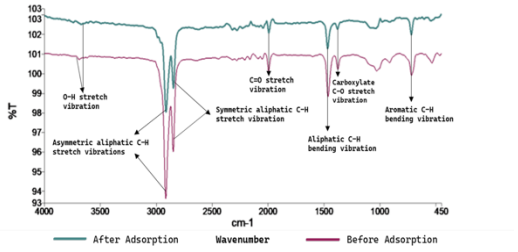

Fig 2: FTIR graph 0f HA before and after adsorption of Zn(II)

4. Conclusion

DCP and HA could be considered potential adsorbents for the removal of heavy metals from aqueous solutions. The feasibility of Ag(I) and Zn(II) removal was demonstrated as a time-efficient, exothermic and spontaneous process. The removal/recovery of metal ions using the composite material was found to be effective in an expanded-scale trial. Stability, reusability, and adsorption/desorption characteristics of the bio-sorbents served as the foundation for their practicality. It would also work as a low-cost bio-sorbent that is acceptable to the environment as "green" idea of producing less sludge.

Acknowledgment: Authors would like to acknowledge the Indian Institute of Technology, Bombay for providing us with BET results.

References

/1/ S.A. Shaikh, H.K. Bagla, Nucl. Engg. Technol. 54 (2022) 456- 461.

Investigation of Precipitation of Iron with Tungstic Acid in The Analysis of Tungsten Containing Compounds by ICPOES and Tracer Studies

*S. Sriram, S. Annapoorani, J. Vithya, Debasish Saha, K. Ushalakshmi, S. Vijayalakshmi**

Analytical Chemistry and Spectroscopy Division, Materials Chemistry and Metal Fuel Cycle Group, Indira Gandhi Centre for Atomic Research, Kalpakkam, India.
*E-mail: sviji@igcar.gov.in

1. Introduction

Carbides and oxides play important roles in nuclear industry. Apart from nuclear fuels, WC, B_4C and WO_3 have applications in shielding and control rod materials and in chemical sensors. Care must be taken for the destructive characterization of these compounds owing to the challenging dissolution conditions. If fusion method is resorted for the dissolution of W compounds, hydrated tungstic oxide is formed in the final acidic condition of the dissolved solution. Presence of Fe was found to have co-precipitation. Co-precipitation issue does not arise in Microwave digestion (MW) using HF with other acid mixtures and has been demonstrated for W containing B_4C [1]. In this study, extent of co-precipitation of Fe with W was examined for different tungsten containing compounds i.e., WC, B_4C and WO_3 by using MW and fusion technique followed by use of ICPOES and radiotracer techniques.

2. Experimental

Microwave digestion: WC powder (100 mg) and 1 mL of Fe standard of concentration 1mg/mL was dissolved using HNO_3 and H_2O_2. The precipitate was filtered. The precipitate with the filter paper was dissolved by HF, HNO_3 and H_2O_2. The solutions were analyzed for Fe by ICPOES. To study the effect of Fe: W ratio, the experiment was carried out using 0.5mL of concentration 1 mg/mL of Fe standard.

Sodium carbonate fusion: Sodium carbonate fusion was carried out for B_4C containing W and Fe. The fused mass was dissolved in HCl and the precipitate was filtered. Filter paper with precipitate was dissolved by MW digestion using HF, HNO_3 and H_2O_2 mixture and were analyzed for Fe by ICPOES.

Digestion experiment was carried out with ^{59}Fe radiotracer for understanding the effect of trace concentration of Fe on co-precipitation. To avoid the localized dissolution of Pt, ^{59}Fe tracer solution in chloride form was converted to sulphate form by heating with sulphuric acid. Concentration of Fe was determined by a modified Ion Chromatograph (IC) suitable to handle radioactive samples.

2.5g of Na_2CO_3 was weighed into a Pt crucible, 0.1mL of ^{59}Fe tracer solution (60 ng) was added and was dried. WO_3 (~100mg) was then added followed by another 2.5 g of Na_2CO_3. The Pt crucible was heated in a glove box at 950ºC for half an hour. The fused mass was taken in a beaker and dissolution was carried out with the step-by-step addition of 1 to 2 ml of 4M HCl. The solution was kept overnight and next day, clear supernatant solution was counted for its activity.

3. Results and Discussion

Treatment of WC in MW with HNO_3 and H_2O_2 precipitated $WO_3 \cdot xH_2O$. The extent of co-precipitation of Fe was 25% for the addition of 1 mg of Fe and 45% for the addition of 0.5 mg of Fe.

Precipitate was also observed in the final solution prepared by sodium carbonate fusion method of B_4C sample containing WC and Fe. Analysis of precipitate indicates 60% co-precipitation of Fe.

Co-precipitation at µg/mL levels of Fe in W matrix was examined using ^{59}Fe tracer. Results of assay of samples for ^{59}Fe by gamma spectrometry indicated 47% co-precipitation.

With increase in Fe: W weight ratio, co-precipitation initially decreased from 50% to 25% and then increased to 60%. The observed variation in co-precipitation may be due to the change in the quantity of formation of various hydrated tungstoferric oxide precipitates such as $Fe_2O_3.3.3WO_3$ and $Fe_2O_3.4.3WO_3$ [2]. Fe in filtrate may be present in the form of soluble tungstoferric acids such as $Fe_2[H_2W_{12}O_{40}]$.

4. Conclusion

Co-precipitation of Fe with tungstic acid was observed to a significant extent at all concentration of Fe from all W-containing compounds in both MW digestion and Fusion.

Acknowledgements: Authors are thankful to Smt. V. Hemalatha, Smt. Uma Maheswari, Dr V. Jayaraman, AD, FMCG, and N. Sivaraman, GD, MC&MFCG for their support.

References:

/1/ J.K. Sekar et. al., IGC report No. 385, 2020.

/2/ J. A. Mair, J. Chem. Soc. (1950) 2364-2372.

A Combination of Thermal and Epithermal Instrumental NAA as well as Cloud Point Extraction Preconcentration NAA to Measure Aluminum Content of Canadian Duplicate Diets

*Eric E. Sullivan, Jason Dalziel, A. Chatt**

Trace Analysis Research Centre, Department of Chemistry, Dalhousie University
6274 Coburg Road, Room 212, PO BOX 15000 , Halifax, NS, B3H 4R2, Canada.
*Email: a.chatt@dal.ca

1. Introduction

Aluminum has not been recognized as an essential element to humans. Exposure to aluminum is of public concern due to its potential toxic biological effects and possible association with Alzheimer's disease. It is one of the most common elements in the human environment. Acid rain can increase its concentration in surface water. Aluminum content of drinking water can be increased during the use of aluminum sulphate in the water purification process. It is naturally present in water and most foods, and its levels vary with geographic location. Typical mass fractions of aluminum in foods are 0.02-5 mg kg^{-1} (wet weight) and typical dietary intakes of aluminum range between 1 and 30 mg d^{-1} (dry weight). Food processing, preparation and storage can also lead to the addition of aluminum to the diet. It is a rather difficult element to determine by almost all analytical techniques. In this work instrumental neutron activation analysis (INAA) and preconcentration neutron activation analysis (PNAA) were used for the determination of aluminum in Canadian duplicate diets.

2. Experimental and Results

A combination of conventional (fission spectrum neutrons) INAA and epithermal INAA (EINAA) was applied in the present work using the Dalhousie university SLOWPOKE-2 reactor facility. The 1779-keV gamma-ray of ^{28}Al (half-life=2.31 min) produced by the reaction $^{27}Al(n,\gamma)^{28}Al$ was used for the determination of aluminum. EINAA was used to correct for contribution to the ^{28}Al activity by the interfering reaction $^{31}P(n,\alpha)^{28}Al$ from phosphorus present in the samples. The contribution to the ^{28}Al

activity due to a second interfering reaction $^{28}Si(n,p)^{28}Al$ was considered negligible because of the very low levels (viz. <1 mg kg^{-1}) of silicon generally present in most food items. Several reference materials were analyzed by the combination of the INAA/EINAA method and our results agreed well with the certified values. The methods were applied to 15 duplicate diet samples. The dietary intakes (dry weight, mg d^{-1}) for this population group had a mean of 7.0, median of 4.4, and a range of 0.08-32.

Additionally, an independent PNAA method using cloud point extraction (CPE) was developed not only to concentrate aluminum but also to significantly reduce phosphorus in the diet samples analyzed. The CPE method consisted of the extraction of aluminum using p-nonylphenol ether 7.5 (PONPE-7.5) as surfactant and 8-hydroxyquinoline as chelating agent. The effects of ionic strength, pH, equilibration temperature, surfactant concentration, and chelating agent concentration were investigated with respect to the extraction potentials of aluminum and phosphorus. The system was shown to exclude phosphorus below the detection limits of NAA and to produce extraction efficiencies of about 90% for aluminum standards. The results of two methods agreed well, as shown in Table 1.

Table 1. Comparison of Mass Fractions of Aluminum in Reference Materials and a Diet by the INAA/EINAA and CPE methods (mg kg^{-1})

Reference material	INAA-EINAA	CPE	Information value
IAEA H-9 Mixed Diet	5.1±1.3[a]	5.0±0.4[a]	(10)
NIST SRM-1549 Milk Powder	2.0±1.0[b]	2.0±0.2[b]	(2)
HMFS Duplicate Diet	5.2 ∀ 0.07[a]	5.2 ∀ 0.05[a]	---

[a] Average of three values; [b] Average of four values

γ-Irradiation Induced Damage on Normal Hepatocytes and Its Protection by Ethyl Cinnamate

Sharmi Mukherjee[#], Anindita Dutta[#], Saba Parveen, Souradyuti Ghosh[*], Anindita Chakraborty

Division of Radiation and Stress Biology, UGC-DAE CSR, Kolkata Centre. Kolkata, India.
[#]Joint 1st author
* Email: souradyutighoshacademic@gmail.com

1. Introduction

In addition to eliminating cancer cells, radiotherapy (RT) causes permanent damage to healthy cells. Radiotherapy is used to treat primary liver cancers like Hepatocellular carcinoma (HCC). However, RT for HCC has diminished efficacy due to radiation-induced liver disease (RILD), also known as radiation hepatitis of normal hepatocytes. There remains a mystery surrounding the signaling mechanism that allows radiation to affect healthy hepatocytes. Also, several natural substances can be used to protect healthy cells from radiation's damaging effects. The objective of this study is to investigate the underlying mechanism and dynamics of γ-radiation induced damage on normal hepatocytes, HCC, and protection of the former using natural substances.

2. Methodology & Results

***2.1. Study design*:** To investigate, normal liver cells (BRL-3A) were exposed to γ-radiation (2Gy, 5Gy, 8Gy) and the effects were studied at early (1 h) and late (24 h) time intervals after irradiation. Cells were treated with EC at a concentration of 75g/mL (IC 50 dose for HepG2 cells) for 24 h before exposure to a single 8 Gy dose of γ-radiation (LD50 dose for HepG2 cells). SOD Assay Kit-WST & MDA assay kit were used to determine SOD activity and MDA level respectively. Assessment of intracellular ROS was carried out by flow cytometry using H2DCFDA. BD-FACS Calibur was used for flow cytometric analysis. Western blot & UV-spectrophotometric methods were also carried out for analysis of samples.

Significant alterations were observed in the DNA repair kinetics and levels of apoptotic indicators, and cell survival mediators. Although oxidative stress and apoptosis were frequent 24 h after

irradiation, they were most pronounced 1 h after. Apoptosis mediators Bax, Bcl2, PARP, cas3, and cas9, as well as cell cycle regulators p53 and p21, were highly activated in the cells. After radiation treatment, survival mediators (PI3K, Akt, p38-MAPK, JNK, NF-kappaB) were downregulated across the board. Pre-treatment with ECs mitigated radio-induced ROS production and restored SOD activity. Additionally, the primary caspase enzymes 3, 9, and Bax were considerably reduced after pre-treatment with EC, and inhibited the γ-radiation-mediated increase in apoptotic signaling. EC significantly attenuated the reduction in p-Bcl-2, p-PI3K, and p-AKT, hence improving cellular survival.

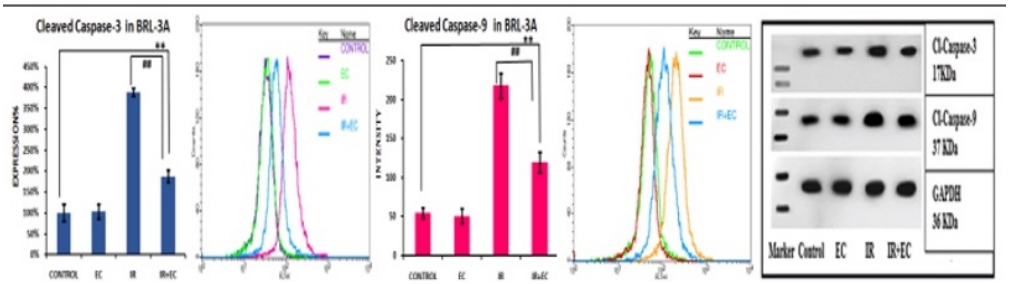

Figure 1: Cleaved Caspase 3 &9 in BRL-3A cells

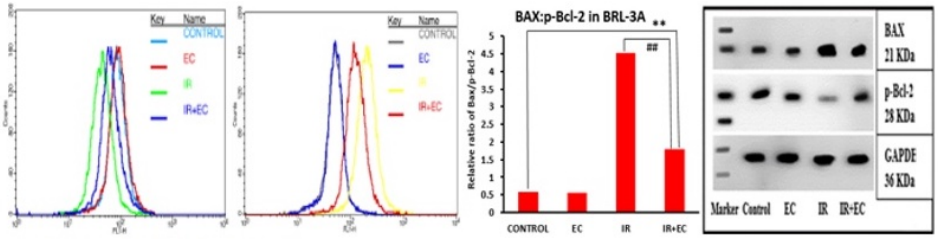

Figure 2: Bax & p-BCl-2 in BRL-3A cells

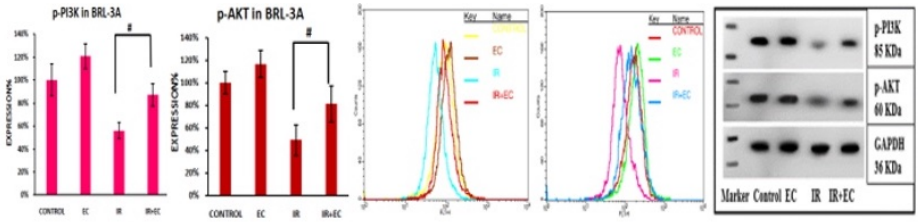

Figure 3: p-PI3K & p-Akt in BRL-3A cells

Overall, persistent damage caused by γ-radiation in normal hepatocytes is mediated in part by ROS-regulated early apoptosis and prolonged inhibition of survival factors. In order to combat ROS-mediated oxidative stress and cell death, EC (i) increases SOD activity, (ii) decreases ROS yield and LPO, (iii) activates the PI3-AKT pathway and p-Bcl-2, and (iv) reduces cleaved caspase-3, -9, and Bax.

Acknowledgement: The financial support received from ICMR and UGC.

Contributed Papers

(Mini Symposium on Earth and Environmental Sciences)

Chemometric Study of Trace Elements in Imported Indonesian Coal Using SRXRF

*S. Srikanth[1], G.J. Naga Raju[1], P. Sarita[2]**

[1]Department of Physics, University College of Engineering Vizianagaram, Jawaharlal Nehru Technological University Kakinada, Vizianagaram 535 003, India.
[2]Department of Physics, Institute of Science, GITAM Deemed to be University, Visakhapatnam 530045, India.
*E-mail: spadala3@gitam.edu

1. Introduction

The coal-fired thermal power stations in Andhra Pradesh and Telangana mostly blend imported Indonesian coal with indigenous coal to generate electric power. The principal objectives of the present study are to investigate the trace elemental concentrations in the imported Indonesian coal samples and compare them with coal Clarke values (average concentration of elements found in the earth's crust) and Swaine's world coal range. This comparison would help to identify the enrichment or depletion of an element in Indonesian coal and thereby assess its impact on the environment and human health. Further, to understand the association among the elemental components of coal, it is planned to analyze the obtained analytical data using chemometric methods.

2. Experiment

Three different thermal power plants situated in the Indian state of Andhra Pradesh were chosen as sample collection sites. The present SRXRF experiments were carryout at RRCAT, Indore, Madhya Pradesh, India and proximate analysis was done at the Centre for Materials Research laboratory of GITAM, Visakhapatnam. Ultimate analysis was carried out at the Facility (STIC-SAIF) of Cochin University of Science and Technology, Kochi, India.

3. Results and Discussion

Sixteen inorganic elements As, Ca, Cr, Co, Cu, Fe, K, Mn, Ni, Pb, Rb, Se, Sr, Ti, V, and Zn were quantified. Measured the enrichment factor for each element to determine its abundance in the analyzed samples compared to Clarke values for world coals. The analytical results were interpreted using

chemometric techniques, namely Pearson's correlation analysis, hierarchical cluster analysis, and principal component analysis, to the data matrix. Fig. 1 represents the SRXRF spectrum of NIST SRM bituminous coal.

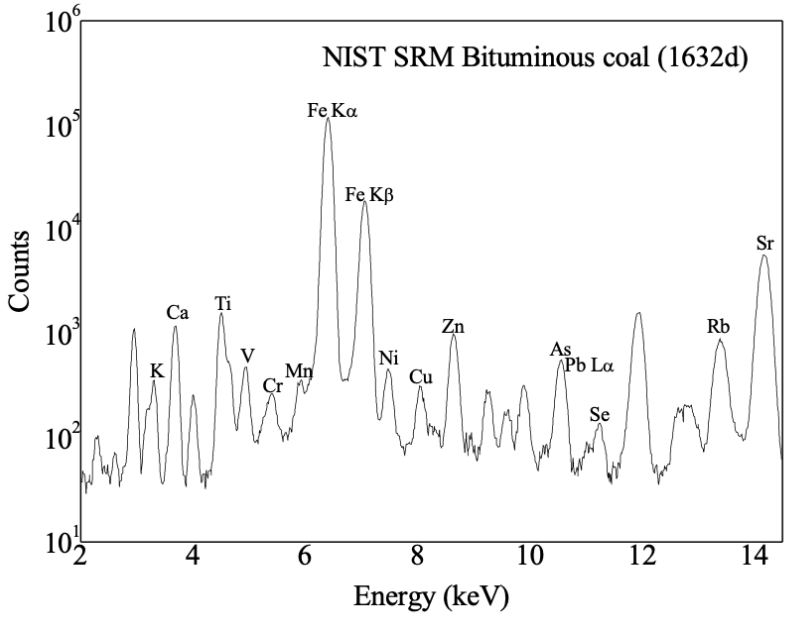

Figure 1: SRXRF spectrum of NIST SRM bituminous coal

4. Conclusion

The results outlined in this work are intended to provide a snapshot of the enrichment of trace elements and their modes of occurrence in Indonesian coal samples. However, it is emphasized that to establish the exact modes of occurrence of trace elements, comprehensive studies on the bulk analysis of Indonesian coal over a long period are required.

Acknowledgement: The authors are thankful to the scientific officers and technicians of RRCAT, Indore, India for providing SRXRF facility at beamline-16, Indus-2 synchrotron high energy photon source. Acknowledgements are due to the authorities of SAIF-STIC, Cochin University, Kochi, India, for the support rendered in performing CHNS elemental analysis.

Measurement of Gross β-γ Activity in Banana Samples from Kerala and Delhi NCR Region

Reetta Sara George, Arpita Datta, Alpana Goel*

Amity Institute of Nuclear Science and Technology, Amity University, Noida, Uttar Pradesh 201313, India.
*Email: adatta@amity.edu

1. Introduction

Banana (Botanical name: Musa sp.) is daily consumed by general public for proper diet and nutrients. Banana contains high amount of potassium (~ 450 mg) [1]. Radiation dose of around 0.01 mrem (0.1 μSv) can be found in each banana because of ^{40}K. Its presence in human tissue is the principal source of irradiation in human body. According to ICRP and AERB, for general public the limit of radiation exposure is 1mSv [2,3]. Studies confirmed that Kerala comes in High Background Radiation Area (HBRA) category. Sonipat near Delhi contains comparatively high amount of radioactivity than in other areas near Delhi because of high usage of phosphate fertilizers in past decades [4,5]. Thus, analyzing samples from Kerala and Delhi will enable researchers to better understand the radioactivity levels of bananas consumed by Indians.

2. Experiment

Banana samples were collected from geographically different Kerala and Delhi. Six samples of several species of bananas were taken from agricultural fields of Wayanad, Kerala. Two same species of banana samples grown in Sonipat, Haryana, were taken from two different marketplaces in Delhi NCR. Collected eight samples were dried in an oven at 80-100 ^{o}C for about 12-14 h and converted into powder form. About 20 g of banana sample was taken in a plastic container and its activity was measured by G.M. counting system (NUCLEONIX GC601A). Efficiency of the detecting system was measured using ^{137}Cs and ^{90}Sr-^{90}Y sources.

3. Results and Discussion

Gross beta and gamma activity was found to be ranged from 3.26±0.11 to 106.4±0.72 Bq kg^{-1} and 13.9±1.17 to 455.7±0.74 Bq kg^{-1}, respectively. ^{40}K was detected using a gamma-spectrometry (RADEAGLET-2SG-H radioisotope identifier which contains 2″×2″ NaI(Tl) detector) (Fig. 1). Absorbed dose rate and exposure rate of each sample were calculated by considering the presence of K-40. The absorbed dose rate of banana samples was found to be between 1.8±1.2 and 16.2±1.4 nSv h^{-1} (Fig. 2). The rate of exposure for banana samples was between 1.5±1.2 nR h^{-1} to 210±0.14 nR h^{-1}, respectively. It is observed that the banana sample collected from Delhi NCR had a higher gross beta and gamma activity, absorbed dose and exposure rate compared to the banana samples collected from Kerala because of high potassium content in Sonipat.

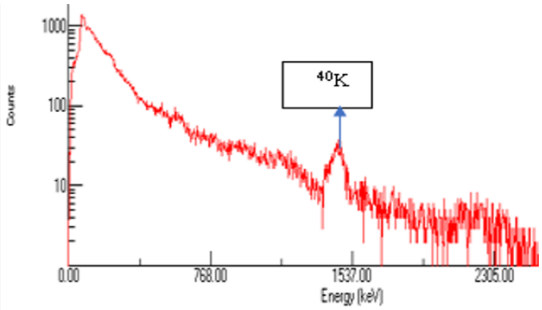

Fig 1: Representative spectrum of banana sample samples

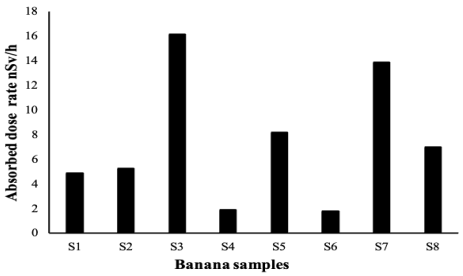

Fig 2: Calculated absorbed dose rate from banana

4. Conclusion

The highest gross gamma activity and gross beta activity were found in the Sonipat sample, with 455.7 ± 0.74 Bq kg^{-1} and 106.4 ± 0.72 Bq kg^{-1}, respectively. The calculated exposure rate and absorbed dosage rate for this sample are 210 ± 0.14 nR h^{-1} and 16.2± 1.4 nSv h^{-1}, respectively. Observed exposure rates were significantly lower for all the banana samples than the ICRP and AERB limit.

References

/1/ G. Shanthi, J.T.T. Kumaran, G.A.G. Raj, et al., Nucl. Instrum. Methods Phys. Res. A 619 (2010) 1.

/2/ A.D. Wrixon, J. Radiol. Prot. 28 (2008) 165.

/3/ K. Agrawal, B.R. Meher, B.M. Padhy, Indian J. Nucl. Med. 34 (2019) 84.

/4/ R. Daulta, V.K. Garg, B.J. Singh, Geol. Soc. India 94 (2019) 1.

/5/ A. Panghal, A. Kumar, S. Kumar, et al., J. Geol. Soc. India 92 (2018) 695.

Determination of Radioactivity in Environmental Samples Around Coal-fired Power Plant in Chennai City, Tamilnadu, India

M. Suhail Ahmed[1], M. Priyadharshini[1], B. Santhanabharathi[1], K. Pradhoshini[1,2], M. Shakeel Ahmed[1], Lubna Alam[2], M. Saiyad Musthafa[1,2]*

[1]Unit of Research in Radiation Biology & Environmental Radioactivity (URRBER), P.G & Research Department of Zoology, The New College (Autonomous), Chennai, Tamil Nadu 600014, India.
[2]Institute for Environment and Development (LESTARI), Research Centre for Sustainability Science and Governance (SKG), University Kebangsaan Malaysia, 43600 Bangi, Selangor, Malaysia
*Email: suhailsch13@gmail.com

1. Introduction

Coal-fired power stations generate 75% of India's electricity. The Indian coal utilised in such thermal power plants has a high fly ash concentration, resulting in massive amounts of fly ash being discharged into the surrounding environment. Such exorbitant generation of fly ash as a by-product during coal combustion elevates the radionuclide concentration of the ground where it gets deposited. This poses a risk of radionuclide exposure to the inhabitants of the environment [2]. The aim is to estimate the concentration of primordial radionuclides (^{238}U, ^{232}Th, ^{40}K) in fly ash, sand, sediment, and soil components around the coal-fired power plants of Chennai city. From the Activity Concentration of radionuclides, we estimated (AEDE), (Hex), (Iγ), (DR) and ELCR for the residents.

2. Experiment

Systematic random sampling Method was performed for sample collection (2kg each) from the targeted sites (S1: 13°16’26” N, 80°18’19” E, S2: 13°9’24” N, 80°20’34” E, S3: 13°16’32” N, 80°18’21” E) as prescribed by [1], post which they were sun and oven dried at 130°C to remove moisture. The samples were sieved in 2 mm ASTM mesh sieve to obtain uniform grain size and stored in cylindrical PVC containers, 250 ml each with tight sealing. After a period of 4 weeks for the radionuclides to attain secular equilibrium with their respective progenies, the samples were analyzed using gamma-ray spectrometer with a NaI (TI) based scintillator. The activity concentration of the radionuclides was

measured using the formula: A = NCPS /W × η, where A= activity concentration in Bq kg^{-1}, NCPS= net counts per sec, W= weight of sample in kg, η= absolute efficiency of the photo peak obtained from efficiency calibration. Radiological risk parameters were evaluated following. [3].

3. Results and Discussion

Mean activities of ^{238}U (407.91 Bq kg^{-1}), ^{232}Th (796.11 Bq kg^{-1}), ^{40}K (1457.9 Bq kg^{-1}) and Radium equivalent (1809.38 Bq kg^{-1}) for all samples (Fig 1), were higher than the recommended world average values of 33, 45, 420 and 370 Bq kg^{-1}, respectively. Absorbed dose rate (796.9 $nGyh^{-1}$), Gamma radiation representative level index (12.7) and External hazard indices (4.8), estimated for the present study were also higher than the permissible limit (59 $nGyh^{-1}$). The Annual Effective Dose Equivalent for the coastal sediments was higher than the recommended value (1 $mSvy^{-1}$). However, the estimated Excessive lifetime cancer risk was below the recommended value of (0.29 $mSvy^{-1}$) according to IAEA 2004. We recommend carrying out remediation measures in such regions with a high load of radionuclides, to reduce the consequent risk of exposure to the public.

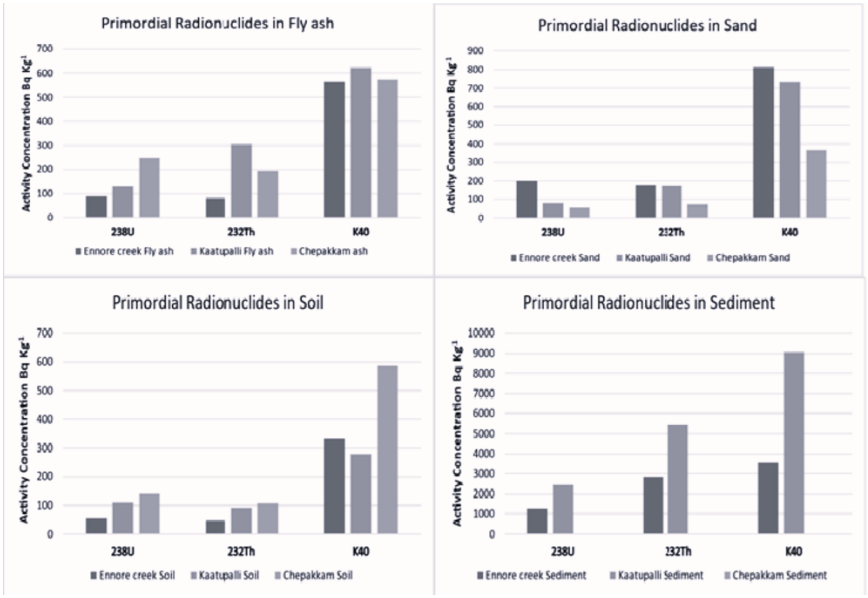

Figure 1: Graphical representation of activities of primordial radionuclides in fly ash, sand, soil and sediment

References

/1/ IAEA (2004) Soil sampling for environmental contaminants. International Atomic Energy Agency, Vienna.

/2/ M. Gupta, A.K. Mahur, R. Varshney et al., Radiat. Meas. 50 (2013) 160-165.

/3/ V. Thangam, A. Rajalakshmi, A. Chandrasekaran, et al., J. Radioanal. Nucl. Chem. 331 (2022) 1207-1223.

Radiological Risk due to Consumption of Most Commonly Consumed Flavoured and Unflavoured Milk Brands in Chennai, India - A Baseline Report

B. Santhanabharathi[1], K. Pradhoshini[1], M. Priyadharshini[1], M. Suhail Ahmed[1], M. Yugan Gogul[1], M. Saiyad Musthafa[1]*

[1]PG and Research Dept. of Zoology, The New College, Chennai, Tamil Nadu, India.
*Email: santhanabharathidpi@gmail.com

1. Introduction

Milk, in one or the other forms, is an indispensable part of our daily food supplements. The contribution of milk towards individual radiation exposure is significant, because, unlike many nutrients, it is harvested each day and can be consumed inside the half-life of radionuclides. The source of radionuclides in milk primarily comes from cattle forage, where the radionuclides get transferred from soil to the plants and finally reach man. Owing to its consumption by all age groups, it is necessary to estimate the internal dose received and other health risks associated with the intake of milk and its products. Accordingly, in our current study, the gross alpha and beta activity of several major brands of milk consumed in and around Chennai city has been analysed.

2. Experiment

Most commonly consumed brands of milk (13 brands), including fresh cow milk and 10 brands of flavoured milk were reduced into ashes at 400°C in an oven, by increasing the temperature gradually at hour intervals. 0.5 g of the sample was spread uniformly in planchettes of alpha and beta counters separately. The activity was then counted after 3 iterations (3600 s for each iteration), following the equation as [1]:

DPM = NET_CPM × 100 / EFF, where, DPM= alpha/beta disintegration per min, NET_CPM= Net alpha/beta count per min, and EFF= alpha/beta efficiency percent. The total effective dose and radiological risk parameters were calculated following references 2 and 3, respectively.

3. Results and discussion

The mean gross alpha activity for unflavoured and flavoured milk ranged from BDL to 0.01Bq/g and BDL to 0.04 Bq g^{-1} respectively, with a beta activity of 0.20 Bq g^{-1} to 0.34 Bq g^{-1} and 0.14 Bq g^{-1} to 0.38 Bq g^{-1}, respectively. Net radiation activity in unflavoured milk was higher than that of flavoured ones. Among unflavoured milk, the highest activity (0.34 Bq g^{-1}) was obtained in fresh cow milk obtained from the farm, which may be due to the processing involved and due to the decay of short-lived radionuclides during transport. The mean AEDE for infants, children and adults due to consumption of unflavoured milk was 18.5, 11.6 & 2.0 mSv y^{-1}, respectively. AEDE for children and adults due to consumption of flavoured milk was 1.8 mSv y^{-1} and 10.5 mSv y^{-1}, respectively. Mean AGDE was 97.4 mSv y^{-1} for infants, 58.5 mSv y^{-1} for children and 9.9 mSv y^{-1} for infants. The AEDE and AGDE were higher than the permissible range of 1 mSv y^{-1} and 0.3 mSv y^{-1}, respectively. However, ELCR for infants (0.06 mSv y^{-1}), children (0.04 mSv y^{-1}) and adults (0.01 mSv y^{-1}) were lower than the suggested level (0.29 mSv y^{-1}).

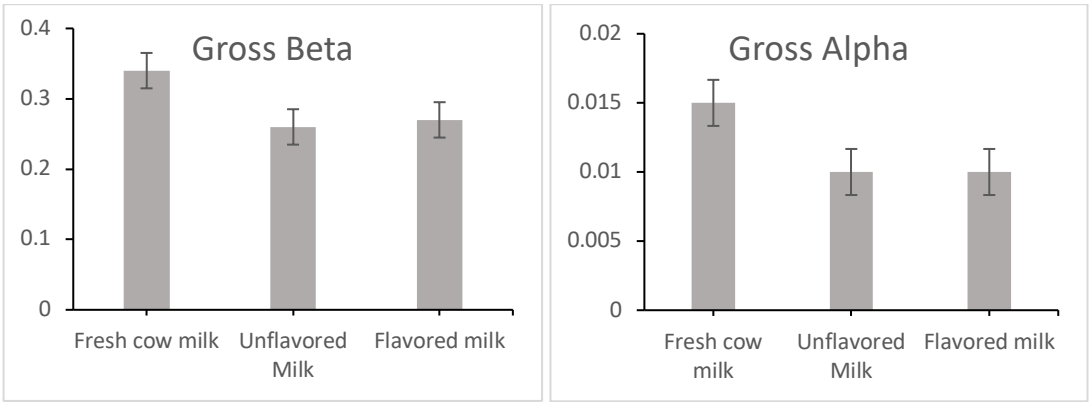

Figure 1: Graphical representation of Gross alpha and gross beta activity

References

/1/ J. Ferdous., S Biswas, A Begum, et al., J. Sci. Res. 7 (2015). 35-44.

/2/ O.S. Zorer, C. Öter, Kerntechnik 80 (2015) 174-179.

/3/ E Agbalagba, E.O., Egarievwe, S.U., Odesiri-Eruteyan, et al., J. Env. Prot. 12 (2021) 526-546.

Radiological Hazard and Natural Radioactivity Assessment in Popular Tea Brands Consumed by People in Tamil Nadu, India - A Pilot Study

K. Pradhoshini[1,2], B. Santhanabharathi[1], M. Suhail Ahmed[1], M. Priyadharshini[1], M. Yugan Gogul[1], Lubna Alam[2], M. Saiyad Musthafa[1,2]*

[1]Unit of Research in Radiation Biology & Environmental Radioactivity (URRBER), P.G & Research Department of Zoology, The New College (Autonomous), Chennai, Tamil Nadu 600014, India.
[2] Institute for Environment and Development (LESTARI), Research Centre for Sustainability Science and Governance (SGK), Universiti Kebangsaan Malaysia, 43600 Bangi, Selangor, Malaysia.
*Email: spradho@gmail.com

1. Introduction

Tea, popularly called as Chai, is India's National drink. An individual's consumption of tea in India ranges from around 1.5 kg per year to 2 cups per day. *Camellia sinensis* grown in suitable climatic conditions in different geographical locations of the world is in no way an exception to natural radioactivity. This is due to the plant's exposure to aerial deposition of radionuclides or the topographical characteristics of the soil in which it is grown, from where it gets transferred to leaves via roots along with minerals and shall result in internal radiation exposure to mankind when consumed. Hence, in the present study, the gross alpha and beta activity in the tea under different commercial tea brands, consumed commonly by people of Tamil Nadu was analysed.

2. Experiment

A total of 25 tea samples, twenty black (TS01-TS25) and five green tea (GT01- GT05) were purchased from various retail and hyper markets. 2 g of tea was used for brewing 1 cup of tea, as followed by people for drinking. Gross alpha and beta activity were calculated in both raw and brewed tea using the alpha counter (Nucleonix, model type: RC605A) and beta counter (Nucleonix, Model type: LB615) respectively. They were calibrated with standard source Am241 (typical activity in the range of 3000-5000dpm) for alpha and ^{90}Sr-^{90}Y standard source (with 1,11,000 DPM) for beta, both the standard

sources provided by BARC, Department of Atomic energy, India. The total activity was determined after subtracting the count rate of samples from the background using the following formula:
Activity= (Net CPS/ Efficiency * weight of the sample) *100, where, Net CPS= (Total count - Background)/3600, Efficiency= (Total count – Background)/Time. Using the activity of the brewed tea solution, the amount of radiation that reaches the human body was estimated through Annual Effective Dose Equivalent (AEDE), using dose conversion factors of reference 1. Other radiological risk parameters and cancer risk were evaluated following reference 2.

3. Results and discussion

Gross alpha activity in all the tea samples was found to be below the detection limit. Hence only gross beta activity was taken for the total effective dose calculation. Gross beta activity in raw tea samples ranged from 0.54 Bq/2g to 1.29 Bq/2g, with a mean value of 0.94 Bq/2g and 0.14 Bq/2g to 0.33 Bq/2g with a mean value of 0.25 Bq/2g in brewed tea samples (Fig. 1). The ratio of dissolution of raw tea samples into water while brewing ranged from 3:1 to 6:1, with an average of 4:1. This indicates that the load of radionuclides gets reduced nearly 4 times when the tea is being brewed. The effective dose and cancer risk due to the consumption of tea was estimated as 0.6 mSv y^{-1} and 0.002 mSv y^{-1}, respectively. They were below the recommended permissible limit of 1 mSv y^{-1} and 0.029 mSv y^{-1}, respectively [1], indicating all the analysed tea brands are safe for consumption.

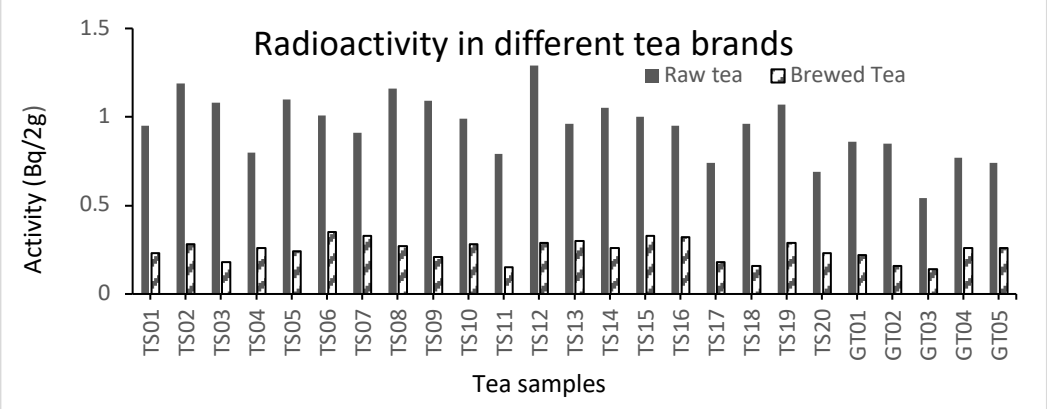

Figure 1: Graphical representation of radioactivity in raw and brewed tea

References

/1/ WHO (2004) Guidelines for Drinking Water Quality, Recommendations, Vol. 1, 3rd Edition, Geneva.

/2/ E.O. Agbalagba, S.U. Egarievwe, E.A. Odesiri-Eruteyan, et al., J. Environ. Prot. 12 (2021) 526-546.

Human Health Risk Assessment due to Consumption of Dried Fish in Chennai, Tamil Nadu, India- A Baseline report

M. Priyadharshini[1], M. Suhail Ahmed[1], K. Pradhoshini[1,2], B. Santhanabharathi[1], M. Shakeel Ahmed[1], Lubna Alam[2], M. Saiyad Musthafa[1,2]*

[1]Unit of Research in Radiation Biology & Environmental Radioactivity (URRBER), P.G & Research Department of Zoology, The New College (Autonomous), Chennai, Tamil Nadu 600 014, India.
[2] Institute for Environment and Development (LESTARI), Research Centre for Sustainability Science and Governance (SGK), Universiti Kebangsaan Malaysia, 43600 Bangi, Selangor, Malaysia.
* Email: mpriyadharshini001@gmail.com

1. Introduction

In India, approximately 17% of the total catch from 32% of marine landings is used for dried fish production. Drying is one of the common and frequently used processes of food preservation. Dried fish is prepared in India by sun drying it for several days. This procedure is ubiquitous on the Indian coast of Tamil Nadu. Regarding nutritional quality, dry fish often exceeds fresh fish. Hence the main objective of the present study was to report baseline data on the gross alpha and beta activity in selected commercial dried fish from Chennai and to estimate the Annual Committed Effective Dose (ACED) and other radiological risk parameters associated with the consumption of dry fish.

2. Experiment

22 types of various species of dried fish were collected from the wholesale markets in and around Chennai city, Tamil Nadu, India, which represents the most commonly consumed species in India. The samples were sun-dried and kept in a hot air oven at 150 ^{o}C for 2 h. Then the samples were milled to powder form and sieved to uniform grain size. About 0.5 g of the sample was spread uniformly in planchettes of alpha and beta counters respectively. Gross alpha and beta activity in the samples were counted using the alpha counter (Nucleonix, model type: RC605A) and beta counter (Nucleonix, Model type: LB615) respectively. They were calibrated with standard source Am241 (typical activity in the

range of 3000-5000 DPM) for alpha and ^{90}Sr-^{90}Y standard source (with 1,11,000 DPM) for beta, both the standard sources provided by BARC, Department of Atomic energy, India:

Activity= (Net CPS/ Efficiency * weight of the sample) *100

where, Net CPS= (Total count - Background)/3600, Efficiency= (Total count – Background)/ Time

The Annual Committed Effective dose and other radiological risk parameters were estimated using standard formulas as suggested by Duong Van et al. [1] and Agbalagba et al. [2].

3. Results and Discussion

The measured gross alpha and beta activity in the selected commercial dry fish from Chennai varied from 6.25 ± 0.12 Bq kg^{-1} to 48.21 ± 0.11 Bq kg^{-1} and 16.27 ± 0.08 Bq kg^{-1} to 479.47 ± 0.65 Bq kg^{-1} with the average value of 20.34 Bq kg^{-1} and 136.83 Bq kg^{-1} (Fig 1). The Annual committed effective dose (ACED), radiological risk parameters such as the total annual gonadal dose equivalent (AGDE), and the total Excessive Lifetime Cancer Risk (ELCR) were examined and were found to be 1.09 mSv y^{-1}, 0.48 µSv y^{-1} and 0.003 µSv y^{-1}, respectively. The Annual Committed Effective Dose (ACED) and total Annual Gonadal Dose Equivalent (AGDE) values are slightly greater than the permissible limit (WHO 2004). However, Excessive Lifetime Cancer Risk (ELCR) values were below permissible limit.

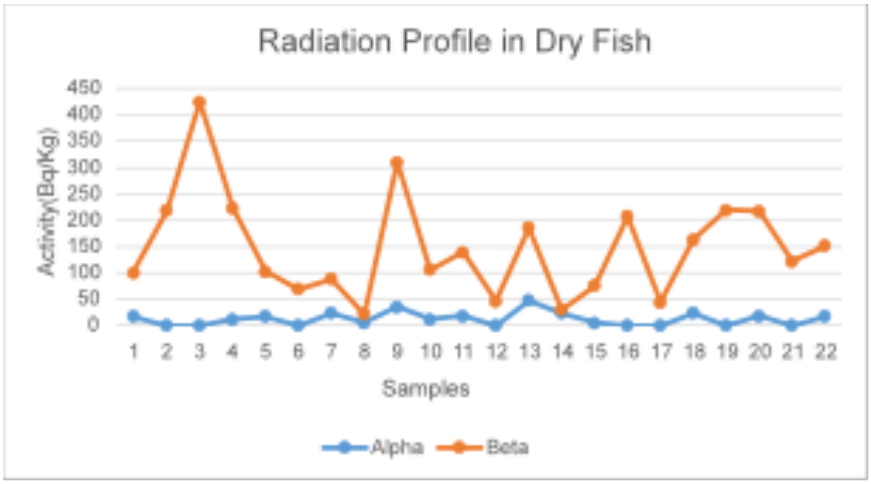

Figure 1. Graphical Representation of Gross Alpha and Gross Beta activity in Dry fish

References

/1/ H. Van, H. Luong, C. Dinh, et al., Environ. Sc. Poll. Res. 27 (2020) 33385-33392.

/2/ E.O. Agbalagba, S.U. Egarievwe, E.A. Odesiri-Eruteyan, et al., J. Environ. Prot. 12 (2021) 526-546.

Radon in the Environment: Occurrence, Effects, Applications

Saheli Chowdhury[1], Chiranjib Barman[2], Argha Deb[1], Md. Nurujjaman[3], Dipok K. Bora[4], Arpita Guha Bose[5], Aditi Das[5], Mahasin Gazi[1,6], Bikas Sinha[7], Debasis Ghose[7]*

[1]Dept. of Physics, Jadavpur University, Kolkata - 700032, India.
[2]Dept. of Physics, Sidho-Kanho-Birsha University, Purulia – 723104, India.
[3]National Institute of Technology Sikkim, Ravangla - 737139, India.
[4]Dept. of Physics, Diphu Government College, Diphu – 782462, India.
[5]Dept. of Physics, Asutosh College, Kolkata – 700026, India.
[6]Apollo Multispecialty Hospitals, Kolkata - 700054, India.
[7]Variable Energy Cyclotron Centre, Kolkata - 700064, India.
*Email: sahelichowdhury2492@gmail.com

1. Introduction

Radon is the predominant source of ionising radiation on earth, occurrence of which is controlled by the presence of uranium in rocks and soils, apart from local geological features and atmospheric factors. Inhalation of air containing excess radon is considered harmful because of its short-lived chemically reactive radioactive decay products. On the other hand, naturally occurring radon may be utilised as a potential precursor for seismic events [1]. A number of these features of environmental radon have been studied in eastern India. Soil radon activity was recorded continuously and simultaneously at three monitoring stations, namely Ravangla and Diphu in the Eastern Himalayas and Tantloi in Bakreswar-Tantloi Geothermal Region of eastern India during several months in 2018, in order to determine possible precursors induced by seismic activity within a few hundred kilometres of the monitoring stations. Ravangla in Sikkim Himalayas is situation amongst an intricate network of faults. Diphu, in Assam Valley, lies at the juncture of the Himalayan arc and the Burmese arc. Tantloi, on the other hand, is located at the eastern end of the Son-Narmada-Tapti (SONATA) Fault. In addition, soil radon concentration was studied together with ionospheric scintillations over Kolkata during April-May 2015, in search of possible pre-seismic signatures for the Nepal earthquakes of 2015. In order to assess hazardous effects of radon, radioactivity was measured in blood samples of 285 individuals, including people diagnosed with cancer. The aim of this study was to look for possible correlation between blood

radon activity, age of the participants, and diseases. Many of these works were the first of their kind in the respective regions.

2. Experiment

Soil radon concentration together with meteorological parameters (air temperature and pressure, rainfall) was recorded by Barasol radon monitor. Ionospheric scintillation data was extracted from GNSS Septentrio satellite. Radioactivity levels in blood were measured by solid state nuclear track detector (SSNTD).

3. Result and discussion

Recorded soil radon data in the Himalayas and the geothermal region were analysed by the 2-step nonlinear technique Empirical Mode Decomposition and Hilbert-Huang Transform, in order to discard environmental influences and identify genuine anomalies [2]. A number of anomalies induced by regional earthquakes were identified in the radon time series of each station. Near-simultaneous anomalies were observed from all three centres preceding a M5.3 earthquake that occurred on September 12, 2018 in Kokrajhar, Assam. The epicentre of the earthquake was found to be located in the overlapping region covered by the three stations. All anomalies were observed within 14 days before the earthquakes, similar to what was observed by Sahoo et al. in Kutch region of Gujarat [3] and Jaishi et al. in the Mat Fault region of Mizoram [1]. For the multiparametric study, pre-seismic radon anomalies and ionospheric scintillations were observed almost simultaneously.

On monitoring radon activity in blood, the average for all participants was found to be 66.3 Bq kg^{-1}, with minimum and maximum being 8.7 Bq kg^{-1} and 221.4 Bq kg^{-1}, respectively. Among cancer patients (100 in number) the average was 73 Bq kg^{-1}, in patients with chronic diseases (110 in number) like hypertension or diabetes it was 66 Bq kg^{-1}, while those with mild diseases like common cold or flu (75 in number) had average activity of 55.5 Bq kg^{-1}. Older participants were found to have higher average blood α-activity, with Pearson correlation coefficient between the two quantities being +0.33. No correlation was seen between blood α-activity and haematological parameters like RBC, platelet, haemoglobin, and white blood cells.

References

/1/ H.P. Jaishi, S. Singh, R.P. Tiwari, et al., Annals of Geophys. 57 (2014) S0544.

/2/ C. Barman, D. Ghose. J. Appl. Geophys. 41 (2016) 123-131.

/3/ S.K. Sahoo, M. Katlamundi, C. Barman, et al., J. Environ. Radioact. 222 (2020) 106353.

Appraisal of Natural Radionuclides Concentration with Reference to the Mineralogy of Various Rock Types in Thrissur district, Kerala, India

Vishnu C V[1], Antony Joseph[1], Vineethkumar V[2], Shimod K P[3]*

[1]Department of Physics, University of Calicut, Malappuram, Kerala- 673635, India.
[2]Department of Physics, Government College of Kasaragod, Kerala-671123, India.
[3]Department of Geography, Government College of Tholanur, Palakkad, Kerala-678722, India.
*Email: venuvishnu24@gmail.com

1. Introduction

Natural radioactivity in rock samples is critical for understanding disruptions in the natural radiation background as a function of geographic location and time. Here, the activity concentration of natural radionuclides viz. ^{238}U, ^{232}Th and ^{40}K, in various rock collected from Athirappilly waterfalls area in Kerala state, India have been measured using HPGe detector. ^{232}Th activity and estimated excess lifetime cancer risk are comparatively higher than the world average values. Higher concentration of radionuclides is observed in the charnockite rocks.

2. Experiment

Thirty-six rock samples (such as dolerite, charnockite, and quartzite) were collected from Athirappilly, Vazhachal, and Thumboormuzhi waterfalls areas in Kerala state. The activities of ^{238}U, ^{232}Th, and ^{40}K were determined using p-type low background HPGe detector. The measured concentration of radionuclides and associated radiological parameters such as absorbed dose (D), annual effective dose (AED), radium equivalent activity (Ra_{eq}), and excess lifetime cancer risk in rock were compared with the values reported in other regions of the world. The radioactive composition of these rocks was also related to the minerals and the mineralogical studies were carried out using XRD and EDXRF techniques.

3. Results and Discussion

The activity concentrations of the primordial radionuclides in the study area are presented in Table 1. The highest levels of ^{238}U and ^{232}Th were observed in the granitic rock of Athirappilly region. The mean activities of ^{238}U, ^{232}Th and ^{40}K were found higher than the world average of 30, 35 and 400 Bq kg^{-1} [1].

Table 1. The activity of the radionuclides (Bq kg^{-1}).

Parameters	^{238}U	^{232}Th	^{40}K
Minimum	16.61	21.38	465.18
Maximum	81.81	91.42	1246.24
N	27	27	27
Mean	42.44	54.49	844.53
Std. Deviation	16.38	21.13	196.03
Skewness	0.440	0.167	-0.088
Kurtosis	-0.056	-1.297	-0.485

Table 2. Average activity concentrations (Bq kg^{-1}) of the radionuclides with types of rock

Rock Type	^{238}U	^{232}Th	^{40}K
Dolerite	39.36±2.5	52.41±3.4	795.92±15.7
Quartzite	30.18±2.2	36.35±2.4	735.92±12.1
Charnockite	57.77±3.9	74.72±4.6	1001.76±17.3

The mineralogy of the rock types of present study indicates that a higher concentration of radionuclides is observed in the order charnockite > Dolerite > Quartzite. The enhanced level of natural radioactivity in the rock samples may be due to the presence of heavy minerals such as monazites or zircons. The estimated radiological hazard indices such as radium equivalent activity, gamma index, alpha index, external hazard index, internal hazard index, and annual effective dose rate are within the world average values. The radionuclide linked with the minerals indicates that thorium-rich phosphates and potassium-bearing feldspar minerals are the primary sources of radioactivity in the region's rocks [2].

4. Conclusion

According to the findings, monazite-bearing charnockite rocks are unsuitable for construction because they may pose health risks to those in the vicinity.

Acknowledgement: Assistance from CSIF, University of Calicut laboratory experiments, is acknowledged.

References

/1/ UNSCEAR, Sources, Effects and Risks of Ionizing Radiation. 120 (2008).

/2/ N. Lokesh, P. Ramanand, V. Kavasara, et al., Acta Geophys. (2022) 2149-2160.

Radiation Profile Mapping And Health Impact Assessment Due To ^{222}Rn Exposure In Asansol Mining Zone, India

*Ankita Dawn[1, 2], Hirok Chaudhuri[1,3]**

[1]Department of Physics, National Institute of Technology Durgapur, M G Avenue, Durgapur, India.
[2]Department of Physics, Durgapur Women's College, Durgapur, India.
[3]Center for Research on Environment and Water [CREW], National Institute of Technology, M G Avenue, Durgapur, India.
*Email: hirok.chaudhuri@phy.nitdgp.ac.in

1. Introduction

We are always exposed to natural radiation. Every year we absorb approximately 2 to 3 mSv dose of radiation. 90% of natural radiation mainly comes from radionuclides present in our earth's crust. All types of rocks and soils contain thorium and uranium and produce radon, its progenies and gamma rays through the spontaneous radioactive decay process [1]. Excessive radiation doses may damage our tissues and may lead to cancer. Among these radionuclides, radon has the largest contribution. For non-smokers, Radon (^{222}Rn) is the second leading cause of lung cancer [2]. Therefore, for health-related issues, the survey on radon in the environment is essential. Among the three isotopes of Radon (^{219}Rn, ^{220}Rn and ^{222}Rn) ^{222}Rn has the largest half-life (3.82 days). Here, the authors measured the ^{222}Rn concentration in the environs of the Asansol city of West Bengal, India.

2. Experiment

We surveyed the Asansol municipality area (almost 20 locations). The concentration of ^{222}Rn in the collected water (both surface water and groundwater) samples (500 mL) was measured using a RAD7 Radon detector in the laboratory within 24 h of sample collection. The activity of ^{222}Rn in ambient air and soil gases (1 m depth) was recorded using an Alpha GUARD radon monitor.

3. Results and discussions

Table 1. Measured ^{222}Rn Concentration & calculated TED and HRF for cancer due to ^{222}Rn exposure in the Asansol mining zone

Sampling Location & Sampling Code	Latitude & Longitude	^{222}Rn Concentration			Effective ingestion doses/annum (μSv/y)	Effective inhalation doses/annum (μSv/y)	Total effective doses per annum (μSv/y)	Health Risk Factor (HRF) for cancer
		Ambient Air (Bq/m^3)	Soil gas (Bq/m^3)	Ground-water (Bq/L)				
Daskeary	23.8437°N; 86.9727°E	97.6±13	16007±235	58.002±61	148.2	632.8	781.00	7.81
Bardhang	23.8085°N; 86.9680°E	65.2±22	9910±156	17.005±344	43.45	185.5	228.95	2.28
Amlala	23.7766°N; 86.9713°E	64.9±17	4950±164	11.009±792	28.13	120.1	148.23	1.48
Rasunnur	23.8233°N; 87.0423°E	32.4±57	10006±278	45.002±211	114.9	490.9	605.8	6.06
Kapistha	23.7990°N; 87.0307°E	32.4±15	8990±256	12.001±114	30.66	130.9	161.56	1.61
Keleiora	23.7614°N; 87.0118°E	33.0±28	2080±376	3.910±409	9.99	42.66	52.65	0.52
Chittaranjan	23.8147°N; 86.8858°E	36.8±14	11009±137	23.003±368	58.77	250.9	309.67	3.09
Lohat	23.7860°N; 86.9136°E	32.8±35	2470±695	16.005±252	40.89	174.6	215.49	2.15
Miliakhola	23.7409°N; 86.8943°E	32.6±21	18009±168	26.005±384	66.44	283.7	350.14	3.50
Kulti	23.7397°N; 86.8524°E	132.8±2	24001±189	40.002±545	102.2	436.4	538.6	5.38
Kalyanpur	23.7138°N; 86.9436°E	23.1±12	1520±267	3.714±376	9.49	40.52	50.01	0.50
Newtown	23.6863°N; 86.9231°E	21.8±14	3840±687	7.960±246	20.34	86.84	107.22	1.07
Suryanagar	23.6527°N; 86.8913°E	45.0±13	8210±111	11.007+793	28.12	120.0	148.12	1.48
Dhenua	23.6314°N; 86.9696°E	18.4±12	4720±195	7.960±108	20.34	86.84	107.18	1.07
Sunview	23.6677°N; 86.9714°E	15.7±12	1860±144	3.920±155	10.02	42.77	52.79	0.52
Majiara	23.7149°N; 86.9972°E	10.6±19	1050±122	3.210±112	8.20	35.02	43.22	0.43
Nigha	23.6647°N; 87.0547°E	10.2±11	1280±116	2.640±524	6.74	28.80	35.54	0.35
Taltore	23.7398°N; 87.0897°E	11.7±10	730±230	1.400±164	3.57	15.27	18.84	0.18
Bhaskajuri	23.7397°N; 87.0100°E	14.1±13	1260±438	2.250±436	5.74	24.54	30.28	0.30
Chinchuria	23.7394°N; 86.9716°E	15.7±12	2714±876	8.050±116	20.56	87.82	108.38	1.08

Recorded ^{222}Rn concentration swings between 1.40±164 Bq L^{-1} and 58.002±61 Bq L^{-1} for water samples. For ambient air, it varies from10.2±11 Bq/m^3 to 132.8±29 Bq/m^3 and the activity range seen in soil gases is from 730±23 Bq/m^3 to 24001±189 Bq/m^3. This work is the first of its kind to assess the health risk due to ^{222}Rn exposure to the dwellers of the study area. The authors calculated total effective dose (TED) per annum. For the risk of cancer due to ^{222}Rn exposure, the health risk factor (HRF) is estimated for the residents of the Asansol area. Calculated TED due to ^{222}Rn varies from 18.84 μSv y^{-1} to 781.29 μSv y^{-1}.

References

/1/ UNSCEAR, Sources, Effects and Risks of Ionizing Radiation. (2000).

/2/ T.K. Sethi, M.N. El-Ghamry, G.H. Kloecker, Clin. Adv. Hematol. Oncol. 10 (2012) 157-164.

Study of Pre-Seismic Radon Anomaly near Indo-Burman Subduction Line using Empirical Mode Decomposition based Hilbert Huang Transform and Artificial Neural Network

T. Thuamthansanga, R.C. Tiwari*

Department of Physics, Mizoram University, Aizawl-796004, Mizoram, India
*Email: sangathomte@gmail.com

1. Introduction

The study presents the causal relationship between anomaly in time series radon data and earthquake along Indo-Burman subduction region with an aim to determine the precursory time. The time-series radon data were generated at the soil-air interface with 15 min cycle at the Department of Physics, Mizoram University, Aizawl using ZnS(Ag) based scintillation counter. Nonlinear analysis techniques were used for analyzing the data. Earthquakes data within 500 km radial distance downloaded from US Geological Survey (USGS) archive were considered to calculate the precursory time. The precursory times obtained by the two methods were compared to assigned seismicity of the region.

2. Experiment

The Empirical Mode Decomposition based Hilbert Huang Transform (EMD-HHT) [1, 2] and Machine Learning (Artificial Neural Network, ANN) were used. The EMD-HHT technique discarded periodicities in the time series data by decomposing it into different oscillatory mode. The ANN method estimated the actual radon value using the Levenberg-Marquardt algorithm.

3. Results and Discussion

The precursory time by EMD-HHT and ANN was found approximately one week respectively. The precursory times were in close agreement with other results [3]. Both techniques are proved to be suitable tools for identifying anomalies in the time series radon data.

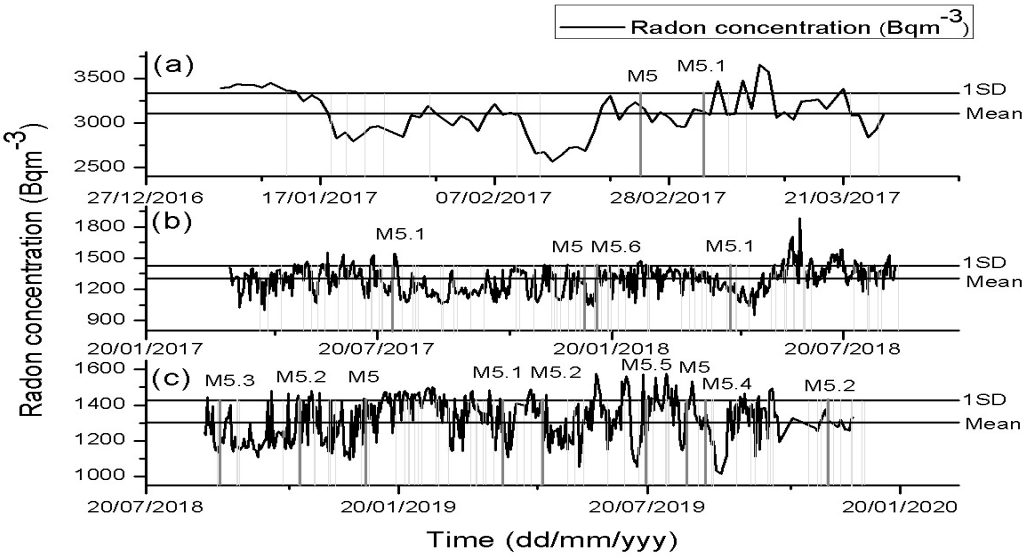

Fig 1: Plot of (a) Instantaneous energy (IE) of time series radon data along with earthquakes (vertical green and red lines represent earthquakes with M<5 and M≥5 on their dates of occurrences respectively) within 500 km radius from the monitoring station between January, 2017 and June, 2017 (b-c) Predicted radon data by ANN along with earthquakes within 500 km radius from the monitoring station from January, 2017 to December, 2019 (vertical green and red lines represent earthquakes with M<5 and M≥5 on their dates of occurrences respectively)

4. Conclusion

The study shows that the region is seismically active and that radon anomaly is a promising indicator. It shows that both the non-linear statistical analysis techniques (EMD-HHT and ANN) successfully discard periodicities in the time series radon data to have genuine geophysically related data.

Acknowledgement: The authors are grateful to Dr Saheli Chowdhury for assisting them in analysis using EMD-HHT technique.

References

/1/ N.E. Huang, Z. Shen, S.R. Long, et al., Proc. of the Royal Society of London. Series A: Math. Phys. Engg. Sci. 454 (1971) 903-995.

/2/ W. Huang, Z. Shen, N.E. Huang, et al., Proc. of the National Academy of Sciences 95 (1998b) 4816-4821.

/3/ S. Chowdhury, A. Deb, M. Nurujjaman, et al., Nat. Haz. 87 (2017) 1587-1606.

Depth Dependence Study of Naturally Occurring Radioactive Materials (NORM) in Soil of the Malwa Region of Punjab

*Neeraj Chauhan[1], Nabanita Naskar[2], Susanta Lahiri[2,3], Rajeev Patnaik[4], Amrit Pal Toor[5], Alok Srivastava[1]**

[1]Department of Chemistry, Panjab University Chandigarh, 160014, India.
[2]Diamond Harbour Women's University, Sarisha, South 24 Parganas 743368, India.
[3]Department of Physics, Sidho Kanho Birsha University, Purulia 723104, India.
[4]Department of Geology, Panjab University Chandigarh, 160014, India.
[5]Dr. Shanti Swarup Bhatnagar University Institute of Chemical Engineering & Technology, Panjab University, Chandigarh, 160014, India.
*Email: alok@pu.ac.in

1. Introduction

The concentrations of naturally occurring radioactive materials (NORM) namely ^{238}U, ^{232}Th and ^{40}K (the main contributors of natural radiation) depend on their geological and geographical locations. More than 350 uranium-rich provenances, mainly in the form of coffinite, uraninite and pitchblende ores have been reported from distinct stratigraphic locations of Shiwalik, Punjab in addition to secondary uranium-bearing minerals [1]. Hence, the concern about uranium mobilization and its related toxicity in the North-Western part of Punjab is increasing. Many reports from various districts of Punjab show higher uranium concentration in groundwater as compared to the permissible limit of 15 ppb provided by WHO [2,3]. Earlier, our group reported uranium content in paleosols, mammalian fossils, and sedimentary rock samples collected from the well-dated Shiwalik region. Interestingly, the activity of ^{238}U varied between 208-5837 Bq kg^{-1} in fossilized bones, perhaps as a result of the deposition of insoluble U^{4+} by replacing Ca^{2+} [4]. However, based on ^{238}U activity concentration measurements in soils, fertilizers and paleosols from the Malwa region which is located in the North-Western part of Punjab, it was concluded that geogenic factors were responsible for uranium mobilization in Malwa [5]. In the present work, a depth dependence study of ^{238}U, ^{232}Th and ^{40}K present in soil collected from Mansa, Bathinda, Mukhtsar, Fazilka and Moga districts of Punjab has been carried out employing low-background gamma-spectrometer.

2. Experiment

Soil samples were collected from different depths (Level A: 30-90 cm, Level B: 90-120 cm, Level C: l50-210 cm). The activity of radionuclides was measured using HPGe detector with 80% relative efficiency and resolution of 1.65 keV at 1.33 MeV and shielded by 1000 kg cylindrical lead shields. After attaining secular equilibrium, sealed samples were measured for 60000 s using the photopeaks of 295.1, 351.9, 609.1 keV for ^{238}U and 338.3, 911.2, 583.2 keV for ^{232}Th and 1460.8 keV for ^{40}K [6,7].

3. Result and Discussion

The activity of ^{238}U in the surface soils samples (Level A) varied between 29.0±0.5 to 38.1±0.4 Bq kg^{-1} with a mean of 33.7±2.8 Bq kg^{-1} and ^{232}Th varied between 47.8±2.1 to 66.4±0.9 Bq kg^{-1} with a mean of 60.3±5.9 Bq kg^{-1}. The activity of ^{238}U in the moderately deep layer (Level B) varied between 28.2±1.6 to 37.9±1.0 Bq kg^{-1} with a mean of 33.4±3.6 Bq kg^{-1} and ^{232}Th varied between 50.6±3.5 to 64.6±1.9 Bq kg^{-1} with a mean of 59.8±5.2 Bq kg^{-1}.

In the deep layer (Level C), the activity concentration of ^{238}U varied from 26.9±1.6 to 41.7±3.8 Bq kg^{-1} with a mean of 32.7±3.9 Bq kg^{-1} and ^{232}Th varied between 49.4±3.3 to 64.6±2.8 Bq kg^{-1} with a mean of 56.7±5.3 Bq kg^{-1}. It is observed from data obtained in the present work on the activity of ^{238}U and ^{232}Th that there is no significant depth dependence, which vouches for the primordial or geogenic origin of ^{238}U and ^{232}Th.

The activity of ^{40}K was also measured in the present work, which ranged from 498.9±7.2 to 764.1±11.2 Bq kg^{-1} with a mean of 637.1.18±76.6 Bq kg^{-1} which is slightly higher than the global average level of 420 Bq kg^{-1}. Punjab State is known for the highest consumption of potassium-based fertilizer in India. The increase in the activity of ^{40}K could perhaps be traced to anthropogenic activity.

References

/1/ R. Kaul, K. Umamaheswar, S. Chandrasekaran, et al., J. Geol. Soc. India. 41 (1993) 243-258.

/2/ K. Saini, P. Singh, B.S. Bajwa, Appl. Radiat. Isot. 118 (2016) 196-202.

/3/ B.S. Bajwa, S. Kumar, S. Singh, et al., J. Radia. Res. Appl. Sci. 10 (2017) 9-13.

/4/ R. Patnaik, S. Lahiri, V. Chahar, et al., J. Radioanal. Nucl. Chem. 308 (2016) 913- 918

/5/ A. Srivastava, V. Chahar, V. Sharma, et al., J. Radioanal. Nucl. Chem. 314 (2017) 1367- 1373.

/6/ P. Chaudhuri, N. Naskar, S. Lahiri. J. Radioanal. Nucl. Chem. 311 (2017) 1947-1952.

/7/ R. Bala, D. Das, N. Naskar, S. Lahiri. J. Radioanal. Nucl. Chem. 331(2022) 2561-2572.

Assessment of Natural Radioactivity and Radiological Hazard Associated with The Commercially Available Tobacco Products in Tamil Nadu - A Pilot Study

M. Shafeeka Parveen[1], M. Suhail Ahmed[2], K. Pradhoshini[2], B. Santhanabharathi[2], M. Priyadharshini[2], Mehraj Ud Din War[1], M. Saiyad Musthafa[2]*

[1]Unit of Aquatic Biology and Aquaculture (UABA), P.G & Research Department of Zoology, The New College, Chennai, Tamil Nadu 600 014, India
[2]Unit of Research in Radiation Biology & Environmental Radioactivity (URRBER), P.G & Research Department of Zoology, The New College, Chennai, Tamil Nadu 600 014, India
*Email: shafeekaparveen94@gmail.com

1. Introduction

Smoking has become a widespread culture where one billion adults are obsessed with it. With an estimated annual production of 800 million kg, India is the second largest producer of tobacco in the world. Tobacco usage is the main cause of six million unwanted death every year due to lung cancer, making it one of the top preventable causes of mortality. Based on the report of various studies conducted, lung cancer caused by tobacco consumption is predominantly due to the internal radiation dose received by smokers [1]. The present study is an attempt to determine the radioactivity level in different brands of tobacco products and the effective dose received subsequently upon smoking.

2. Experiment

A total of 31 brands of commercially available tobacco products among which 20 brands of cigarette (C1-C20), 2 cigar types (G1, G2) 8 brands of Beedi (B1-B8) and fresh tobacco leaves (T1) that are in use for regular smoking were purchased from markets in and around Chennai metropolis. Weight of the individual tobacco products was measured for determining total radioactivity content. Gross alpha and beta activity were calculated in alpha counter (Nucleonix, model type: RC605A) and beta counter (Nucleonix, Model type: LB615), respectively. They were calibrated with standard source Am241 (typical activity in the range of 73,500 DPM) for alpha and ^{90}Sr-^{90}Y standard source (with 1,11,000 DPM) for beta, both obtained from BARC, DAE, India. Total activity was determined after subtracting

the count rate of samples from the background using the following formula: Activity= (Net CPS/ Efficiency * weight of the sample) *100, where Net CPS= (Total count - Background)/3600, Efficiency= (Total count – Background)/ Time. The annual effective dose to smokers upon inhalation of these tobacco products was calculated using the dose conversion factors [2].

3. Results and discussion

Gross alpha activity ranged between 1-98.4 Bq/stick, with average of 4.6 Bq/stick in cigarettes, 54.2 Bq/stick in Cigar, 18.5 Bq/stick in Beedi and 58 Bq/5g in fresh tobacco leaves. Gross beta activity had a range of 346-903 Bq/stick, the mean value being 651 Bq/stick in cigarettes, 3273 Bq/stick in Cigar, 381 Bq/stick in Beedi and 605 Bq/5g in fresh tobacco leaves. Gross beta activity was comparatively very high than alpha activity. indicating more contribution of beta emitters than alpha particle emitting radionuclides. Among the tobacco products, high radioactivity was observed in Cigar, followed by Cigarettes, Beedi and fresh tobacco leaves. Within the cigarettes, highest activity was observed in C6 and C11, which is the most commonly smoked one by all age groups. The internal radiation / annual effective dose (AED) received by a smoker upon inhalation of the tested tobacco products were above 1 mSv y^{-1}, being higher than the permissible limit [3]. AED received upon smoking Cigar is much higher (18 mSv y^{-1}), indicating high risk to Cigar smokers than who smokes cigarettes and Beedi.

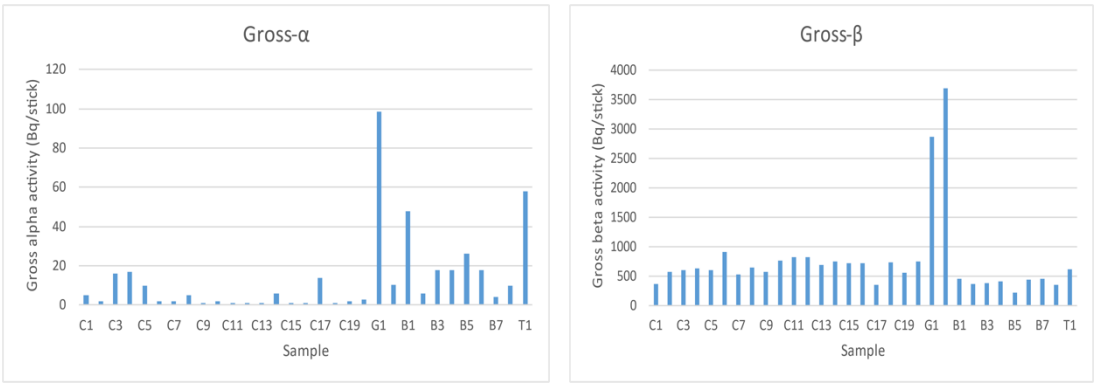

Figure 1: Activity concentration of Gross α and Gross β in Cigarettes and other tobacco products.

References

/1/ S.A. Abbas, S.F. Hassan, M.S. Karim, J Phys.: Conf. series 1660 (2020) 012048, IOP Publishing.

/2/ C. Papastefanou, Radiat. Prot. Dos. 123 (2007). 68-73.

/3/ United Nations Scientific Committee on the Effects of Atomic Radiation. Sources and effects of ionizing radiation (New York: United Nations) (2000).

Assessment of Gross α-β and ^{3}H Activities in Groundwater Samples in and around Tantloi Geothermal Region, Jharkhand, India

*Sayantan Mitra[1], Nabanita Naskar[2], Joydeep Mukherjee[1], Sushanta Sutradhar[1], Susanta Lahiri[1,2], Sonjoy Mondal[1], Chiranjib Barman[1]**

[1]Department of Physics, Sidho-Kanho-Birsha University, Purulia 723104, India.
[2]Diamond Harbour Women's University, Sarisha, South 24 Parganas 743368, India.
*Email: chiranjib-barman@skbu.ac.in

1. Introduction

Depending on its origin, radiation can be divided into two categories: primordial and cosmogenic. The dose of radiation exposure majorly comes from naturally occurring radioactive materials (NORMs) [1]. NORMs are present everywhere in different matrices such as soil, sediment, and waterbodies [2]. The study of radioactive content of water has gained a lot of interest owing to the effects of natural radioactivity on water quality and its influence on the radioactive dose ingested by humans [3]. The present study is an attempt to assess the radiogenic quality of groundwater on the basis of gross α, gross β and Tritium (^{3}H) activities in the Tantloi geothermal region of Chhotanagpur Plateau, Jharkhand, India.

2. Experiment

Gross Alpha-Beta: Water samples were collected from Tantloi geothermal region. For each sample, 2000 mL were pre-concentrated to 100 mL and subjected to several chemical procedures as described in reference 4 for low-level detection of gross alpha-beta. After cooling, 8 mL of each sample was taken in a 20 mL plastic vial, mixed with 12 mL aqualite (make: Hidex) cocktail and measured using liquid scintillation counter [4]. The minimum detectable activities (MDA) for gross α and β at 10000 s counting time were found to be 1.32 Bq L^{-1} and 0.26 Bq L^{-1}.

Tritium (^{3}H): 1000 mL sample was filtered through 42 Whatman filter paper and the filtrate was then subjected to double-distillation. 8 mL of the distillate sample was taken in a plastic vial with the addition

of 12 mL aqualite (make: Hidex) cocktail and ^{3}H measurement was carried out by LSC-TDCR. The MDA of ^{3}H activity was calculated to be 1.4 Bq L^{-1} at 10000 s counting time.

3. Result and Discussion

The groundwater samples collected from Tantloi geothermal region show gross alpha activities from below detection limit (BDL) to 0.5±0.05 Bq L^{-1}, gross beta activities from BDL to 0.2±0.01 Bq L^{-1} and ^{3}H activities from BDL to 63.42 Bq L^{-1}. Figure 1 shows the frequency of gross alpha-beta and tritium activities in groundwater samples. Most of the samples are found to be BDL in case of gross alpha and tritium. The average gross alpha, gross beta and tritium activities are also within the permissible limits of 0.5, 1 and 7000 Bq L^{-1}, respectively in drinking water prescribed by WHO [5]. Tritium activities have been observed in the water samples collected from Dalahi hot spring (87.16236 E, 24.08361N) and two different deep tube wells, lying in close proximity to the former, which indicate that the mixing of geothermal water and groundwater is occurring in this geothermal region.

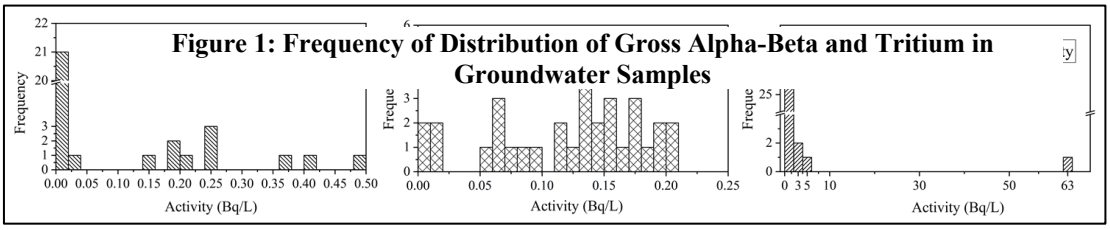

Figure 1: Frequency of Distribution of Gross Alpha-Beta and Tritium in Groundwater Samples

4. Conclusion

To the best of our knowledge, this is the first methodical study on radiogenic water quality assessment in terms of gross α-β and ^{3}H in and around Tantloi geothermal region and may be considered as a baseline data for future radiogenic assessments. The current results suggest that the groundwater in Tantloi geothermal region is radiologically safe and there are no considerable radiation hazards for public.

References

/1/ T. Rajeshwari, S. Rajesh, J. Radioanal. Nucl. Chem. 300 (2014) 61-65.

/2/ F. Caridi, M. D'Agostino, J. Inst. 11 (2016) C10012.

/3/ K.F. Al-Shboul, A. Alali, J. Environ. Radioact.178 (2017) 245-252.

/4/ N. Naskar, S. Lahiri, Environ. Res. 185 (2020) 109407.

/5/ Guidelines for drinking-water quality. WHO, Geneva. 216 (2011) 303-304.

Dynamics of Thoron Concentration in Dwellings of the Industrial Sites in Kannur District, Kerala

*Neeraja N[1], Sahadiya Nazar[2], Nadira Mahamood K[2], Prakash, V[1]**

[1]Department of PG Studies & Research in Physics, Payyanur College, Edat - 670327, India.
[2]Department of PG Studies in Physics, Sir Syed College, Taliparamba - 670142, India.
*E-mail: prakashamv@gmail.com

1. Introduction

The radionuclides from the decay series of ^{232}Th and ^{238}U are the major contributors to the terrestrial gamma radiations in the environment. Among those radionuclides, ^{220}Rn (Thoron) from the decay chain of ^{232}Th is known to be hazardous due to various characteristics of the radionuclide. The radioactive gas emanating from ^{220}Rn can cause severe health issues including lung cancer, leukemia etc as per various reports. In view of this, here is an attempt to probe the ^{220}Rn activity concentration in dwellings of the industrial sites in Kannur district, Kerala. The dwellings were categorized depending upon the various materials used for construction.

2. Experiment

A pinhole based dosimeter mounted with LR-115 type Solid State Nuclear Track Detector (SSNTD) and Direct Thoron Progeny Sensors (DTPS) respectively were used to measure the indoor thoron concentration (in Bqm^{-3}) [1] and equilibrium equivalent thoron concentration (in Bqm^{-3}) [2,3]. Both the dosimeters were placed in different types of dwellings categorized as; Mud House (MH), Tile floor and Concrete roof (TC), Odu and wood roof and Red oxide floor (OR), Granite floor and Concrete roof (GC), and Marble floor and Concrete roof (MC). After the 3 months (90 days) of exposure time, the exposed SSNTD films were etched with 2.5N NaOH solution at a temperature of 600 ºC in a water bath for 90 minutes. The track density (in $Trcm^{-2}d^{-1}$) of alpha particles was then counted using a spark counter. The indoor thoron concentration and equilibrium equivalent concentration (EEC) were measured, and radiological parameters such as annual effective dose (in mSv), excess lifetime cancer risk (ELCR) were estimated.

3. Result and Discussion

The indoor thoron activity concentration in dwellings varies from 125 Bqm^{-3} - 454 Bqm^{-3}. The values estimated for different houses clearly indicate thoron activity concentration varies significantly with the type of house. The contributing factors may be ventilation conditions, types of construction, materials used for construction and site specific characteristics. The maximum concentration of 454 Bqm^{-3} (track density of 409 $Trcm^{-2}d^{-1}$) observed in dwellings with marble floor and concrete roof. The poor ventilation and cracks in floor due to age might be contributed to the higher level of activity concentration in addition to the considerable role of construction materials. The marble floor house followed by granite floor house with activity concentration of 288 Bqm^{-3}. Granite is a natural source of radiation, like most natural stones. The minimum concentration of 125 Bqm^{-3} (track density of 113 $Trcm^{-2}d^{-1}$) observed in mud house with good ventilation. The annual effective dose in the dwellings ranges from 3mSv to11mSv with the observed maximum for the marble floor and concrete roof house. Based upon calculated values of annual effective dose, excess lifetime cancer risk (ELCR) was calculated and found to vary from $13x10^{-3}$ to $45x10^{-3}$. The track density associated with DTPS varies from 48 $Trcm^{-2}d^{-1}$ to 268 $Trcm^{-2}d^{-1}$. The equilibrium equivalent thoron concentration ($EETC_{Rn\text{-}220}$) varies from 0.033 Bqm^{-3} to 2.63 Bqm^{-3} with observed minimum value for granite floor with concrete roof house and maximum value for mud house.

4. Conclusion

The higher concentration observed in the houses with marble/granite floor and concrete roof and lower concentration in mud houses clearly indicates the substantial contribution of construction material and type of construction in the enrichment of thoron activity. The concentration might also get affected with climatic condition, human interference, and site specific characteristics. The estimated annual effective dose and ELCR values are higher than the world's average indicating an additional risk of getting cancer due to occupancy inside the dwellings for a longer time.

References

/1/ K. Kaur, M.S. Heer, R. Mehra, et al., International J. Pure Appl. Phys. 13 (2017) 65-70.

/2/ R. Mishra, Y. S. Mayya, Radiat. Meas. 43 (2008) 1408-1416.

/3/ P. Singh, P. Singh, S. Singh, et al., J. Radiat. Res. Appl. Sc. 8 (2015), 226-233.

Multi-Elemental Analysis of Terrestrial and Aquatic Flora in Visakhapatnam

Tanushree Panigrahi[1], Sulagna Dutta[2], Anima Sunil Dadhich[1], Anindita Chakraborty[3]*

[1]Department. of Chemistry (GIS, GITAM), Visakhapatnam-530045, India.
[2]Department of Zoology, Bidhannagar College, Kolkata-700064, India.
[3]UGC-DAE Consortium for Scientific Research, Kolkata Center, Kolkata-700106, India.
*Email: tanushreepanigrahi2015@gmail.com

1. Introduction

Energy dispersive X-Ray fluorescence (EDXRF) is a versatile, efficient method for multi-elemental quantification in samples of diverse origins. Recorded X-ray fluorescence spectrum has to be carefully processed (de-noising, background estimation, subtraction) to obtain the area under the characteristic X-ray peak(s), so as to derive the corresponding elemental concentration. A novel method based on the scaled intensity of the characteristic X-ray line of the element under consideration has been developed to obtain the elemental concentration. Trace element concentrations in several plant species and seaweeds collected from different sites in Visakhapatnam have been obtained using this method.

2. Experiment

Sample collection was done randomly from specific study stations/ locations of various study sites in Visakhapatnam, to explore the trace element profile therein, and investigate the presence of heavy metal (HM). Anthropogenic activities, traffic emissions, industrial discharges [1], waste from municipal activities, and atmospheric deposition are the primary sources of heavy metals (HMs) .Four commonly grown plant species and three algae samples were collected.

SOD Assay Kit-WST was used to determine SOD inhibition activity for fresh samples. EDXRF measurements were carried out using the Jordan Valley EDXRF-3600 system. The spectrum (Fig. 1) was subjected to the conventional smoothening (Fig. 2) and background subtraction (Fig. 3).

The measured intensity of the characteristic X-ray peak has to be mapped to the corresponding elemental concentration. This mapping involves several factors (instrumental and fundamental physical parameters). Scattered peak(s) and background region (Fig. 4) were used for this mapping, so as to

extract the corresponding elemental concentration. This process is expected to appropriately account for the matrix and self-absorption effects. The elemental profile would be discussed in details during the presentation. In the case of superoxide dismutase activity, *G. corticate* showed the most favourable result (Fig. 5). The metal accumulation in the studied plant samples is pictorially summarized in Fig. 6. It is expected that the collation of the results would help us estimate the effectiveness of the specimens under investigation concerning their scavenging of toxic elements.

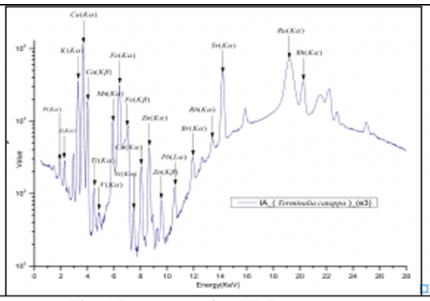

Fig. 1 Representative XRF spectrum

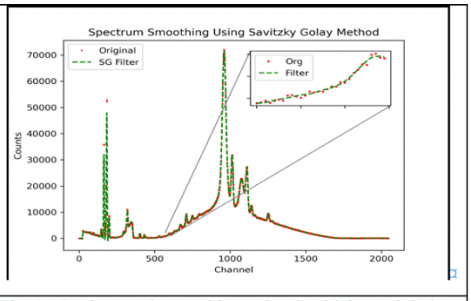

Fig. 2: Background smoothing using Savitzky and Golay filter

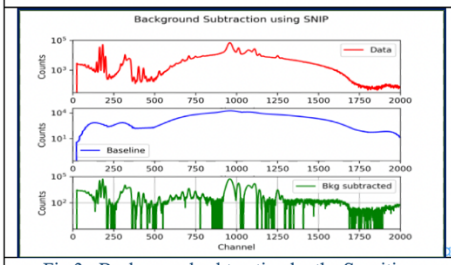

Fig 3: Background subtraction by the Sensitive Nonlinear Iterative Peak clipping method

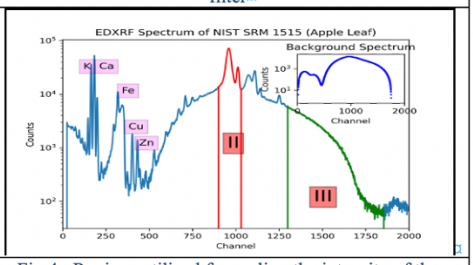

Fig 4: Regions utilized for scaling the intensity of the characteristic X-ray peak

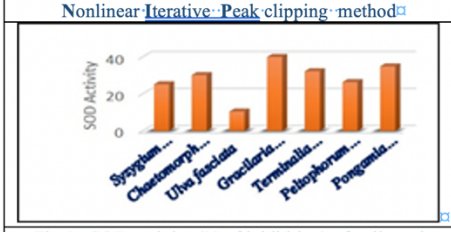

Fig 5: SOD activity (% of inhibition) of collected species

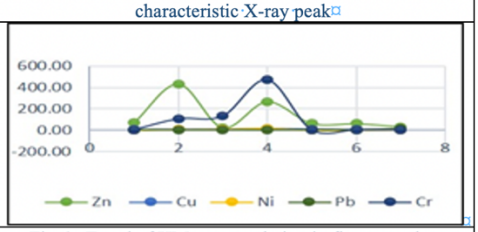

Fig 6: Trend of HMs accumulation in flora samples

Acknowledgement: The authors are thankful to Dr S.S. Ghugre, for the support and interest in this work. The financial support from the UGC-DAE-CSR Kolkata Centre in the form of a fellowship is acknowledged.

References

/1/ M. Dietrich, J. Huling, M.P. Krekeler, Sc. Total Environ. 618 (2018) 1350-1362.

Radon (Rn-222) Concentration in Groundwater of Bokaro District, Jharkhand, INDIA

*Sushanta Sutradhar[1], Joydeep Mukherjee[1], Sayantan Mitra[1], Sonjoy Mondal[1], Chiranjib Barman[1]**

[1]Department of Physics, Sidho-Kanho-Birsha University, Purulia 723104, India.
*Email: chiranjib-barman@skbu.ac.in

1. Introduction

Radon is naturally occurring radioactive noble gas, which poses severe carcinogenic threat to humans, mainly to the stomach and lungs [1]. It is produced by alpha decay of radium-226 [2,3] and found in rocks and soil [4]. Groundwaters contain natural radionuclides in various concentrations and these radio nuclides release radon into water. On the other hand, radon in water may also come from the dissolution of airborne radon into the water [5]. Radon contributes roughly 55% of the total internal radiation exposure to human beings (ICRP, 1993) [6]. In the present work, radon concentration has been analyzed in deep tube well waters collected from all nine administrative blocks of Bokaro district, Jharkhand. This is the first attempt to assess the radiogenic features of groundwater in Bokaro district.

2. Experiment

Water samples have been collected and sealed in 150 mL of glass bottles from deep tube wells. The radon concentrations were measured on the same day using AlphaGuard DF2000 ionization chamber (make: Bertin Instruments) following the protocol prescribed by the manufacturer. Additionally, pH of the samples was measured using a digital pH meter pH80 (make: HM Digital) and the major cations have been measured using Microcontroller based Flame Photometer G-301 (make: HPG Instruments) to identify any possible correlation between pH/cations and water radon.

3. Result and Discussion

The radon activities in groundwater samples of Bokaro district have been found to vary from 3.5 Bq L^{-1} to 598.9 Bq L^{-1} with an average of 145.8 Bq L^{-1} 54% of samples exceeds100 Bq L^{-1}, which implies that

control is needed for consumption of this radon rich water as recommended in guidelines of World Health Organization (WHO) [7]. Annual effective dose rates for three different categories have also been calculated as described in Ademola and Oyebode, 2017 [8]. From figure 1 it can be observed that for adult, children, and infant the average dose rates are beyond the value of 0.1 mSv y^{-1}. Additionally, pH and some major cations (Na^{+}, K^{+}, Li^{+}, and Ca^{2+}) of the groundwater samples have also been analysed and no correlation has been observed between these parameters and radon.

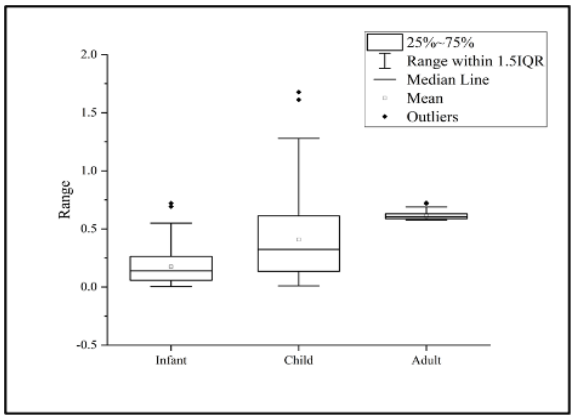

Figure 2. Box Plot of Annual Effective Dose Rates

4. Conclusion

54% of measured samples show higher activity of radon than the controllable limit recommended by WHO. Also, the high annual effective dose rates due to radon exposure are indicators of potential health risks for the local population and the importance of radiation protection. The present work creates a baseline database for future radiogenic studies in this specific area.

References

/1/ L. Villalba, M. Cabrera, Radiat. Prot. Dosim. 121 (2006) 148-157.

/2/ O. Baykara, M. Dogru. Radiat. Meas. 41-3 (2006) 362-367.

/3/ J. Adams, W. Lowder. *The natural radiation environment*. (1964) University of Chicago Press.

/4/ https://www.who.int/news-room/fact-sheets/detail/radon-and-health

/5/ V. Jobbágy, T. Altzitzoglou, J Env. Rad. 173 (2017) 18-24.

/6/ https://www.icrp.org/publication.

/7/ Guidelines for drinking-water quality. WHO (2004), Vol-1, 3rdedn, Geneva.

/8/ J.A. Ademola, A.O. Oyebode. J. Radiat. Prot. 37 (2017) 189.

Water Radon (Rn-222) Assessment in Raghunathpur and Jhalda Municipalities of Purulia District, West Bengal, INDIA

*Joydeep Mukherjee[1], Sayantan Mitra[1], Sushanta Sutradhar[1], Sonjoy Mondal[1], Chiranjib Barman[1]**

[1]Department of Physics, Sidho-Kanho-Birsha University, Purulia 723104, India.
*Email: chiranjib-barman@skbu.ac.in

1. Introduction

The only naturally occurring colourless, odourless radioactive gas radon, is produced by the decay of radium-226, thorium-232, uranium-235 that remain in the rocks of the Earth's crust. There exist three naturally occurring isotopes of radon nuclides viz. Rn-222, Rn-220 and Rn-219. Radon (Rn-222) is the most important in terms of physical behaviour and the effects due to the abundance and long-lived progeny of isotopes [1]. Diffusion of radon gas through the pores and cracks of Earth crust into the groundwater and water solubility of radon gas are the main reasons behind the presence of radon in groundwater. This radon containing groundwater, exhales radon gas into the air and consequently increases the radon concentration limit of air [2]. As a result, the consumption of radon enriched water and inhalation of radon rich air may lead to several harmful radiological effects on the local population.

2. Experiment

Water samples from deep tube wells of two municipalities, Raghunathpur and Jhalda, were collected and sealed in 250 mL air tight glass bottles. Then the samples were brought into the laboratory for water radon measurement using an ionization chamber type detector AlphaGuard DF 2000 with associated AquaKIT [3]. A microcontroller-based Flame-Photometer (G-301 Series, HPG Instruments, India) was used to measure the cations (Na^+, K^+, Li^+, Ca^{++}) concentration and pH of the water samples were measured using a digital pH meter (HM_PH80).

3. Results and Conclusion

The radon concentration of water samples that were collected from Raghunathpur municipality varies from 11.82 Bq L^{-1} to 155.64 Bq L^{-1} with an average of 49.78 Bq L^{-1} and the samples from Jhalda municipality ranges from 12.08 Bq L^{-1} to 74.74 Bq L^{-1} with an average of 39.06 Bq L^{-1}. Most of the water samples have lower activity of radon concentration than 100 Bq L^{-1}, for which no controls are to be implemented as per guidelines prescribed by WHO 2004 except for two samples from Raghunathpur municipality [4].

Table 2: Radon activities and AED levels for water samples collected from Raghunathpur and Jhalda Municipality

Place	**Raghunathpur**		**Jhalda**	
	Sample Size	**50**	**Sample Size**	**48**
Radon (Bq L^{-1})	Minimum	11.82	Minimum	12.08
	Maximum	155.64	Maximum	74.74
	Average	49.78	Average	39.06
AED (mSv y^{-1})	Adults	98% above 0.1 mSv y^{-1}	Adults	98% above 0.1 mSv y^{-1}
	Children	72% above 0.1 mSv y^{-1}	Children	62.5% above 0.1 mSv y^{-1}
	Infant	8% above 0.1 mSv y^{-1}	Infant	All below 0.1 mSv y^{-1}

Dose (AED) for adults, children and infants due to exposure to radon was calculated using the standard equation [5]. It is clearly visible from table-1 that in case of infants, maximum number of samples from these two municipalities has lower AED than 0.1 mSv y^{-1}. Additionally, the concentration of cations (Na^{+}, K^{+}, Li^{+}, Ca^{++}) present in the water samples and pH of the samples have been analysed and no correlation has been observed between radon and these parameters.

References

/1/ H. Bem, U. Plota, et al., J. Radioanal. Nucl. Chem. 299 (2014) 1307-1312.

/2/ A. Lima-Flores, V. Castaño, et al., J. Radioanal. Nucl. Chem. 329 (2021) 527-536.

/3/ S. Mitra, S. Chowdhury, et al., J. Radioanal. Nucl. Chem.330 (2021) 1331-1338.

/4/ Guidelines for Drinking Water Quality. Vol.1 3rd edition, WHO (2004) Geneva, Switzerland.

/5/ J.A. Ademola, O.A. Oyeleke, J. Radiol. Prot. 37 (2017) 189.

Study of Radiological and Non-Radiological Toxicants in The Aquatic Ecosystem of Coal Powered Thermal Power Plant

*Neeraj Chauhan[1], Pavitra Kumar[2], Pankaj Kumar[2], W. Alam[3], Amrit Pal Toor[4], Roland Bol[5], Ulrich W. Scherer[6] and Alok Srivastava[1]**

[1]Department of Chemistry, Panjab University Chandigarh, India.
[2]National Geochronology Facility, Inter-University Accelerator Centre, Aruna Asaf Ali Marg, New Delhi, India.
[3]Department of Forestry and Environmental Science, Manipur University Imphal, India.
[4]Dr.SSB University Institute of Chemical Engineering & Technology, Panjab University, Chandigarh, India.
[5]Institute for Biosphere and Geosphere-3, Forschungzetrum Juelich, Juelich 52428 Juelich, Germany.
[6]Institute for Physical Chemistry and Radiochemistry, Hochschule Mannheim, Mannheim, Germany.
*Email: alok@pu.ac.in

1. Introduction

Malwa region of Punjab State located in North-Western part of India is known to have an increased incidence of cancer. This belt has also been found to have significantly increased levels of uranium in its groundwater [1]. The increased incidences of cancer can be directly related to elevated uranium levels in groundwater [2]. The higher level of uranium concentration in the groundwater can be traced either to anthropogenic or to geogenic contribution [3]. The burning of coal could be considered as the significant source of anthropologically driven contamination of the aquatic environment as coal is known to consist of many radiological and non-radiological toxicants in trace amounts some of which have the potential to pollute the surrounding environment. In the present work, the concentration of radiological toxicant uranium along with non-radiological toxicants have been determined in water samples collected from aquatic sources inside and outside of a coal-powered thermal power plant located in the Malwa region of Punjab State using the Inductively Coupled Plasma Mass Spectrometry Technique (ICP-MS) to understand the contribution of coal in polluting local aquatic bodies.

2. Experiment

The study area is located in Punjab State of India which lies between 30.91–31.18^0 N latitude and 75.88–74.94^0 E longitude. 21 different water samples were collected in and around the coal-powered thermal

power plant. Polyethylene bottles soaked in 10% HNO_3 (65% ultra-pure, Himedia) for 24 h were used to collect water. The pH was maintained at 2 to preserve the water samples by adding ultra-pure nitric acid. Water samples were filtered through 0.45 μm filter paper to remove insoluble particles if any. The elemental concentration of collected water samples was determined using Inductively Coupled Plasma Mass Spectrometry (ICP-MS) facility of Inter University Accelerator Centre, New Delhi. Multi-element standard solution from Merck was used for calibration purpose and the detection limit of the elements identified was found to be in the range of 0.01 ppb to 1 ppb.

3. Results and Discussion

The measurement carried out in the present work showed presence of 14 different elements in water samples collected from locations in and around a thermal power plant besides from far away locations. Concentration of radiological toxicant uranium in water samples varied between 1.12 ppb and 47.07 ppb. The concentration of uranium in water used for various processes in the power plant was found to vary between 1.12 ppb and 5.29 ppb. The concentration of uranium in remaining water samples was found to be comparably higher as the observed uranium concentration level was observed to be in the range of 5.29 ppb to 47.07 ppb. It is interesting to point out here that the power plant uses canal and pond water for its operation whereas the remaining water samples were groundwater samples collected from locations within as well as outside the power plant. It is further observed that concentration of uranium in 18 out of 21 samples studied lay within the permissible limit of 30 ppb recommended World Health Organization (WHO) for drinking water [4]. However, if one goes by the more stringent limit of 10 ppb prescribed for uranium by the German Ordinance on Drinking Water [5] only 12 out of 21 samples could be considered fit for drinking purpose. The concentration of non-radiological elements in general was found to be within permissible limits except for Arsenic and Antimony where some samples showed levels higher than that prescribed by WHO for drinking water purpose.

References

/1/ M. Alrakabi, G. Singh, A. Bhalla, et al., J. Radioanal. Nucl. Chem. 294 (2012) 221-227.

/2/ E. Blaurock-Busch, Y.M. Busch, A. Friedle, et al., Clin. Med. Ins. Onco. 8 (2014) CMO-S13410.

/3/ A. Srivastava, V. Chahar, V. Sharma, et al., J. Radioanal. Nucl. Chem. 314 (2017)1367-1373.

/4/ World Health Report, 1998, World Health Organisation, Geneva.

/5/ Trinwasserverordnung https://www.gesetze-im-internet.de/trinkwv_2001/BJNR095910001.html

Spatial Distribution and Radiological Risk Assessment of Soil Radon (^{222}Rn) in Gandhinagar City, Gujarat

Sushanta Ku Sahoo[1], Madhusudhanarao Katlamudi[2], Bala Chander[3]*

Institute of Seismological Research, Gandhinagar, Gujarat, India
*Email: madhuspl@yahoo.com

1. Introduction

Radon is a found as a decay product of naturally occurring radionuclides ^{238}U, ^{232}Th, etc. ^{222}Rn travels through the pores of the soil and diffuses into the air. There are three processes of diffusion of radon into the air e.g., emanation, migration and exhalation. During the emanation process, radon enters the soil pores and during the migration process, radon moves through the soil pores and diffuses into the air upon exhalation [1,2]. Other factors such as concentration of uranium and thorium in the soil, porosity of soil and rocks, differences in atmospheric pressure between interfaces, soil moisture content, etc., contribute to the concentration of radon in the soil. The main contributor to total exposure to ionizing radiation in the environment comes from this radon. ^{222}Rn has a serious influence on human health.

2. Experiment

In order to decipher the distribution of soil radon and thoron, a soil radon survey was conducted in and around Gandhinagar, the capital of Gujarat, India. Measurements were taken at 70 locations in the study area at an average depth of 3 feet below ground. For data collection, the area of even distribution of soil without stones was selected. Samples were collected during daylight hours (04:00-12:30 GMT) in January. The survey is carried out with RAD7, supplied by Durridge Company Inc. (USA). The instrument can instantly distinguish radon from thoron based on the energy of the alpha particles released.

3. Results and Discussion

A variation in the soil radon concentration observed from 175 Bq/m^3 to 14,807 Bq/m^3 with an average value of 175.6 Bq/m^3 to 12,200 Bq/m^3, at different sites during the monitoring period. The concentration of thoron is higher than the concentration of radon at each observation point. It is observed that maximum thoron concentration varies between 100 Bq/m^3 and 16,100 Bq/m^3 and the average thoron value varies between 28 Bq/m^3 and 15,033 Bq/m^3. In the northern and eastern parts of Gandhinagar, the soil radon concentration is higher than in the western part. The high soil radon concentration in the northern part may be due to the fly ash content of the soil discharged from the Gandhinagar thermal power station. The annual effective dose that people living in the study area receive by inhaling radon is calculated. It is observed that the annual dose rate varies between 0.0013 mSv/year and 0.1337 mSv/y during the study. This dose rate range is below the ICRP recommended global average of 1 mSv/y. The coal fired in the thermal power plant contains organic substances as well as some inorganic radioactive elements such as U, Th and their decay products such as Ra and Rn. During the combustion of coal, such decomposition products are released from the coal and deposit at the interfaces between the gas phase and the solid combustion product (fly ash) and therefore occur in high concentrations. Apart from this, there are also places with high radon concentrations in the southern and eastern part of Gandhinagar in the RTO circle, Bhaijipura and Sarita Udyan regions. These small spots are due to fly ash contamination in the soil, which was dumped earlier. In addition, areas with high radon concentration are also observed in areas with high seismic risk.

Acknowledgement: The authors thank the Director General of the Institute of Seismological Research (ISR), Gandhinagar for giving permission to carry out the work. The authors also express their sincere thanks to the Dept. of Science and Technology, Govt. of Gujarat for providing the necessary funding for the investigation.

References

/1/ W.W. Nazaroff, B.A. Moed, R.G. Sextro, (1988) Soil as a source of indoor radon: Generation, migration and entry. In: W. W. Nazaroff, A.V. Nero (eds) Radon and its decay products in indoor air. Wiley-Interscience, New York, pp 57-112.

/2/ R. Schumann, D. Owen, S, Asher-Bolinder (1988) Weather Factors affecting soil-gas radon concentrations at a single site in the semiarid western U.S. In: EPA Symposium on Radon and Radon Reduction Technology 2.

Author Index

D

E

F

G

H

I

J

K

L

M

N

P

R

S